FINAL

Engineering Development of Coal-Fired High Performance Power Systems Phase II and III

DE-AC22-95PC95144

Quarterly Progress Report

January 1 - March 31, 1999

Prepared for

Federal Energy Technology Center
Pittsburgh, Pennsylvania

United Technologies Research Center
411 Silver Lane, East Hartford, Connecticut 06108

FINAL

Engineering Development of Coal-Fired High Performance Power Systems Phase II and III

DE-AC22-95PC95144

Quarterly Progress Report

January 1 - March 31, 1999

Prepared for

Federal Energy Technology Center
Pittsburgh, Pennsylvania

United Technologies Research Center
411 Silver Lane, East Hartford, Connecticut 06108

Abstract

This report presents work carried out under contract DE-AC22-95PC95144 "Engineering Development of Coal-Fired High Performance Systems Phase II and III." The goals of the program are to develop a coal-fired high performance power generation system (HIPPS) that is capable of:

- ◊ thermal efficiency (HHV) ≥ 47%
- ◊ NOx, SOx, and particulates ≤ 10% NSPS (New Source Performance Standard)
- ◊ coal providing ≥ 65% of heat input
- ◊ all solid wastes benign
- ◊ cost of electricity ≤ 90% of present plants

Phase I, which began in 1992, focused on the analysis of various configurations of indirectly fired cycles and on technical assessments of alternative plant subsystems and components, including performance requirements, developmental status, design options, complexity and reliability, and capital and operating costs. Phase I also included preliminary R&D and the preparation of designs for HIPPS commercial plants approximately 300 MWe in size. This phase, Phase II, involves the development and testing of plant subsystems, refinement and updating of the HIPPS commercial plant design, and the site selection and engineering design of a HIPPS prototype plant.

Work reported herein is from:

- ◊ Task 2.1 HITAC Combustors;
- ◊ Task 2.2 HITAF Air Heaters;
- ◊ Task 6 HIPPS Commercial Plant Design Update

Table of Contents

List of Exhibits

Executive Summary

This report represents work carried out under contract DE-AC22-95PC95144 "Engineering Development of Coal-Fired High Performance Systems Phase II and III." The goals of the program are to develop a coal-fired high performance power generation system (HIPPS) that is capable of:

- ◊ ≥ 47% thermal efficiency (HHV)
- ◊ NOx, SOx, and particulates ≤ 10% NSPS
- ◊ coal providing ≥ 65% of heat input
- ◊ all solid wastes benign
- ◊ cost of electricity ≤ 90% of present plant

Work presented in this report is from Task 2.1 HITAF Combustor, Task 2.2 HITAF Air Heaters, and Task 6 Commercial Plant Design Update.

Task 2.1 HITAF Combustors

Efforts are underway to improve the coal off-gas mixing and reaction model by incorporating three new coal off-gas mixture fractions coupled to a detailed mixing and reacting model. These three mixture fractions will allow mechanistic variations in coal off-gas compositions for "early" and "late" devolatilization reactions and will allow a single specified composition of the mass of coal off-gas evolved during the early and late stages of char oxidation. These three new mixture fractions are: the mixture fraction of coal off-gas originating from early devolatilization, the mixture fraction of the coal off-gas originating from late devolatilization; and the mixture fraction of coal off-gas which originates during the heterogeneous chemical char oxidation regime. This formulation retains the important ability to predict an overall time temperature dependent yield of char through two competing devolatilization reaction pathways.

The HIPPS design proposed in this program uses crossflow mixing as a critical technology for both flue gas recirculation (FGR) and for the rapid mixing nozzle used in the duct heater. The FGR design requires the incoming relatively cool gas to mix and quench the flue gas rapidly and produce a nearly flat temperature profile at the entrance to the SNCR zone. The duct heater design requires rapid mixing of the fuel and the heated air (>1700F) to minimize fuel-rich pockets which can be sources of NOx. Consequently, a benchmark database of concentration and velocity measurements is being acquired for a single jet injected normal to a confined crossflow. The database will include both mean and fluctuating quantities of the inlet conditions and mixing field acquired at high spatial resolution.

Task 2.2 HITAF Air Heaters

The pilot-scale SFS was fired on natural gas and Illinois No. 6 coal during the period January 24–29 and on natural gas and an eastern Kentucky bituminous coal during the period February 14–19. The purpose of the January test was: to evaluate the LRAH panel following its reassembly and installation in early January; to test the new inner-layer refractory design while coal was fired; and to test two refractory coatings painted on small areas of the inner refractory

layer to determine if they would help reduce slag corrosion of the refractory. The purpose of the February test was to continue the evaluation of the LRAH panel. However, the fuel used in February was selected because of its significant commercial interest and because it presented significantly different ash/slag properties compared to the Illinois No. 6 coal.

The following summarizes the results and observations for the January and February tests as well as SFS maintenance and modification activities.

- The fuel feed system was operated in January (60 hr, Illinois No. 6 coal) and in February (38 hr, Kentucky bituminous coal) at nominal feed rates of 180 to 195 lb/hr (82 to 89 kg/hr) and 150 to 170 lb/hr (68 to 77 kg/hr), respectively. These feed rates were chosen in an attempt to maintain a flue gas temperature near the LRAH tile surfaces of 2800 F (1538 C).
- The slagging furnace heatup rate during the January and February test periods was limited to 100 F/hr (56 C/hr) while natural gas was fired.
- In January, after an attempt to achieve a furnace temperature of 2950 F (1621 C) by increasing the natural gas firing rate through the main burner to 3.2 MMBtu/hr (3.3×10^6 kJ/hr) , the main burner natural gas firing rate was reduced to 2.3 MMBtu/hr (2.4×10^6 kJ/hr) to reduce the furnace temperature to 2800 F (1538 C). When the furnace reached normal operating temperature (2800 F/1538 C), the main burner was switched from natural gas to coal firing. The coal firing rate through the main burner in January was 2.1 to 2.25 MMBtu/hr (2.2 to 2.3×10^6 kJ/hr) with an auxiliary burner firing rate of 0.65 to 0.80 MMBtu/hr (0.7 to 0.9×10^6 kJ/hr). These firing conditions were maintained for 60 hours while personnel attempted to maintain a furnace flue gas temperature near the LRAH panel of 2800 F (1538 C).
- In February, the main burner natural gas firing rate was nearly 3.0 MMBtu/hr (3.1×10^6 kJ/hr) during preheating of the furnace prior to switching to coal-firing during the February test. The coal firing rate through the main burner in February was 2.1 to 2.3 MMBtu/hr (2.2 to 2.4 $\times 10^6$ kJ/hr) once the furnace refractory reached thermal equilibrium, with an auxiliary burner firing rate of 0.48 to 0.60 MMBtu/hr (0.6 to 0.7×10^6 kJ/hr). These firing conditions were maintained for 38 hours of coal.
- The firing rate for February was different than the January test probably because of the higher moisture content of the Illinois No. 6 coal (5.1 versus 2.5 wt%).
- Inspection of the furnace refractory after the January and February tests indicated that the new high-density refractory was in excellent condition.
- The main and auxiliary burners performed well during the January and February tests.
- Slag screen flue gas temperatures during the January test were typically 2585 to 2655 F (1419 to 1458 C) at the inlet and 2550 to 2600 F (1399 to 1427 C) at the outlet. Slag screen operating temperature is selected on the basis of ash fusion data for the fuel to be fired. There was no need to complete extensive maintenance or repairs to the slag screen following the January test with Illinois No. 6 coal. However, because of the large amount of residual slag left in the slag screen following the February test, the EERC elected to rebuild the screen prior to a test planned for April.

- During the January test, slag deposits formed in the vicinity of the FGR nozzles. Because of the slag flow from the slag screen into the dilution/quench zone, it was necessary to clean slag deposits from the area of the FGR nozzles on a periodic basis, however, cleaning frequency was somewhat variable, about every 2–4 hours. During the February test, slag deposits formed in the vicinity of the FGR nozzles. However, the deposition was minimal and no cleaning was required during the 38 hours of coal firing.
- Although the cooling air preheater heat-transfer rate degraded with time as ash deposits developed on the tube surfaces, cooling air temperature and flow rate control were adequate to support operation of the CAH tube bank and LRAH panel.
- The clean air plenum was removed from the pulse-jet baghouse following each test. One bag was pulled for inspection following the January test, with multiple bags pulled for inspection following the test in February. In both cases, the tube sheet appeared to be very clean, consistent with the low level of particulate emissions generally measured, and the bags pulled for inspection were found to be in good condition. As a result, the bags were not pulled for cleaning after either the January or February tests.
- In January, while natural gas was fired and the tubes were clean, heat recovery from the CAH tube bank was roughly 44,000 Btu/hr (46,420 kJ/hr). The cooling air flow rate was 138 scfm (3.9 m^3/min). The inlet cooling air was 1080 F (582 C), outlet cooling air was 1240 (671), and flue gas was 1800 (982) entering the CAH tube bank. As ash deposits developed on the tube surfaces, heat recovery from the CAH tube bank decreased from roughly 44,060 Btu/hr (46,483 kJ/hr) to 17,625 Btu/hr (18,594 kJ/hr).
- In February, while natural gas was fired and the tubes were clean, heat recovery from the CAH tube bank was roughly 44,474 Btu/hr (46,921 kJ/hr). The cooling air flow rate was 127 scfm (3.6 m^3/min). The inlet cooling air was 1010 F (544 C), outlet cooling air was 1195 F (646 C), and flue gas was 1800 F (982 C) entering the CAH tube bank. As ash deposits developed on the tube surfaces, heat recovery from the CAH tube bank decreased from roughly 46,500 Btu/hr (49,058 kJ/hr) to 27,000 Btu/hr (28,485 kJ/hr).
- A comparison of the LRAH panel data for both the January and February coal-fired test and the previous tests firing bituminous coal indicates that there has been a significant improvement in the heat recovery rate. During previous test periods, the heat recovery rate in the LRAH panel was <120,000 Btu/hr (<126,600 kJ/hr). However, in January and February the heat recovery rate was generally >120,000 Btu/hr (>126,600 kJ/hr). The higher heat recovery rate observed in January was a function of many factors: the SRAH panel was no longer in place, a minimal main burner swirl setting resulted in a more uniform temperature over the length of the furnace, the total furnace firing rate was somewhat higher in January and February than tests completed in late 1997 and early 1998, and the new condition of the high-density refractory may have resulted in a slight reduction in furnace heat loss.
- An examination of the Monofrax M refractory panels that were tested in the small radiant air heater (SRAH) and large radiant air heater (LRAH) during 1998 was conducted. The purpose of the examination was to evaluate the panel performance and durability. Examination of the removed tiles indicated that little or minimal changes occurred in the tile dimensions (especially in the thickness).

- The discoloration of the white Monofrax M was noticeable in the early runs, but apparently the continued rate of discoloration into the material decreased with increasing exposure time. Samples with 562 hours of furnace time had a discoloration depth averaging about 5 - 6mm, while those with 1006 hours had an average depth of 7 - 8mm.
- The application of a plasma sprayed chromia/alumina layer on the face of a tile did not seem to reduce the thickness of the discolored zone. However, it did have a significant effect on limiting the extent of the major corrosive action of the slag to the outer 1 mm from the surface.

Task 6 HIPPS Commercial Plant Design Update

Two repowering concepts were investigated: The first concept is "conventional" repowering wherein a gas turbine(s) is used to supply additional power as well as heated air for use in the steam bottoming cycle; and the second uses a high temperature fuel cell in addition to the gas turbine.

- Several conventional repowering concepts were estimated to provide power at the approximately 45%(HHV) efficiency level.
- A preliminary configuration developed for a Solid Oxide Fuel Cell system produces was estimated to provide power at the approximately 54%(LHV) efficiency level.

Introduction

The High Performance Power Systems (HIPPS) electric power generation plant integrates a combustion gas turbine and heat recovery steam generator (HRSG) combined cycle arrangement with an advanced coal-fired boiler. The unique feature of the HIPPS plant is the partial heating of gas turbine (GT) compressor outlet air using energy released by firing coal in the high temperature advanced furnace (HITAF). The compressed air is additionally heated prior to entering the GT expander section by burning natural gas. Thermal energy in the gas turbine exhaust and in the HITAF flue gas are used in a steam cycle to maximize electric power production. The HIPPS plant arrangement is thus a combination of existing technologies (gas turbine, heat recovery boilers, conventional steam cycle) and new technologies (the HITAF design including the air heaters, and especially the heater located in the radiant section).

The HITAF provides heat to the compressor outlet air using two air heaters, a convective air heater (CAH), and a radiant air heater (RAH). The HITAF is a slagging furnace which contains the radiant air heater, as well as waterwalls and steam drum for the high pressure (HP) steam system. Hot flue gas leaving the HITAF furnace passes over the CAH prior to entering a heat recovery steam generator (HRSG). Hot exhaust gas from the gas turbine is ducted to another HRSG in a typical combined cycle arrangement. The HITAF, gas turbine and HRSGs are configured to achieve the required high efficiency of the HIPPS plant.

The key to the success of the concept is the development of integrated combustor/air heater that will fire a wide range of US coals with minimal natural gas and with the reliability of current coal-fired plants. The compatibility of the slagging combustor with the high temperature radiant air heater is the critical challenge.

Task 2.1 HITAF Combustors

Improvement of Existing Models

Ongoing studies include the augmentation of the total number of progress variables currently used to characterize the turbulent mixing and reaction effects of coal off-gas within a detailed three-dimensional multiphase computational simulation code. Specifically, we seek to improve the coal off-gas mixing and reaction model by tracking three new coal off-gas mixture fractions as defined within a two step devolatilization model.

Typically one coal off-gas mixture fraction progress variable is defined and requires the model assumption of a uniform coal off-gas composition throughout both the coal devolatilization and heterogeneous char oxidation regime. Exhibit 2.1-1 graphically represents the concept of a single coal off-gas mixture fraction progress variable. In such single coal off-gas mixture fraction formulations, a single partial differential equation is solved to determine this coal off gas mixture fraction. Source terms are given by the solution of a set of ordinary differential equations within the context of a Lagrangian dispersion cloud model. The mass source terms due to the devolatilization and char oxidation pathways are distributed by the Particle-Source-in-Cell technique.

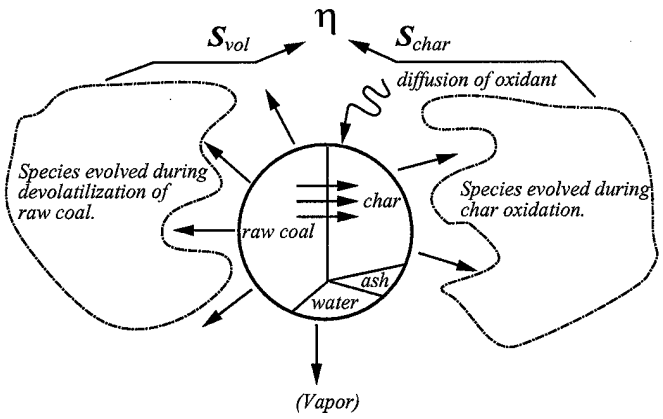

Exhibit 2.1-1
Conceptual Diagram of a Single Coal Off-Gas Mixture Fraction

Exhibit 2.1-2 represents a conceptual diagram whereby the mass source of coal off-gas contributions is separated. This formulation explicitly allows the capability to define different coal off-gas compositions based on the experimental observations of a nonuniform composition during the transition from coal devolatilization to char oxidation.

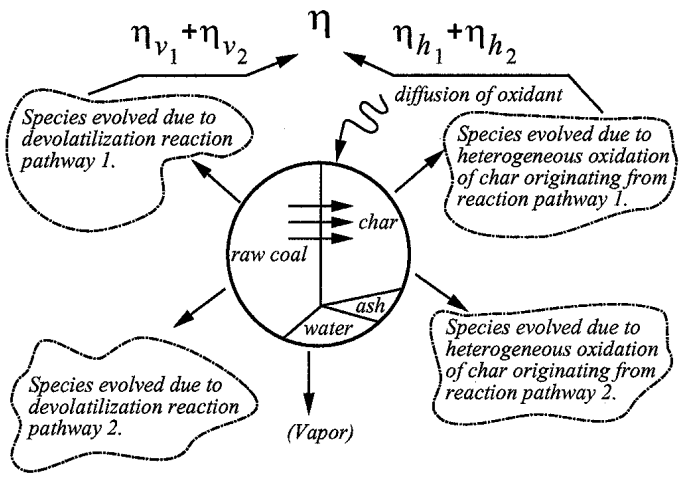

Exhibit 2.1-2
Conceptual Diagram of the Potential Different Sources of Coal Off-Gas within the Context of a Two Step Devolatilization Mechanism

Efforts are now concentrated on the incorporation of three new coal off-gas mixture fractions coupled to a detailed mixing and reacting model. These three mixture fractions will allow mechanistic variations in coal off-gas compositions for "early" and "late" devolatilization reactions and will allow a single specified composition of the mass of coal off-gas evolved during the early and late stages of char oxidation. These three new mixture fractions are:

1) the mixture fraction of coal off-gas originating from devolatilization pathway one,
2) the mixture fraction of the coal off-gas originating from devolatilization pathway two; and
3) the mixture fraction of coal off-gas which originates during the heterogeneous chemical char oxidation regime.

This formulation retains the important ability to predict an overall time temperature dependent yield of char through two competing devolatilization reaction pathways. Experimental composition data does exist for the specification of the composition of coal off-gas originating during the heterogeneous char oxidation process. There are three aspects of this project which need to be developed. They are:

1) writing the code for the transport of the progress variables,
2) incorporating the new progress variable information within a reaction model, and
3) sub-grid micromixing effects through an appropriate mixing model.

In our coal simulation efforts, we use a presumed Probability Distribution Function approach whereby the shape of the PDF is assumed to be of a clipped Gaussian shape. This formulation requires local information of both a mean mixture fraction and its respective variance of the PDR Incorporation of fluctuation effects for all three coal off-gas mixture fractions require solving a total of six new PDEs (three for the mixture fractions and three for each associative variance). These calculated mean mixture fraction values are used in a local Gibbs minimization equilibrium solution. Turbulent fluctuation effects are included by the convolution of the joint PDF over all scalar quantities.

The transport code of the three coal off-gas mixture fractions and the three associative variances of the presumed PDF are fully coded. The next step is to work towards incorporating this information within the mixing and reacting model.

Cross-Flow Mixing

Injection of a jet into a crossflow is a commonly employed mixing technique which consists of a jet entering into a freestream flow at a large angle. The distinguishing characteristics of this flowfield are the deflection of the jet by the mainstream to follow a curved path downstream, and the concurrent change of the jet cross section to a kidney-like shape. Farther downstream the jet shears into a counter-rotating vortex pair. This basic flowfield is used for dispersion of plumes, gas turbine combustor cooling, thrust control and many other commercial applications where rapid mixing of two streams is desired. In the HIPPS design, proposed by UTRC, crossflow mixing is a critical technology for both flue gas recirculation (FGR) and for the rapid mixing nozzle used in the duct heater. The FGR design requires the incoming relatively cool gas to mix and quench the flue gas rapidly and produce a nearly flat temperature profile at the entrance to the SNCR zone. The duct heater design requires rapid mixing of the fuel and the heated air (>1700F) to minimize fuel-rich pockets which can be sources of NOx.

In this program a benchmark database of concentration and velocity measurements are being acquired for a single jet injected normal to a confined crossflow. The database will include both mean and fluctuating quantities of the inlet conditions and mixing field acquired at high spatial resolution. This data will be used to validate CFD codes and will be particularly valuable in evaluating turbulence sub-models.

To date one component velocity measurements have been completed using a thermal anemometer. Measurements of average and rms velocity have been acquired at 10,000 points in the flowfield for a jet-to-mainstream momentum-flux ratio of 42.2. The data points were spaced on a 0.125" grid throughout the flowfield. Exhibit 2.1-3 shows the average velocity distribution in the x-z plane (plane parallel to the mainstream flow direction) on the centerline of the jet, which illustrates the jet trajectory feature of this flowfield. Exhibit 2.1-4 shows the distribution of rms velocity in the y-z plane (plane perpendicular to the flowfield) at a downstream distance of 1" which illustrates the development of the counter-rotating vortex pair. These figures contain 700 data points and are shown to illustrate typical data frames.

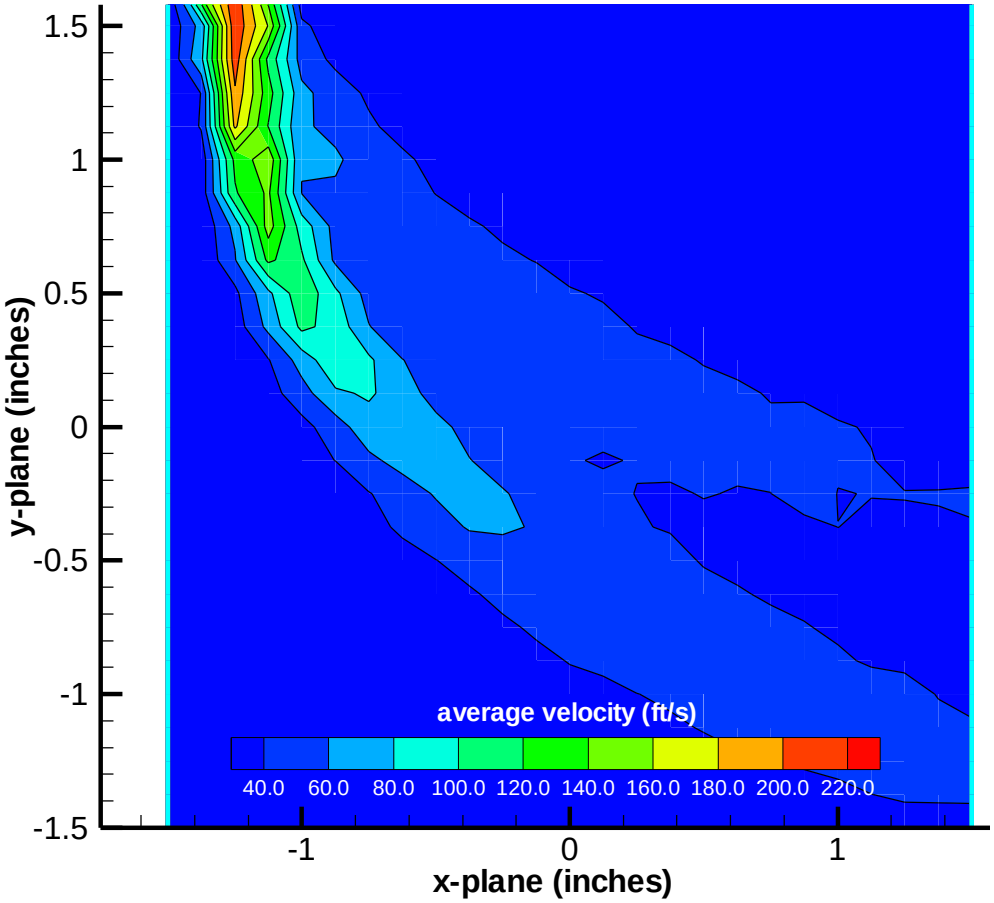

Exhibit 2.1-3
Distribution of Average Velocity
at J = 42.2

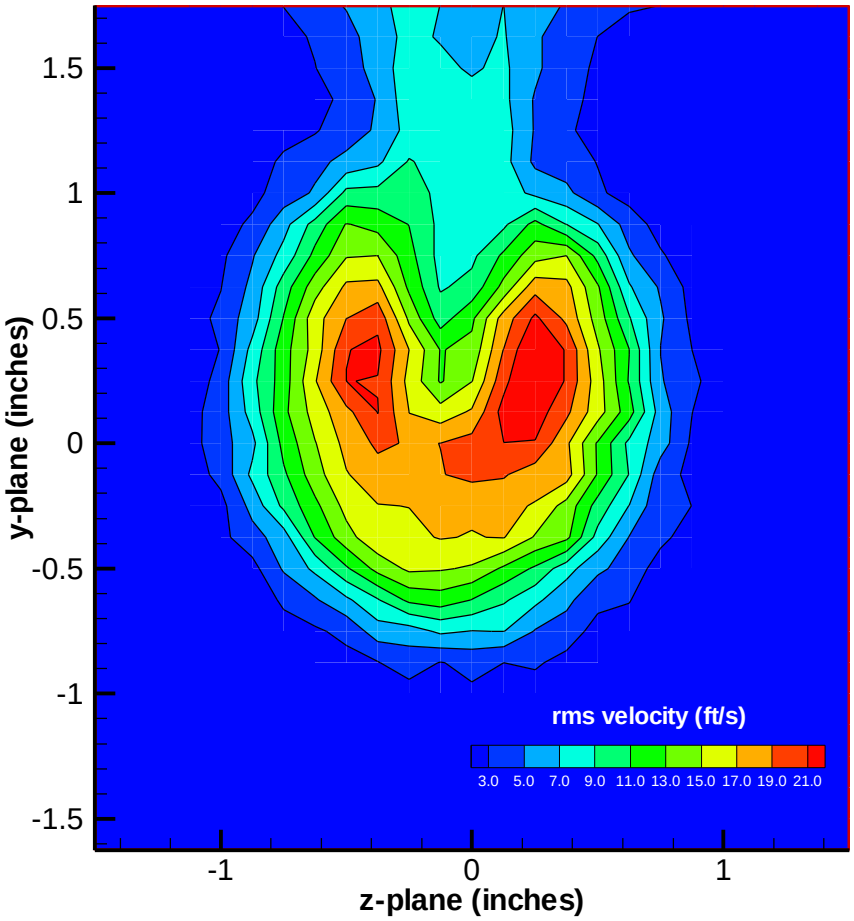

Exhibit 2.1-4
Distribution of RMS Velocity
at J = 42.2; Height of the Tunnel is 4.0"; Jet Enters at Top; and x = 1.0"

Collection of velocity data on the single jet configuration is in progress. The following is a brief summary of the experiment configuration, the data acquired to date, and future plans / schedule:

Exhibit 2.1-5
Specifications and Setpoints for the Reference Single Jet Configuration

(jet-to-mainstream momentum-flux ratio (J) = 42.2)

[note: $J = \rho_j V_j^2 / \rho_o V_o^2 = (m_j/m_o)^2/(C_d)^2(\rho_j/\rho_o)(A_j/A_o)^2$]

Mainstream (tunnel) width	**12.0**	inches
Mainstream height	4.0	inches
Mainstream velocity (V_o)	35.0	ft/s
Jet plenum width	12.0	inches
Jet plenum height	2.0	inches
Orifice (jet) diameter (tunnel side)	0.330	inches
Orifice diameter (plenum side)	0.370	inches
Orifice plate thickness (total)	0.07	inches
Tunnel side jet diameter thickness	0.02	inches
Measured orifice discharge coefficient	0.86	
Metered mainstream mass flowrate	0.881	lbm/s
Metered jet plenum mass flowrate	0.00877	lbm/s

The approach flow velocity distribution of the mainstream (tunnel) has been measured at x=0 (upstream edge of the orifice). The distribution of mean velocity and rms velocity is shown as contour plots in Exhibits 2.1-6 and -7. Each plot contains 705 individual points that are equally spaced on 0.25" centers. These measurements were made with a single hot-wire probe sensing the axial velocity at the reference tunnel set-point of 35 ft/s. Tunnel uniformity is about +/- 1 ft/s in mean velocity with a turbulence level of about 3.5% over the tunnel mid-section.

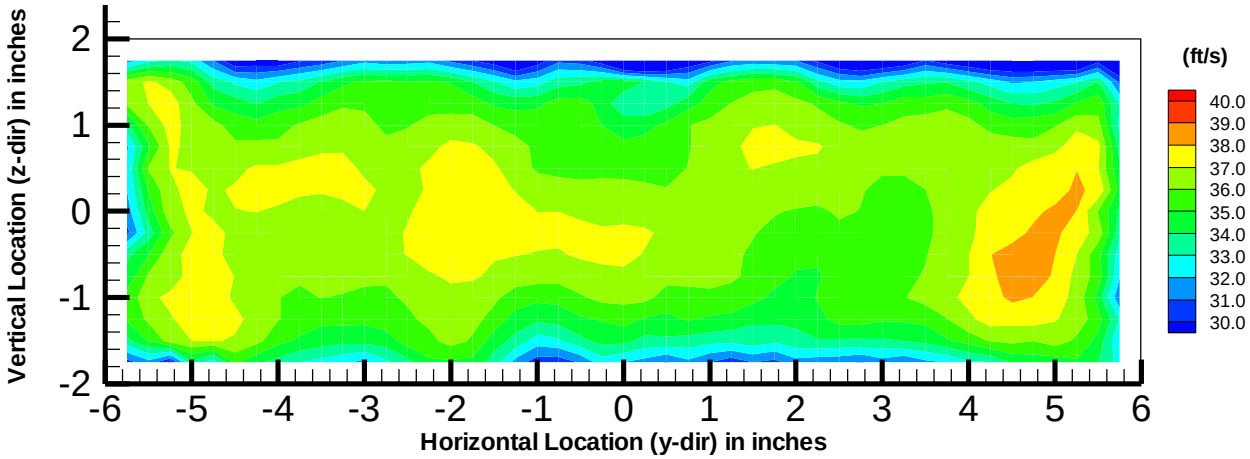

Exhibit 2.1-6
Mean Velocity Distribution of the Mainstream
at x=0 at a Set-Point of 35 ft/s

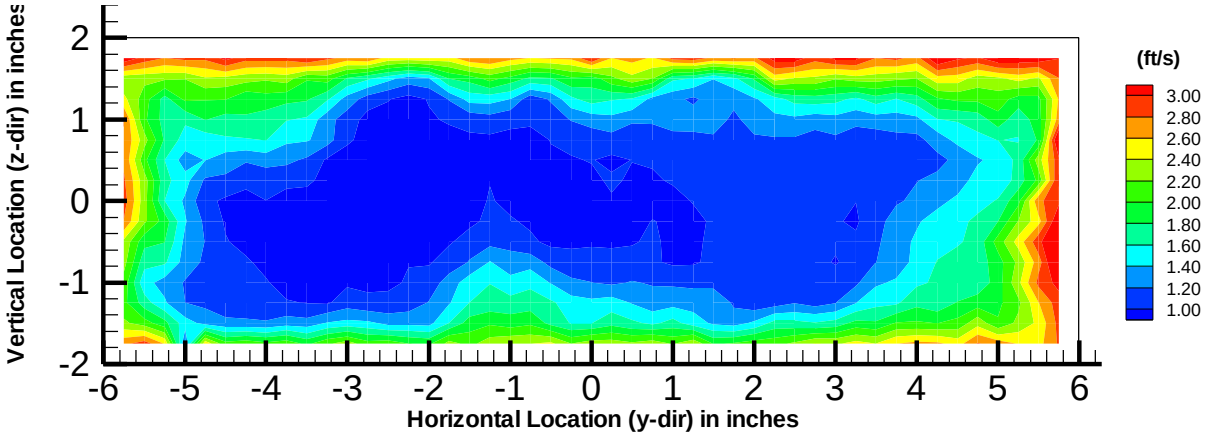

Exhibit 2.1-7
RMS Velocity Distribution of the Mainstream
at x=0 at a Set-Point of 35 ft/s

Mean and rms velocity distributions at a J of 42.2 have been measured at 16 downstream locations. Each distribution consists of 752 data points that are equally spaced on 0.125" centers. A few of the distributions are shown in Exhibit 2.1-8 (mean velocity) & -9 (rms velocity) to illustrate the resolution of the single wire data. A comparison of the jet trajectory of this dataset with the empirical correlation of Holdeman for a single jet in crossflow at J=42.2 is shown in Exhibit 2.1-10

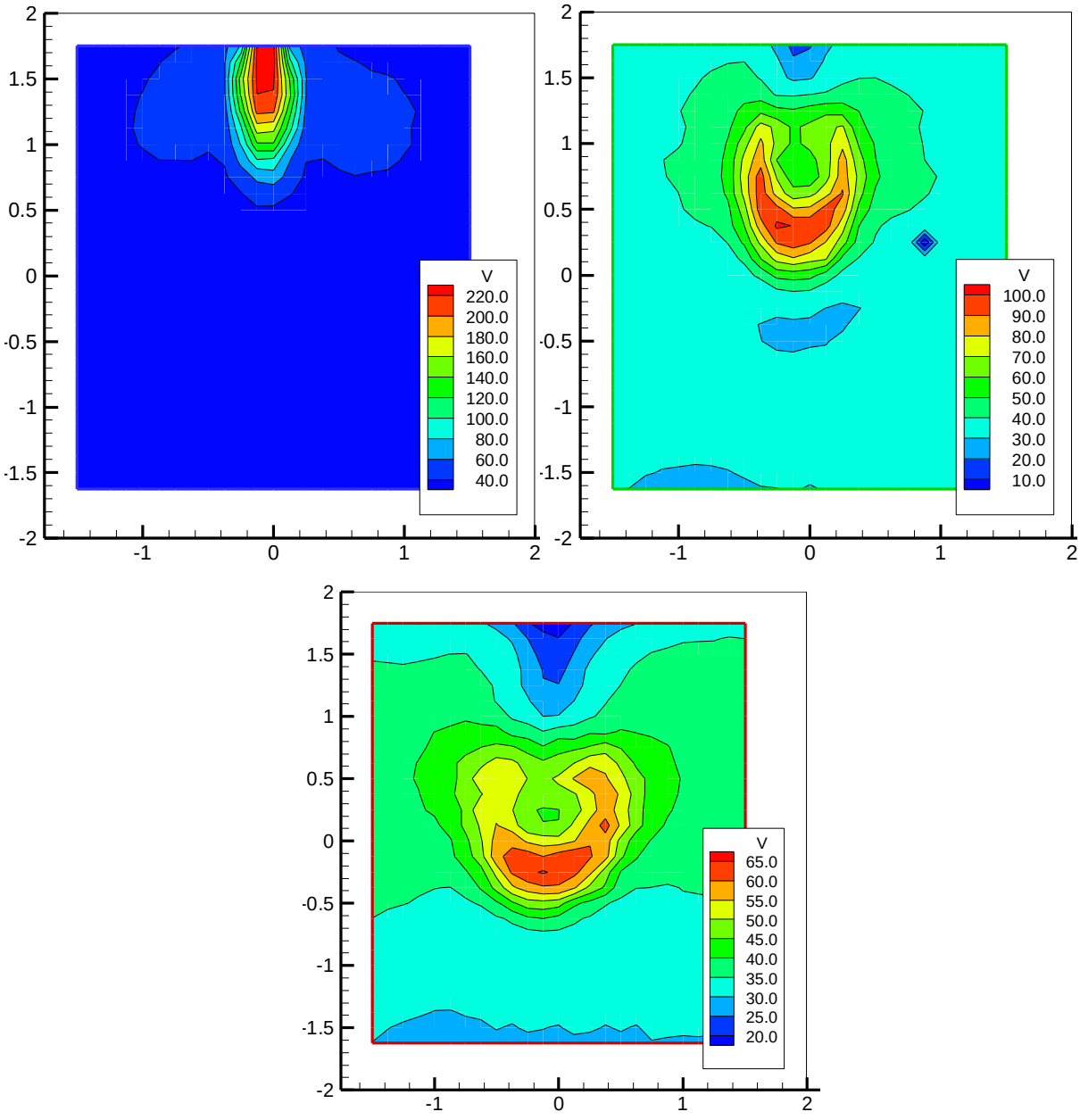

Exhibit 2.1-8
Mean Velocity Distribution
at x = 0.125, 0.500 and 1.00 for J = 42.2

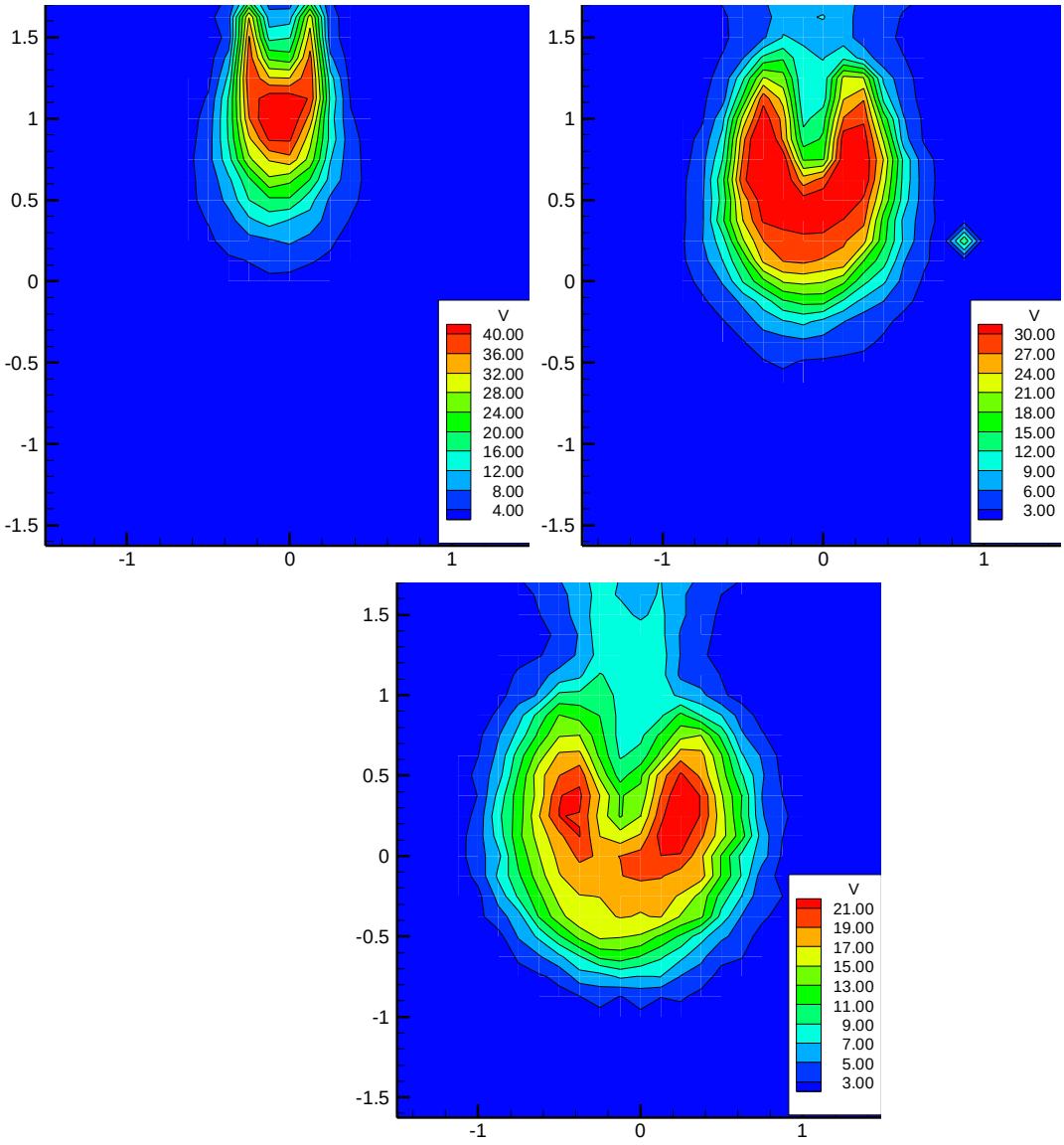

Exhibit 2.1-9
RMS Velocity Distribution
at x = 0.125, 0.500 and 1.00 for J = 42.2

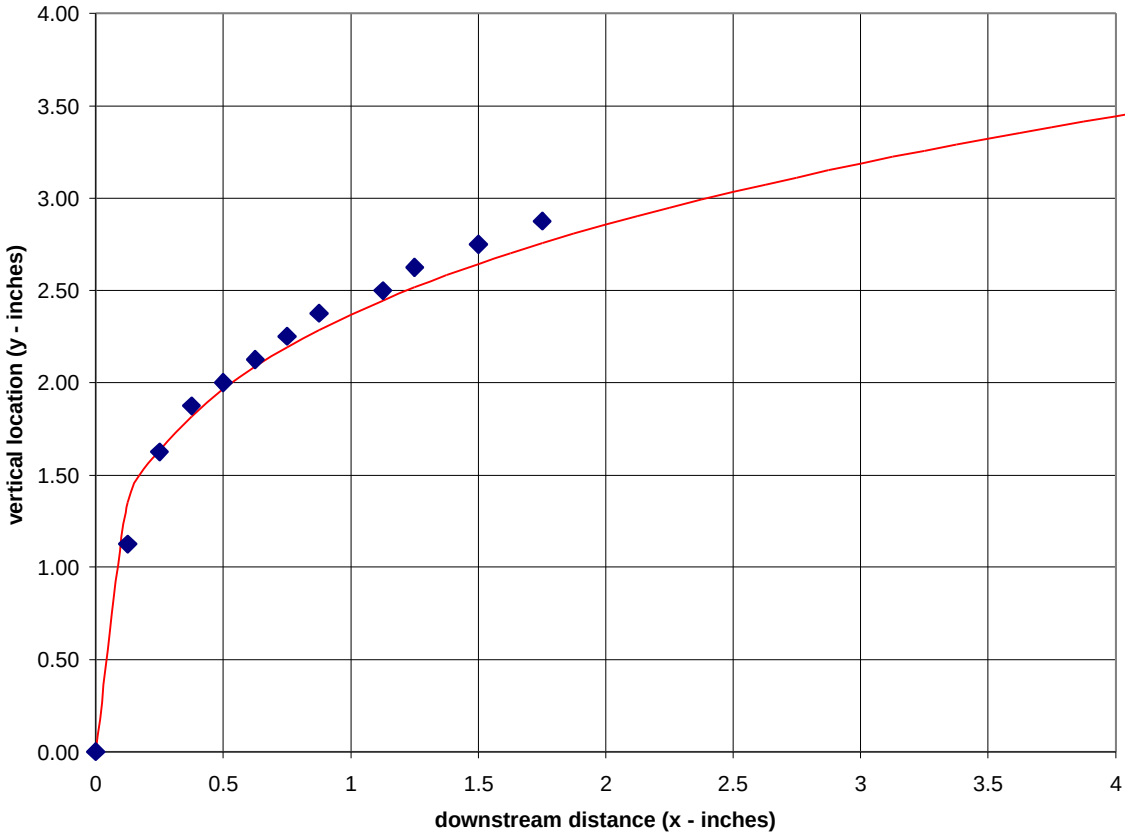

Exhibit 2.1-10
Comparsion of Jet Velocity Trajectories

at J = 42.2

(line = Holdeman's correlation (NASA TN D-6966, 1972), symbols = UTRC data)

Future work includes acquisition of three component velocity data, including turbulence level and measurement of the scalar distributions using planar light scattering once the velocity measurements is complete.

Task 2.2 HITAF Air Heaters

Pilot-Scale Testing

EERC pilot-scale activities this past quarter involved HITAF Testing. The remainder of this section discusses system modifications, observations, and results from the SFS operating periods completed in January and February 1999. Funding for the furnace modifications was provided through the subcontract to UTRC for Combustion 2000 work. However, funding for the actual combustion tests performed in January and February was provided through the Cooperative Agreement between the EERC and the Federal Energy Technology Center (FETC) under Task 3.3, High-Temperature Heat Exchanger Testing in a Pilot-Scale Slagging Furnace System (Contract No. DE-FC26-98FT40320).

Description of Pilot-Scale SFS

Exhibit 2.2-1 is a simplified illustration of the overall slagging furnace system. There have been no changes to the Exhibit in the past quarter nor has there been any additional equipment procured. Electrical work this past quarter focused on identifying the source of intermittent power surges to the process control/data acquisition computers observed on January 29. No equipment damage occurred. However, although the source of the power surges was not identified, they did not recur during the February test. Other activities were limited to miscellaneous maintenance items in support of overall system operation.

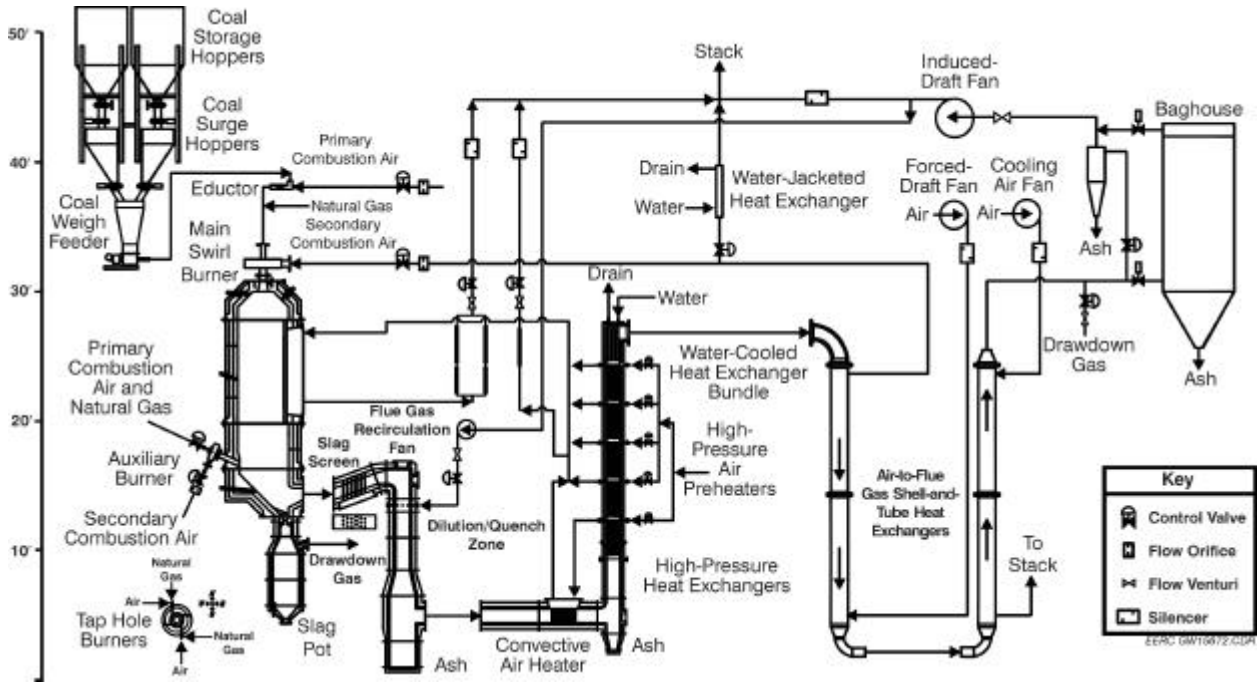

Exhibit 2.2-1
Combustion 2000 Slagging Furnace and Support Systems

SFS process noise within the high-bay facility was further reduced this past quarter with the installation of an available flow control valve in the balance air piping supporting the coal feed venturi. The flow control valve was smaller than the manual hand valve it replaced, substantially decreasing the valve noise and simplifying air flow control.

During the January operating period, the induced-draft (ID) fan tripped once when natural gas was fired in an attempt to increase the furnace flue gas temperature near the walls to >2900 F (1594 C) while curing refractory coatings applied to the high-density refractory in specific areas of the furnace. Therefore, the maximum flue gas temperature that can be achieved near the walls of the furnace with the LRAH panel installed while natural gas is fired is nominally 2900 F (1594 C). On the basis of operating experience, the EERC believes that a 3000 F (1649 C) flue gas temperature can be achieved while a bituminous coal is fired with the LRAH panel installed.

Fuel Feed System

Other than routine maintenance and cleaning, no changes or modifications were made to the fuel feed system this past quarter. During the January (firing Illinois No. 6 bituminous coal) and February (firing Kentucky bituminous coal) tests, the screw feeder operated effectively at <25% capacity.

Mechanical seals associated with the screw feeder were replaced prior to the February test because of pulverized coal leaks observed during the January test. EERC personnel anticipate that seal replacement will be required every 300+ hours, depending on the fuel type, feed rate, and the need to change the feeder screws.

Slagging Furnace

The pilot-scale slagging furnace design is intended to be as fuel-flexible as possible, with maximum furnace exit temperatures of 2700 to 2900 F (1483 to 1593 C) to maintain the desired heat transfer to the LRAH panel and slag flow. It has a nominal firing rate of 2.5 MMBtu/hr (2.6×10^6 kJ/hr) and a range of 2.0 to 3.0 MMBtu/hr (2.1 to 3.2×10^6 kJ/hr). It uses a single burner.

The design is based on Illinois No. 6 bituminous coal (11,100 Btu/lb or 25,800 kJ/kg) and a nominal furnace residence time of 3.5 s. Flue gas flow rates range from roughly 425 to 645 scfm (12.0 to 18.6 m^3/min), with a nominal value of 530 scfm (15 m^3/min) based on 20% excess air. Firing a subbituminous coal or lignite increases the flue gas volume, decreasing residence time to roughly 2.6 s. However, the high volatility of the low-rank fuels results in high combustion efficiency (>99%). The EERC oriented the furnace vertically (downfired) and based the burner design on that of a swirl burner used on two smaller EERC pilot-scale pulverized coal (pc)-fired units (600,000 Btu/hr [633,000 kJ/hr]). Slagging furnace dimensions are 47 in. (119 cm) inside diameter by roughly 16 ft (4.9 m) in total length.

The vertically oriented furnace shell was designed to include four distinct furnace sections. The top section of the furnace supports the main burner connection, while the upper middle furnace section provides a location for installation of the RAH panels. The lower middle furnace section supports the auxiliary gas burner; the bottom section of the furnace includes the furnace exit to the slag screen as well as the slag tap opening.

Flue gas temperature measurements have been made using four Type S thermocouples protruding 1 in. (2.5 cm) into the furnace through the refractory wall, and more recently, using three optical pyrometers. Furnace temperature is also measured using thermocouples located at the interface between the high-density and intermediate refractory layers as well as between the intermediate and insulating refractory layers. A pressure transmitter and gauges are used to monitor static pressures in order to monitor furnace performance. These data (temperatures and pressures) are automatically logged into the data acquisition system and recorded manually on data sheets on a periodic basis as backup.

The slag tap is intended to be as simple and functional as possible. To that end, the design is a simple refractory-lined hole in the bottom of the furnace. The diameter of the slag tap is nominally 4 in. (10 cm), with a well-defined drip edge. A two-port natural gas-fired tap hole burner is used to maintain slag tap temperature for good slag flow. Although some slag tap deposits did form and slag tap erosion was observed, no severe slag tap plugging was encountered this past quarter. When the slag tap has plugged in the past year, the plug was removed on-line after a switch was made to natural gas firing for a short period of time (2 hours) in the main burner. To minimize heat losses, slag is collected in an uncooled, dry container with refractory walls.

The refractory walls in the slagging furnace are composed of three layers of castable refractory. They consist of an inner 4-in. (10.2-cm) layer of high-density (14-Btu-in./ft^2-F-hr or 2.0-W/m-K) slag-resistant material, 4 in. (10.2 cm) of an intermediate refractory (4.0-Btu-in./ft^2 F-hr or 0.6 W/m-K), and a 3.25-in. (8.3-cm) outer layer of a low-density insulating refractory (1.3-Btu-in./ft^2-F-hr or 0.2 W/m-K). Three refractory layers were selected as a cost-effective approach to keep the overall size and weight of the system to a minimum while reducing slag corrosion and heat loss.

Complete replacement of the high-density furnace refractory was anticipated in the original Combustion 2000 scope of work, although the lifetime of the material was uncertain because of the variable slag deposition that was anticipated. Most of the original high-density refractory lasted until after the August 1998 test period. At that time a decision was made to replace it because of extensive cracking caused by the differences in the expansion and contraction of the inner and middle liners during each heatup and cooldown cycle. Actual corrosion of the high-density liner was minimal, except for newer patches that were not completely sintered and for areas of flame impingement. The timing worked out well with the need to replace/reassemble ceramic components in the LRAH panel. Exhibit 2.2-2 summarizes properties for refractories used in the SFS.

Although the Narco Cast 60 refractory in the top section of the furnace appeared to be in good shape, refractory deterioration was evident as a result of two weeks of lignite firing. Therefore, it was replaced with a Plibrico Plicast Cement-Free 96V refractory. This material will be less prone to corrosion than the Narco Cast 60 refractory, yet stronger. It will also be less prone to shrinkage than the Plibrico Plicast Cement-Free 98V KK refractory originally used in this section of the furnace.

Exhibit 2.2-2
Refractory Properties

Refractory:	Plicast Cement-Free 99V KK/99V[1]	Plicast Cement-Free 98V KK/98V[1]	Plicast Cement-Free 96V KK/96V[1]	Narco Cast 60	Plicast LWI-28	Plicast LWI-20	Harbison-Walker 26
Function	High density	High density	High density	High density	Insulating	Insulating	Insulating
Service Limit, °F	3400	3400	3300	3100	2800	2000	2600
Density, lb/ft^3	185	185	185	145	80	55	66
K, Btu-in./ft^2 °F-hr @ 2000°F	14.5	14.5	14.0	6.5	4.0	NA[2]	2.2
K, Btu-in./ft^2 °F-hr @ 1500°F	14.7	14.7	14.2	6.0	3.0	1.7	1.9
K, Btu-in./ft^2 °F-hr @ 1000°F	15.5	15.5	15.0	5.6	2.7	1.3	1.7
Hot MOR[3] @ 2500°F, psi	650	750	1400	NA	NA	NA	NA
Hot MOR @ 1500 °F, psi	–	–	2000	1000	250	100	110
Cold Crush Strength @ 1500 °F, psi	–	–	10000	NA	750	400	350
Typical Chemical Analysis, wt% (calcined)							
Al_2O_3	99.6	98.6	95.5	62.2	54.2	39.6	53.8
SiO_2	0.1	1.0	3.8	28.0	36.3	31.5	36.3
Fe_2O_3	0.1	0.1	0.1	1.0	0.8	5.4	0.5
TiO_2	0.0	0.0	0.0	1.7	0.5	1.5	0.6
CaO	0.1	0.1	0.1	2.8	5.7	19.5	7.2
MgO	0.0	0.0	0.0	0.1	0.2	0.8	0.2
Alkalies	0.2	0.2	0.2	0.2	1.5	1.4	1.4

[1] The "KK" designation indicates the presence of fibers that promote dewatering during curing.

[2] Not applicable.

[3] Modulus of rupture.

Because of its greater structural strength and high corrosion resistance, Plibrico Plicast Cement-Free 98V alumina castable was used to replace the high-density refractory in the three lower furnace sections. Based on vendor information and bench-scale data, Plicast Cement-Free 98V was expected to be less prone to shrinkage than the 98V KK and 99V KK materials originally used in these furnace sections while having comparable slag corrosion resistance. The condition of the high-density refractory following the tests completed in January and February appears to be excellent. It appears that removal of the KK fibers from the refractory had little or no effect on high-density refractory shrinkage. In addition, the approach used for high-density refractory replacement resulted in a complete separation of the high-density and intermediate refractory surfaces. This separation should limit cracking and other refractory damage resulting from differential thermal expansion during heatup and cooldown cycles.

Main and Auxiliary Burners

The main burner is natural gas- and pulverized fuel-capable. The basic design is an International Flame Research Foundation (IFRF)-type adjustable secondary air swirl generator which uses primary and secondary air at approximately 15% and 85% of the total air, respectively, to adjust swirl. Increasing swirl to provide flame stability and increased carbon conversion can also affect the formation of NO_x. Carbon conversion has been >99% when bituminous and subbituminous coal and lignite are fired. High carbon conversions can be obtained at low swirl settings because of the high operating temperature and adequate residence time. Combustion air flow rates through the main burner range from about 400 to 600 scfm (11 to 17 m^3/min), depending on furnace firing rate and the fuel type (bituminous, subbituminous, or lignite) fired.

An auxiliary gas burner (850,000 Btu/hr or 896,750 kJ/hr) is located near the furnace exit to control furnace exit temperature, ensuring desired slag flow from the furnace and the slag screen. This auxiliary burner is used to compensate for heat losses through the furnace walls, sight ports, and RAH test panel. Use of the auxiliary gas burner is beneficial during start-up to reduce heatup time and to prevent slag from freezing on the slag screen when the switch is initially made to coal firing.

Radiant Air Heater Panels

The LRAH test panel arrived at the EERC on September 15, 1997. Final assembly and installation of the LRAH panel into the furnace took place in November 1997. A key design feature of the furnace is accessibility for installation and testing of the LRAH panel. The furnace design will accept one LRAH panel with a maximum active size of 1.5 × 6.4 ft (0.46 × 1.96 m). This size, which was selected to minimize furnace heat losses, was based on panel-manufacturing constraints identified by UTRC. Flame impingement on the RAH panel is not necessarily a problem. Cooling air for the LRAH panel is provided by an existing EERC air compressor system having a maximum delivery rate of 510 scfm (14.4 m^3/min) and a maximum stable delivery pressure of 275 psig (19 bar). Backup cooling air is available from a smaller compressor at a maximum delivery rate of 300 scfm (8.5 m^3/min) and pressure of <100 psig (<7 bar). A tie-in to an existing nitrogen system is also available as a backup to the existing air compressor system. In the event of a failure of inlet cooling air piping, a backflow emergency piping system was installed

so that overheating of the LRAH panel could be avoided. UTRC designed and fabricated the LRAH test panel.

Slag Screen

The slag screen design for the pilot-scale slagging furnace system is the result of a cooperative effort between the EERC, UTRC, and PSI personnel. The primary objective for the pilot-scale slag screen is to reduce the concentration of ash particles entering the CAH. Design criteria specific to the pilot-scale slag screen include:

1. a simple design permitting modifications using readily available, inexpensive materials;
2. matching duct dimensions and flue gas flow rates to maintain turbulent flow conditions;
3. minimizing the potential for plugging as the result of slag deposit growth on tube surfaces or the sloped floor;
4. limiting differential pressure across the slag screen to 2 in. W.C. (4 mm Hg); and
5. limiting heat losses to assure desired slag flow from the slag screen to the furnace slag tap.

The walls of the slag screen consist of two refractory layers. The inner, high-density layer is a Plicast Cement-Free 98V KK with an outer insulating layer of Harbison-Walker Castable 26. The high-density refractory is 2.25 in. (5.7 cm) thick in the sidewalls and 4 in. (10.2 cm) thick in the roof and floor of the slag screen. The insulating refractory is 3.75 in. (9.5 cm) thick in the sidewalls, roof, and floor. A Plicast LWI-28 refractory was used around the sight ports in the wall of the slag screen. Properties for the high-density and insulating refractories selected for use in the slag screen are summarized in Exhibit 2.2-2. Water-cooled surfaces were installed inside of the refractory tubes to cool the tubes and reduce the erosion/corrosion observed during shakedown tests. Specific details concerning slag screen modifications and performance this past quarter are addressed later in this report.

Dilution/Quench Zone

The dilution/quench zone design was a cooperative effort between the EERC and UTRC. The circular dilution/quench zone is oriented vertically and maintains a 1.17-ft (0.36-m) diameter in the area of the flue gas recirculation (FGR) nozzles. The duct diameter expands to 2 ft (0.6 m) to provide adequate residence time within duct length constraints. The duct section containing the flue gas recirculation nozzles is a spool piece to accommodate potential changes to the size, number, and orientation of the flue gas recirculation nozzles. The vertically oriented dilution/ quench zone is refractory-lined and located immediately downstream of the slag screen and upstream of the CAH duct.

Routine cleaning of the dilution/quench zone has been required during each weeklong bituminous and subbituminous coal test period. To better monitor and document the slag deposition in the dilution/quench zone, a pressure transmitter is used to monitor and record differential pressure. On the basis of observations during the August 1998 test and the frequent cleaning required, the EERC modified the spool piece section of the dilution/quench zone. The specific modification involved the addition of a water-cooled wall around the flue gas recirculation (FGR) nozzles. This water-cooled wall should embrittle the slag deposits that form in this area, making them easier to remove on-line. Performance observations as a result of the January and February tests are summarized later in this report.

Convective Air Heater (CAH)

The CAH design was a cooperative effort between the EERC and UTRC. It was constructed by UTRC and installed in September 1997. The flue gas flow rate to the CAH tube bank has been calculated to range from 3553 to 4619 acfm at 1800 F (101 to 131 m^3/min at 982 C). A rectangular inside duct dimension of 1.17 ft^2 (0.11 m^2) results in a flue gas approach velocity of 50 to 73 ft/s (15 to 22 m/s) to the CAH.

The CAH originally consisted of twelve 2-in.- (5-cm)-diameter tubes installed in a staggered three-row array. The first five tubes in the flue gas path were uncooled ceramic material, with the remaining seven tubes cooled by heated air. The uncooled ceramic tubes were replaced in May 1998 with uncooled stainless steel tubes. Replacement of the ceramic tubes was necessary because they were repeatedly damaged when the tube bank was removed from the duct after the test periods in February, March, and April 1998.

In September 1998, the uncooled tubes were again replaced. The replacement tubes represented three high-temperature alloy types (Incoloy MA956, Incoloy MA956HT, and PM2000) and three pipe sizes (1.5-in. [3.8-cm] Schedule 80, 1-in. [2.5-cm] Schedule 40, and 0.75-in. [1.9-cm] Schedule 40, respectively). Exhibit 2.2-3 illustrates the position, size, and alloy type for the five uncooled tubes.

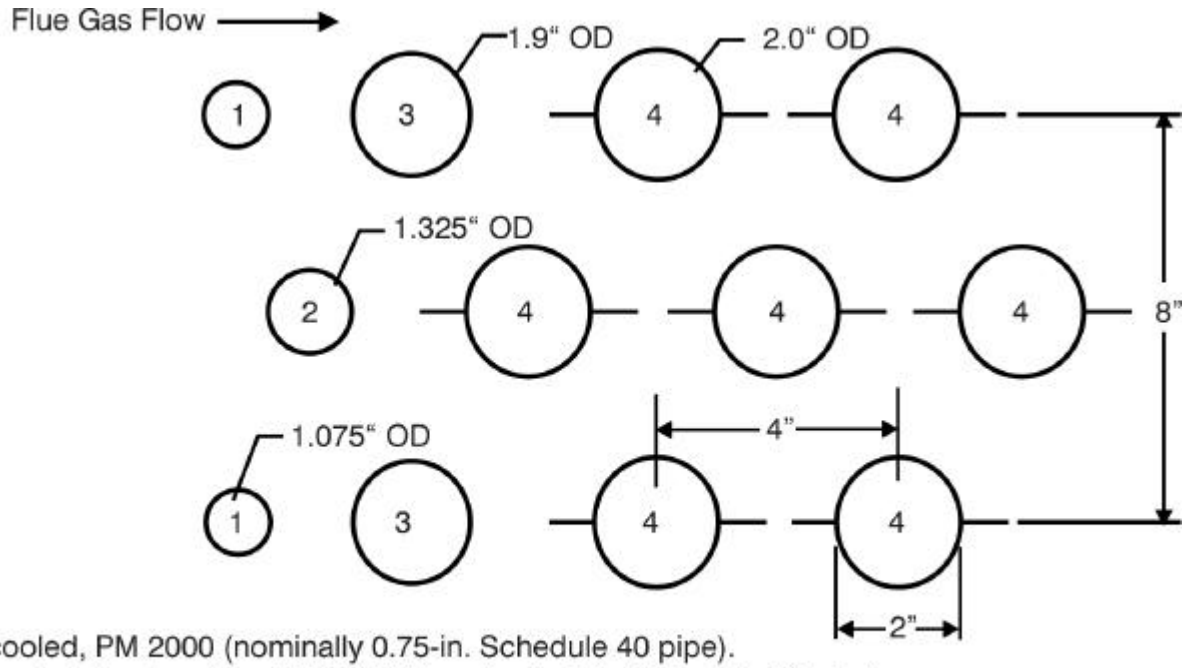

Exhibit 2.2-3
Illustration of the Uncooled Tubes in the CAH Tube Bank

Emission Control

A pulse-jet baghouse is used for final particulate control on the pilot-scale SFS. The baghouse design permits operation at both cold-side (250 to 400 F/121 to 205 C) and hot-side (600 to 700 F/316 to 371 C) temperatures. The primary baghouse chamber and ash hopper walls are electrically heated and insulated to provide adequate temperature control to minimize heat loss and avoid condensation problems on start-up and shutdown. The main baghouse chamber was designed with internal angle iron supports to handle a negative static pressure of 20 in. W.C. (37 mm Hg).

During the past quarter a single tube sheet was used, permitting the installation of 36 bags arranged in a six-by-six array. Bag dimensions are nominally 6 in. (15.2 cm) in diameter by 10 ft (3.0 m) in length, providing a total filtration area of (565 ft^2 [52.5 m^2]). The bag type being used at this time is a 22-oz/yd^2 (747-g/m^2) woven glass bag with a polytetrafluoroethylene (PTFE) membrane. Pulse cleaning of the bags was accomplished on-line using a reservoir pulse-air pressure of nominally 40 psig (2.8 bar). Baghouse performance observations as a result of the January and February tests are summarized later in this report.

Flue gas sample ports were installed in the inlet and outlet piping of the baghouse to permit flue gas sampling for gaseous/vapor-phase constituents as well as fly ash. Fly ash particle-size distribution and mass loading are determined periodically using standard U.S. Environmental Protection Agency (EPA) methods. Hazardous air pollutant (HAP) measurements can be taken through existing sample ports using EPA Method 29 and the Ontario Hydro method for mercury speciation.

Instrumentation and Data Acquisition

The instrumentation and data acquisition components for the pilot-scale SFS address combustion air, flue gas, cooling air, cooling water, temperatures, static and differential pressures, and flow rates. The data acquisition system is based on a Genesis software package and three personal computers. Two sets of flue gas instrumentation (oxygen, carbon dioxide, carbon monoxide, sulfur dioxide, and nitrogen species) are dedicated to support the operation of the SFS. Flue gas is transferred from the sample point through a heated filter and sample line to the sample conditioner before it reaches the analyzers. Flue gas is routinely sampled in the slag screen at the furnace exit and the exit of the baghouse. Total flue gas flow rate through the SFS is measured using a venturi. The only instrumentation work completed this past quarter involved routine maintenance.

Pilot-Scale SFS Activities

The pilot-scale SFS was fired on natural gas and Illinois No. 6 coal during the period January 24–29 and on natural gas and an eastern Kentucky bituminous coal during the period February 14–19. The purpose of the January test was:

- to evaluate the LRAH panel following its reassembly and installation in early January,
- to test the new inner-layer refractory design (described in the October through December 1998 quarterly technical progress report) while coal was fired, and
- to test two refractory coatings painted on small areas of the inner refractory layer to determine if they would help reduce slag corrosion of the refractory.

The purpose of the February test was to continue the evaluation of the LRAH panel. However, the fuel used in February was selected because of its significant commercial interest and because it presented significantly different ash/slag properties compared to the Illinois No. 6 coal. Data evaluation and sample analysis have been completed. Therefore, this report summarizes the results and observations for the January and February tests as well as SFS maintenance and modification activities.

Fuel Feed System

The fuel feed system was operated in January (60 hr, Illinois No. 6 coal) and in February (38 hr, Kentucky bituminous coal) at nominal feed rates of 180 to 195 lb/hr (82 to 89 kg/hr) and 150 to 170 lb/hr (68 to 77 kg/hr), respectively. These feed rates were chosen in an attempt to maintain a flue gas temperature near the LRAH tile surfaces of 2800 F (1538 C). Exhibits 2.2-4 and 2.2-5 illustrate the coal feed rate data for the January and February tests, respectively. During both tests, the coal feed rate was quite stable except for a few minor spikes (high and low) associated with coal hopper refill cycles.

Exhibits 2.2-6 and 2.2-7 summarize analytical results for the Illinois No. 6 bituminous, Kentucky bituminous, and Rochelle subbituminous coal and the Coal Creek Station (CCS) and Milton R. Young Station (MRYS) lignites, respectively, that have been fired in the pilot-scale slagging furnace. For the January test, the analyses of the composite Illinois No. 6 coal sample indicated that the as-fired fuel contained 5.1 wt% moisture, 11.3 wt% ash, and 3.7 wt% sulfur. The heating value was 11,328 Btu/lb (26,365 kJ/kg) on an as-fired basis. Coal ash was analyzed for ash fusion properties under oxidizing conditions. Results indicate a softening temperature of 2417 F (1325 C) and a fluid temperature of 2491 F (1366 C).

For the February test, the analyses of the composite Kentucky coal sample indicated that the as-fired fuel contained 2.5 wt% moisture, 3.9 wt% ash, and 0.8 wt% sulfur. The heating value was 14,120 Btu/lb (26,365 kJ/kg) on an as-fired basis. Coal ash was analyzed for ash fusion properties under oxidizing conditions. Results indicate a softening temperature of 2440 F (1338 C) and a fluid temperature of 2588 F (1420 C). The fluid temperature of the coal ash in the Kentucky coal was 50 F (28 C) higher than any of the previous fuels fired.

Dry-sieve analysis indicated that the pulverized Illinois No. 6 coal was nominally 80 wt% 200 mesh (74 microns [μm]). Dry-sieve analysis data for the pulverized Kentucky coal indicated nominally 64 wt% 200 mesh (74 μm). The poorer pulverization efficiency for the Kentucky bituminous coal is believed to have been caused by surface moisture. However, because of the high furnace operating temperature, combustion efficiency was not affected. For both fuels, the carbon content of the fly ash collected in the baghouse was low, 0.50 wt% for the Illinois No. 6 coal and 0.24 wt% for the Kentucky coal.

X-ray fluorescence (XRF) analysis results for the various ashed fuels are summarized in Exhibits 2.2-6 and 2.2-7 and reported as oxides. Comparison of the Illinois No. 6 and Kentucky coal ash indicates that the Kentucky coal ash contains significantly less silica and iron and significantly more calcium. Since the Illinois No. 6 coal contains more than three times the sulfur observed in the Kentucky coal, one might expect to find a higher level of sulfur trioxide (SO_3) in the ashed coal. However, the higher calcium content of the Kentucky coal ash is responsible for the SO_3 of the ashed coal.

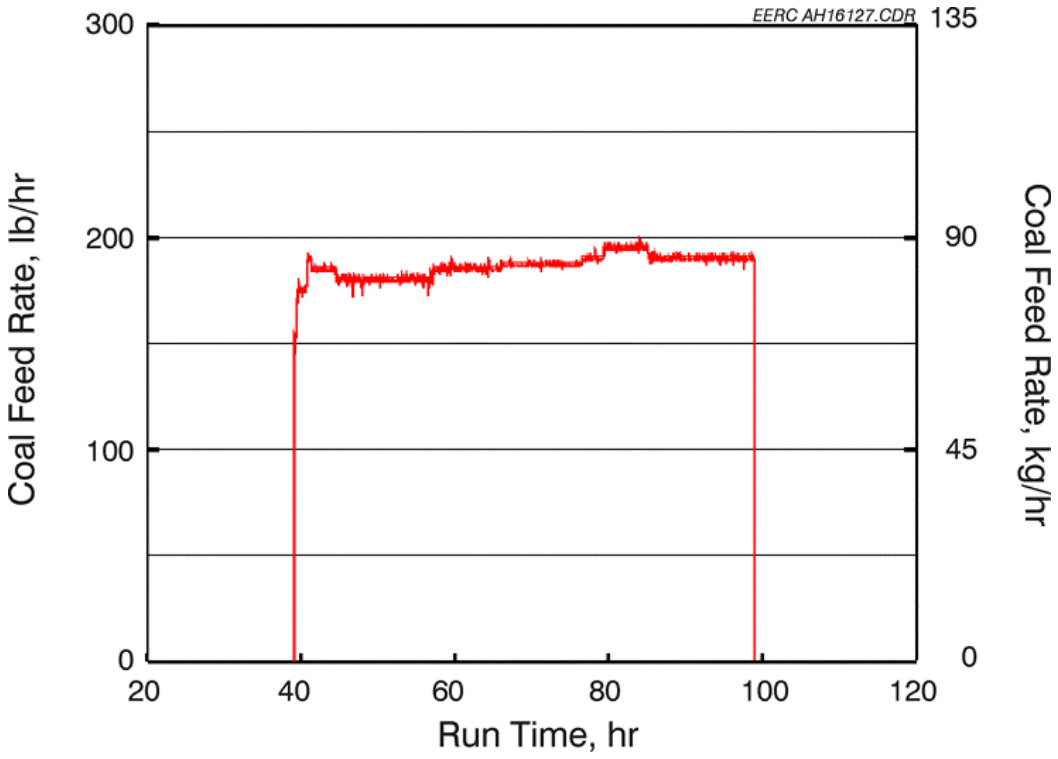

Exhibit 2.2-4
Coal Feed Rate Versus Run Time for the January 1999 Test

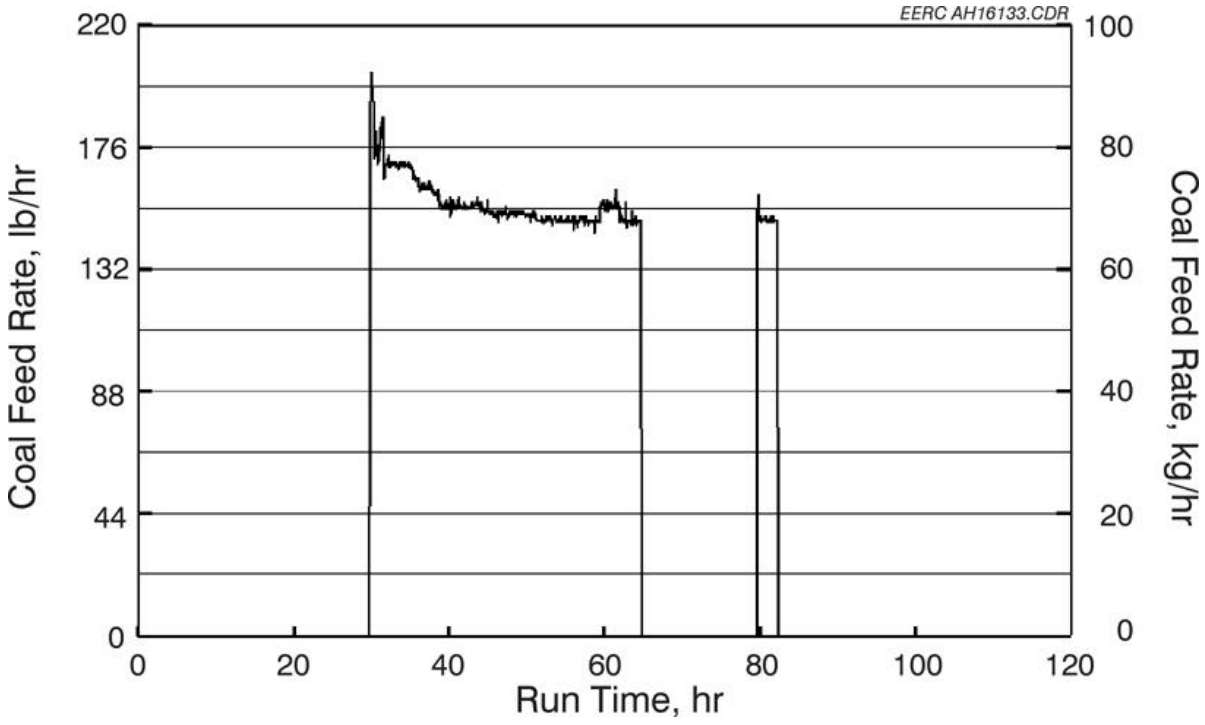

Exhibit 2.2-5
Coal Feed Rate Versus Run Time for the February 1999 Test

Exhibit 2.2-6
Results of Coal and Coal Ash Analysis for Coal-Fired Slagging Furnace Tests [1]

	Illinois No. 6 Bituminous Coal	Kentucky Bituminous Coal	Rochelle Subbituminous Coal
Proximate Analysis, wt%			
Moisture	4.8–10.3	2.5–2.6	21.6–24.3
Volatile Matter	35.9–38.8	38.7–39.6	35.6–37.4
Fixed Carbon	43.3–46.3	53.7–54.9	35.8–36.7
Ash	10.6–11.3	3.9–4.0	4.3–4.7
Ultimate Analysis, wt%			
Hydrogen	4.9–5.8	5.3–5.5	6.1–6.4
Carbon	61.6–64.9	77.6–78.2	53.0–55.2
Nitrogen	0.8–1.4	1.8	0.6–0.7
Sulfur	3.2–3.7	0.8–1.0	0.3–0.3
Oxygen	14.7–17.6	9.7–10.2	32.9–33.4
Ash	10.6–11.3	3.9–4.0	4.3–4.7
Heating Value, Btu/lb	11,036–11,658	14,120–14,173	9021–9328
Percent as Oxides, wt%			
SiO_2	52.0–53.9	37.7	26.7–27.1
Al_2O_3	20.6–21.2	28.8	15.5–16.3
Fe_2O_3	13.6–14.9	9.9	6.3–6.6
TiO_2	0.9	1.0	1.2–1.4
P_2O_5	0.1–0.2	0.1	0.7–0.9
CaO	3.0–3.5	10.1	21.6–24.3
MgO	1.5–2.0	2.1	6.7–6.9
Na_2O	1.1–1.4	1.4	1.5
K_2O	1.9–2.1	2.1	0.1–0.4
SO_3	2.5–2.7	6.7	15.6–17.0
Ash Fusion Temp., °F			
Initial	2315–2361	2358–2398	2202–2295
Softening	2342–2417	2377–2440	2205–2308
Hemisphere	2392–2448	2423–2474	2214–2311
Fluid	2491–2534	2451–2588	2221–2325
Sieve Analysis			
Screen Mesh Size		Weight Percent Retained	
100	1.8–6.2	11.4	7.6–8.8
140	0–11.2	12.9	14.2–15.4
170	0–14.9	NA[2]	NA
200	9.6–13.5	11.4	14.3–14.4
230	0–16.2	8.7	8.4–9.1
270	0.8–14.6	1.6	2.0–5.6
325	7.4–14.7	12.7	4.8–11.6
400	0–4.7	NA	NA
Pan	41.6–57.8	41.2	39.7–43.4
Total %	99–100.2	99.9	98.6–100.6

[1] Coal analysis is presented on an as-fired basis.

[2] Not available.

Exhibit 2.2-7
Results of Lignite and Lignite Ash Analysis for Lignite-Fired Slagging Furnace Tests [1]

Item / Lignite type	Coal Creek Station	Milton R. Young Station
Proximate Analysis, wt%		
Moisture	31.6–37.9	33.8–37.1
Volatile Matter	29.4–31.5	30.4–32.1
Fixed Carbon	26.4–26.8	26.9–27.9
Ash	6.3–10.2	5.6–6.2
Ultimate Analysis, wt%		
Hydrogen	6.4–6.8	7.0–7.2
Carbon	38.5–40.9	41.1–43.4
Nitrogen	0.6–0.6	0.6–0.6
Sulfur	0.5–0.7	0.7–0.9
Oxygen	41.1–47.3	42.1–44.9
Ash	6.3–10.2	5.6–6.2
Heating Value, Btu/lb	6300–6708	6933–7144
Percent as Oxides, wt%		
SiO_2	31.8–35.5	11.2
Al_2O_3	11.7–12.0	8.6
Fe_2O_3	6.4–8.0	13.2
TiO_2	0.5	0.2
P_2O_5	0.3	0.1
CaO	17.0–18.7	21.3
MgO	6.5–7.0	7.3
Na_2O	2.9–3.2	11.7
K_2O	1.3	0.2
SO_3	16.0–19.0	26.2
Ash Fusion Temp., °F		
Initial	2170–2188	2370–2371
Softening	2181–2196	2381–2384
Hemisphere	2189–2203	2384–2387
Fluid	2196–2219	2392–2428
Sieve Analysis		
Screen Mesh Size	Weight Percent Retained	
100	6.4–10.3	14.9
140	12.3–13.8	15.7
170	NA [2]	4.6
200	11.9–12.3	8.5
230	3.7–8.5	NA
270	6.2–10.2	3.1
325	6.4–6.5	14.9
400	NA	NA
Pan	41.5–48.2	38.2
Total %	98.3–99.9	99.9

[1] Lignite analysis is presented on an as-fired basis.

[2] Not available.

Slagging Furnace Operation

The slagging furnace heatup rate during the January and February test periods was limited to 100 F/hr (56 C/hr) while natural gas was fired. This is the heatup rate recommended for the LRAH panel by UTRC. To sinter anticorrosion coatings placed on the surface of the high-density refractory prior to the January test, the natural gas firing rate through the main burner was increased to 3.2 MMBtu/hr (3.3×10^6 kJ/hr) in an attempt to achieve a furnace temperature of 2950 F (1621 C). Although this natural gas firing rate was maintained for nearly 2 hours, furnace temperature near the wall never exceeded 2900 F (1594 C). Further increases in the main burner natural gas firing rate were not possible because of ID fan limitations. Subsequently, the main burner natural gas firing rate was reduced to 2.3 MMBtu/hr (2.4×10^6 kJ/hr) in order to reduce the furnace temperature to 2800 F (1538 C).

When the furnace reached normal operating temperature (2800 F/1538 C), the main burner was switched from natural gas to coal firing. The coal firing rate through the main burner in January was 2.1 to 2.25 MMBtu/hr (2.2 to 2.3×10^6 kJ/hr) with an auxiliary burner firing rate of 0.65 to 0.80 MMBtu/hr (0.7 to 0.9×10^6 kJ/hr). These firing conditions were maintained for 60 hours while personnel attempted to maintain a furnace flue gas temperature near the LRAH panel of 2800 F (1538 C). This temperature measurement was made using an optical pyrometer with secondary measurements using Type S thermocouples. Summary of furnace and slag screen temperatures are presented as a function of run time in Exhibits 2.2-8 and 2.2-9 for the January and February tests, respectively. Corresponding slagging furnace firing rate data are summarized in Exhibits 2.2-10 and 2.2-11.

During the week of January 24–29 , the furnace was fired on Illinois No. 6 bituminous coal and the main burner swirl setting was maintained at a minimum. No attempt was made to maximize and minimize the main and auxiliary burner firing rates, respectively, because of slag damming/flow problems in the slag screen. The total furnace-firing rate (main plus auxiliary burners) ranged from 2.9 to 3.0 MMBtu/hr (3.0 to 3.1×10^6 kJ/hr). The main burner-firing rate ranged from 2.1 to 2.25 MMBtu/hr (2.2 to 2.3×10^6 kJ/hr) accounting for 73% to 77% of the total energy input. The resulting flue gas temperature near the furnace wall/LRAH panel was 2775 to 2840 F (1524 to 1560 C).

Furnace refractory temperatures ranged from 1060 to 1300 F (571 to 705 C) for the hot side of the insulating refractory to as high as 2480 F (1360 C) for the cold side of the high-density refractory. Compared to previous test periods with the Illinois No. 6 coal, the insulating refractory temperatures are 15 to 100 F (8 to 56 C) lower, and high-density refractory temperatures are 160 F (89 C) lower. The lower insulating refractory temperatures are probably the result of the planned gap/air space between the high-density and intermediate refractory layers. However, there is no obvious explanation for the lower cold-side high-density refractory temperature. One possibility is poor temperature data because of aging thermocouples. All of the thermocouples measuring furnace refractory temperatures will be inspected and replaced where necessary.

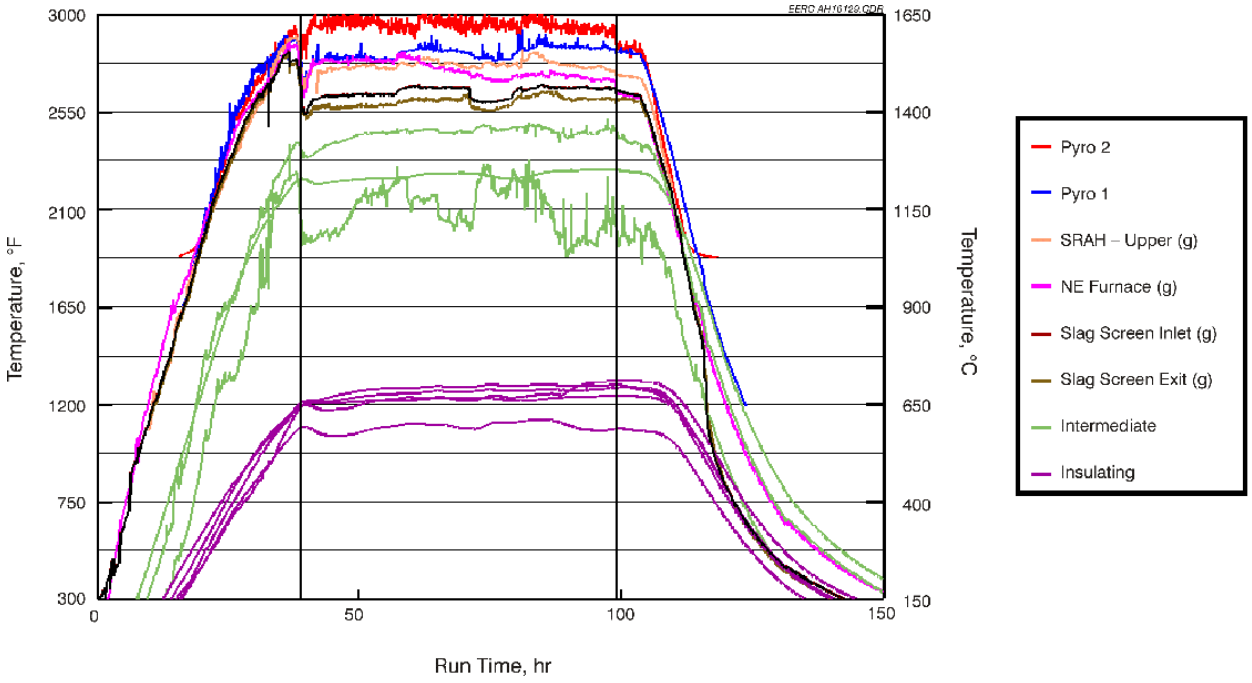

Exhibit 2.2-8
Furnace and Slag Screen Temperatures Versus Run Time for the January 1999 Test

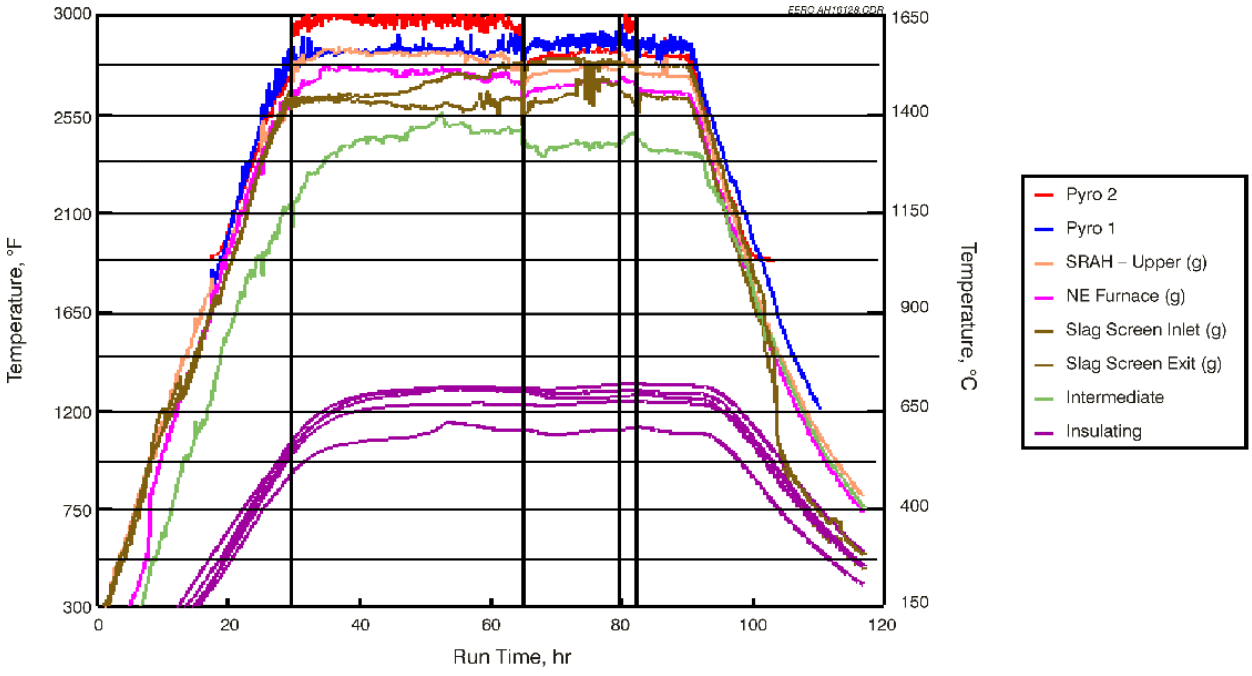

Exhibit 2.2-9
Furnace and Slag Screen Temperatures Versus Run Time for the February 1999 Test

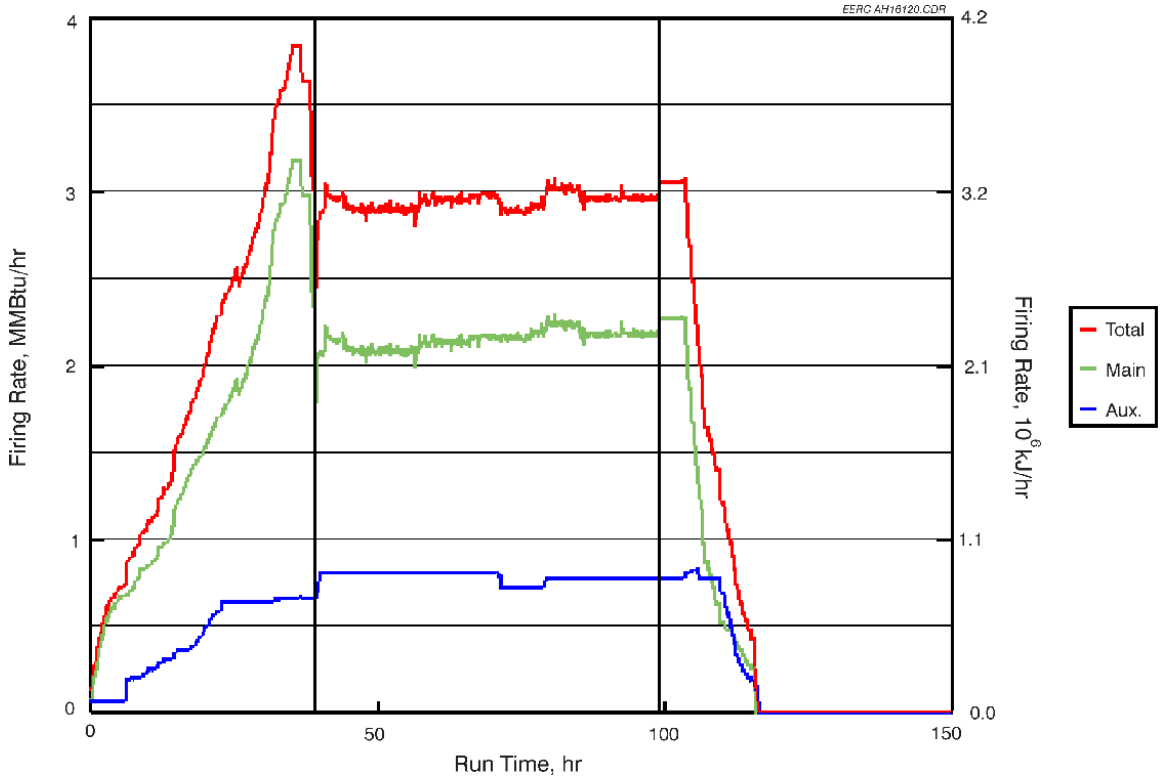

Exhibit 2.2-10
Slagging Furnace Firing Rate Versus Run Time for the January 1999 Test

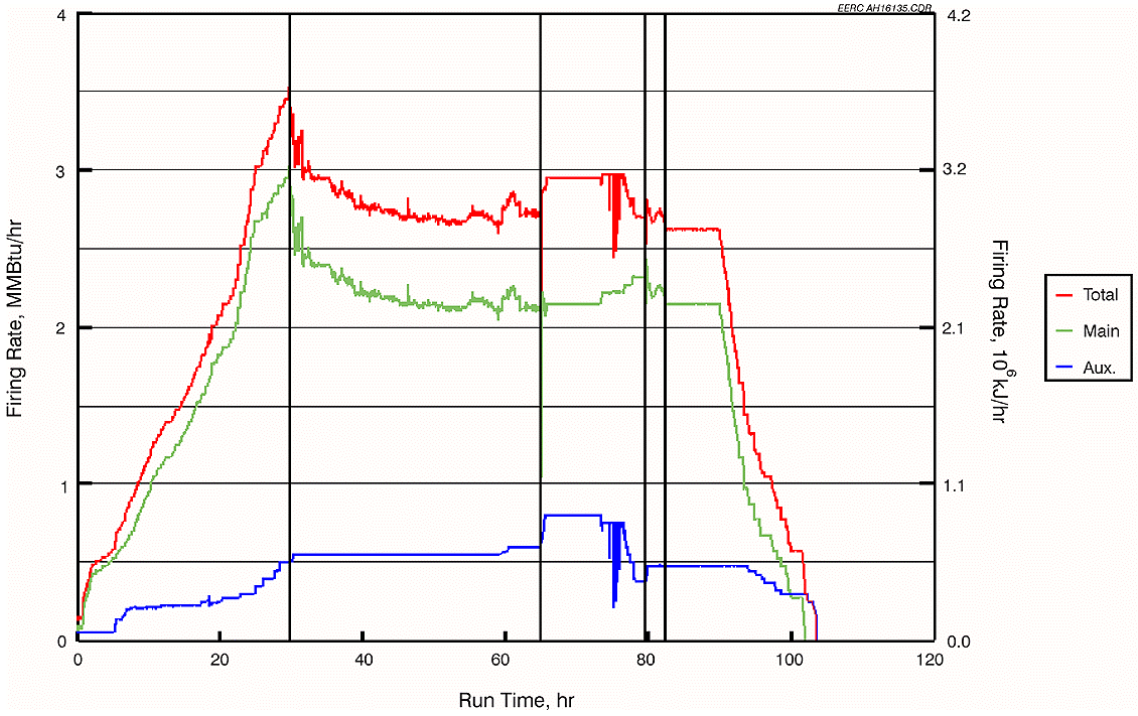

Exhibit 2.2-11
Slagging Furnace Firing Rate Versus Run Time for the February 1999 Test

During the January test, the slag tap never plugged and slag flow was not a problem. The refractory in the slag tap was replaced in the third quarter of 1998 in conjunction with the replacement of the high-density refractory furnace liner. As reported in the October through December 1998 quarterly technical progress report, the inner liner was poured in such a way that it would not bond to the middle refractory layer, and in approximately 2-ft-square sections to allow it to move independently during heatup and cooldown. This design was very successful in preventing the extensive cracking that was seen in the original furnace liner, so extensive patching was not required following the January test. Also, the slag tap was found to be in good condition and no repairs were required prior to the February test.

The main burner natural gas firing rate was nearly 3.0 MMBtu/hr (3.1×10^6 kJ/hr) during preheating of the furnace prior to switching to coal-firing during the February test. The coal firing rate through the main burner in February was 2.1 to 2.3 MMBtu/hr (2.2 to 2.4×10^6 kJ/hr) once the furnace refractory reached thermal equilibrium, with an auxiliary burner firing rate of 0.48 to 0.60 MMBtu/hr (0.6 to 0.7×10^6 kJ/hr). These firing conditions were maintained for 38 hours of coal firing while it was attempted to maintain a furnace flue gas temperature of 2800 F (1538 C) near the LRAH panel.

During the week of February 14–19, the furnace was fired on an eastern Kentucky bituminous coal and the main burner swirl setting was maintained at a minimum. A modest attempt was made to maximize and minimize the main and auxiliary burner firing rates, respectively, near the end of the week. However, because of plugging problems in the slag screen, the effort was limited. The total furnace firing rate (main plus auxiliary burners) ranged from 2.7 to 2.9 MMBtu/hr (2.8 to 3.0 $\times 10^6$ kJ/hr). This firing rate is similar to, but slightly lower than, that required when the Illinois No. 6 coal was fired in January. One reason for the difference in firing rates may have been the higher moisture content of the Illinois No. 6 coal (5.1 versus 2.5 wt%). The main burner firing rate ranged from 2.1 to 2.27 MMBtu/hr (2.2 to 2.3×10^6 kJ/hr) accounting for 78% to 82% of the total energy input. The resulting flue gas temperature near the furnace wall/LRAH panel was 2775° to 2830°F (1524° to 1555°C).

Furnace refractory temperatures ranged from 1080 to 1320 F (582 to 716 C) for the hot side of the insulating refractory to as high as 2490 F (1366 C) for the cold side of the high-density refractory. Compared to the January test with the Illinois No. 6 coal, the refractory temperatures are 10 to 20 F (6 to 11 C) higher. These slightly higher refractory temperatures may be the result of fuel moisture differences.

Following the February test, the high-density refractory lining the furnace was found to be in excellent condition without the cracking observed in the previous liner. Also, the slag tap never plugged and slag flow was not a problem during the test. The slag tap was found to be in good condition, and no repairs will be required prior to the upcoming April test.

Minor pressure surges (a few inches of W.C.) are not uncommon in the slagging furnace. They happen on a periodic basis as a result of baghouse cleaning, opening of access ports to clean the dilution/quench zone and CAH tube bank, opening of access ports to insert or remove sampling probes, and when flue gas flow distribution through the baghouse or cyclone is altered. However, pressure surges in the furnace did not cause any operating problems during the January or February tests.

Inspection of the furnace refractory after the January and February tests indicated that the new high-density refractory was in excellent condition. The only area showing any deterioration was below the LRAH panel where slag from the panel was dripping onto the horizontal surface below. However, no refractory repairs/replacement are expected to be necessary in the near future. In addition, the approach used to install the new high-density refractory has apparently eliminated the cracking observed immediately after the original high-density refractory was cured.

Main and Auxiliary Burners

The main and auxiliary burners performed well during the January and February tests. As previously stated, the main burner swirl was maintained at a minimum while the auxiliary burner swirl setting was nominally 80%. Carbon efficiency for both bituminous coals was 99.5% or greater because of the high furnace operating temperature. On the basis of slagging furnace operating experience, the EERC intends to continue minimum main burner swirl as necessary to establish a stable flame, to establish uniform temperatures over the length of the furnace, and to minimize NO_x emissions.

Slag Screen

Slag screen flue gas temperatures during the January test were typically 2585 to 2655 F (1419 to 1458 C) at the inlet and 2550 to 2600 F (1399 to 1427 C) at the outlet. Slag screen operating temperature is selected on the basis of ash fusion data for the fuel to be fired. The EERC tries to operate the slag screen at flue gas temperatures of 100 to 200 F (56 to 112 C) above the fluid temperature of the fuel ash to ensure slag flow from the slag screen to the slag tap. The ash fluid temperature (under oxidizing conditions) of the composite sample of Illinois No. 6 coal analyzed following the January test period was determined to be 2491 F (1366 C). A composite slag sample collected from the slag pot was found to have a fluid temperature of 2545 F (1396 C).

Exhibit 2.2-12 presents photographs of the slag screen inlet following the January (top) and February tests (bottom). In the top photograph erosion/corrosion of the slag screen tubes is evident along with some accumulation of slag on the floor of the slag screen in the vicinity of the third and fourth rows of tubes. Partial plugging of the slag screen did occur during the January test. However, once the slag began to flow into the dilution/quench zone, slag screen operation remained stable at an elevated differential pressure, 3 to 7 in. W.C. (6 to 14 mm Hg). Normally the slag screen differential pressure is 2 in. W.C. (4 mm Hg). Once coal feed was terminated, the slag screen differential pressure decreased over the 4-hour period of natural gas firing as slag slowly flowed to the slag tap. As a result, there was no need to complete extensive maintenance or repairs to the slag screen following the January test.

Exhibit 2.2-12
Photographs of Slag Screen Tubes Following the January (top) and February (bottom) Tests

The bottom photograph in Exhibit 2.2-12 shows that the first row of tubes experienced additional erosion/corrosion during the February test as well as significant slag buildup on the floor of the slag screen in the vicinity of the second, third, and fourth rows of tubes. As the degree of slag screen plugging developed, differential pressure eventually exceeded 8 in. W.C. (16 mm Hg), forcing a termination of the coal feed after 36 hours. After a number of hours of natural gas firing, the slag screen differential pressure decreased to 4.5 in. W.C. (9 mm Hg). The differential pressure reduction during this period of natural gas firing was the result of a reduction in the auxiliary burner firing rate and possibly in the slag flow from the slag screen to the slag tap. The auxiliary burner firing rate was reduced while a consistent temperature was maintained in the slag screen by increasing the main burner natural gas firing rate. However, after nearly 3 additional hours of coal feed, slag screen differential pressure again exceeded 8 in. W.C. (16 mm Hg) and termination of coal feed was again required.

The composition of the Kentucky coal ash as compared to the compositions of slag samples collected from the slag pot and slag screen are shown in Exhibits 2.2-13 and 2.2-14. The oxide values are reported on an oxide basis normalized to an SO_3-free basis, while the SO_3 numbers are reported on a basis normalized with the other oxides. The slag pot samples were collected from the bottom and top of the slag collected in the pot, and from the slag tap itself to determine if the composition of the slag dripping into the pot changed during the course of the test. This was done in order to explain why the slag initially flowed quickly into the pot from the slag screen, but later in the test it appeared to become more viscous, ultimately leading to the formation of the slag dam.

Exhibit 2.2-13
Slag Pot Samples

Oxides,[1] wt%	Kentucky Coal	Pot Bottom	Pot Top	Slag Tap
SiO_2	40.4	45.6	43.6	46.8
Al_2O_3	30.8	23.6	27.7	26.9
Fe_2O_3	10.6	16.4	17.4	17.9
TiO_2	1.1	1.0	0.9	0.9
P_2O_5	0.1	0.1	0.1	0.1
CaO	10.9	6.6	4.9	2.0
MgO	2.3	4.0	2.5	1.9
Na_2O	1.5	1.0	1.1	1.0
K_2O	2.3	1.7	1.9	2.6
SO_3[2]	6.7	0.1	0.1	0.1

[1] Oxide concentrations normalized to an SO_3-free basis.

[2] SO_3 concentrations normalized with other oxides.

Exhibit 2.2-14
Slag Screen Samples

Oxides,[1] wt%	Kentucky Coal	Screen Front	Screen Back	Quench Entrance
SiO_2	40.4	49.5	48.2	49.4
Al_2O_3	30.8	26.4	28.3	25.1
Fe_2O_3	10.6	15.6	13.9	11.1
TiO_2	1.1	1.0	1.1	0.9
P_2O_5	0.1	0.1	0.0	0.1
CaO	10.9	1.9	2.7	8.0
MgO	2.3	1.9	2.2	1.9
Na_2O	1.5	1.1	1.2	1.7
K_2O	2.3	2.6	2.3	1.9
SO_3[2]	6.7	0.1	0.1	0.1

[1] Oxide concentrations normalized to a SO_3-free basis.

[2] SO_3 concentrations normalized with other oxides.

The data show that all of the slag samples contained much less calcia, slightly less alumina, slightly more silica, and much more iron oxide than the original coal ash. Computer-controlled scanning electron microscope (CCSEM) analyses of the minerals in the coal indicate that the alumina and silica in the coal were concentrated in clay particles, with the larger clay particles being more enriched in silica compared to the smaller clay particles. The calcia in the coal was concentrated in larger limestone particles and the iron in larger pyrite particles. The reduced alumina content in the slag pot samples most likely occurred because the smaller, alumina-rich clay particles stayed entrained in the gas stream as it passed around the slag screen tubes rather than impacting the tubes. The alumina content in the slag did increase, however, as the run proceeded, possibly because the screen efficiency increased slightly, causing more of the smaller clay-derived particles to be captured. The lower calcia content in the slag samples as compared to the coal ash is most likely due to the limestone fragmenting on heating, forming small particles that also passed around the tubes. Note that the calcia content did not increase in the samples collected higher in the pot, indicating that any increase in capture efficiency later in the test was not enough to begin significant capture of limestone-derived particles. The enrichment in iron oxide in the slag is due to the high capture efficiency for the relatively large pyrite-derived ash particles.

The compositions of the residual slag held in dams in the slag screen itself are compared to that of the coal ash in Exhibit 2.2-14. As is true for the slag pot samples, the slag dams are depleted in alumina and calcia and enriched in silica and iron. However, the enrichment in silica is greater than and the iron less than the enrichments found in the slag pot samples. These changes would give the slag dam samples even higher viscosities than the slag pot samples. However, slag

flow patterns in the main furnace indicate that essentially all of the slag in the slag pot flowed from the slag screen. The fact that the higher-viscosity slag remained in the screen and the lower-viscosity slag flowed out into the pot may indicate that the slag is not a true solution but is instead a mixture.

Because of the large amount of residual slag left in the slag screen following the February test, the EERC elected to rebuild the screen prior to a test planned for April. To improve the performance of the slag screen when the Kentucky bituminous coal is fired, only three rows of tubes will be installed (1, 3, and 5). Eliminating three rows of tubes should accomplish three objectives:

1. reduce the heat loss in the slag screen,
2. reduce the collection efficiency of the slag screen, and
3. lessen the drag on the flow of the slag out of the screen.

Reducing the heat loss in the slag screen should result in a higher slag temperature and a lower slag viscosity, improving slag flow from the slag screen to the slag tap. Reducing the collection efficiency of the slag screen will permit smaller aluminum and silicon-rich clay-derived slag particles to escape to the dilution/quench zone and CAH section of the SFS.

Following the January test, slag and ash samples from system components and piping were collected and weighed in order to prepare a mass balance. A total theoretical ash quantity was calculated (2107 lb or 956 kg) on the basis of the total coal feed and the measured ash content of the composite coal sample. Total slag and ash recovery from the January test was only 48% (1019 lb or 463 kg). Slag recovery from the furnace, slag pot, and dilution/quench zone represented 42% of the theoretical ash. Additional slag is evident on the furnace wall, LRAH panel, in the bottom of the furnace, in the slag screen, and in the upper section of the dilution/quench zone. However, this material is not recoverable from the high-density refractory. The EERC estimates that this unrecoverable slag may represent as much as 30% to 40% of the theoretical ash. Collected material and these estimates indicate that over 75% of the coal ash was captured in the system as slag. The 48% closure on ash and slag for the January Illinois No. 6 test was lowest mass balance observed for the SFS to-date.

Fly ash recovered from other system components (drawdown gas line, CAH duct, cooling air preheater tubes, tube-and-shell heat exchangers, cyclone, baghouse, and flue gas piping) represented 6% of the theoretical ash for the January test. Nominally 10% to 15% of the ash in the fuels fired in the SFS has been reaching the baghouse. However, the baghouse ash recovered following the January test period represented <3% of the total ash/slag. While the bags were not removed from the baghouse and thoroughly cleaned following the January test, the residual dust cake on the bags is not likely to increase the baghouse ash to more than 7% of the total.

Following the February test, slag and ash samples were again collected from system components and piping and weighed in order to prepare a mass balance. A total theoretical ash quantity was calculated (230 lb or 104 kg) on the basis of the total coal feed and the measured ash content of the composite coal sample. Total slag and ash recovery from the February test was only 71% (163 lb or 74 kg). Slag recovery from the furnace, slag pot, and dilution/quench zone represented nominally 53% of the theoretical ash.

On the basis of previous experience and inspection following the February test, additional slag appears to have been adsorbed/absorbed into the furnace wall, collected in the slag screen, and collected in the upper section of the dilution/quench zone. However, this material is not recoverable from the high-density refractory. The EERC estimates that this unrecoverable slag may represent as much as 25% of the theoretical ash. The collected material measurements and these estimates both indicate that over 75% of the coal ash was captured in the system as slag. The 71% closure on ash and slag for the February Kentucky coal test is much better than the January Illinois No. 6 test. However, it is still lower than most of the closures observed for the SFS to date when a bituminous coal was fired.

Fly ash recovered from other system components (drawdown gas line, CAH duct, cooling air preheater tubes, tube-and-shell heat exchangers, cyclone, baghouse, and flue gas piping) represented 18% of the theoretical ash for the February test. For most SFS tests, 10% to 15% of the ash in the fuels fired in the SFS has been reaching the baghouse. Baghouse ash recovered following the February test period represented about 10% of the total ash/slag. Again, the bags were not removed from the baghouse and thoroughly cleaned following the February test. However, the residual dust cake on the bags would likely be comparable to that present following the January test. Therefore, recovery of the ash from the bags would not be an appropriate contribution to the February mass balance.

The EERC believes that the primary factors contributing to the poor material balances observed this past quarter were slag adsorption/absorption into the new high-density furnace refractory, slag screen plugging, and unrecovered ash from refractory surfaces and the surfaces of the new bags in the baghouse. Mass balances will be completed for all future test periods to further document the distribution of slag and ash in the system.

Dilution/Quench Zone

During the January test, slag deposits formed in the vicinity of the FGR nozzles. Because of the slag flow from the slag screen into the dilution/quench zone, it was necessary to clean slag deposits from the area of the FGR nozzles on a periodic basis. However, as a result of modifications made to the nozzle spool piece (the addition of a water-cooled wall), the slag deposits were more efficiently removed. As a result, cleaning frequency was somewhat variable, about every 2–4 hours. About 10% of the ash/slag recovered from the SFS was recovered in the dilution/quench zone. This quantity of material is comparable to that from previous tests.

During the February test, slag deposits formed in the vicinity of the FGR nozzles. However, the deposition was minimal and no cleaning was required during the 38 hours of coal firing. This result was most likely due to the high collection efficiency of the slag screen and the low ash content and high heating value of the Kentucky bituminous coal. The amount of slag entering the dilution/quench zone was illustrated by the fact that only 8% of the ash/slag recovered from the SFS was recovered in the dilution/quench zone.

Material recovered from the dilution/quench zone during previous tests was typically <13%. Downstream of the FGR nozzles, the small quantity of ash observed on the refractory walls was weakly sintered for both the January and February tests.

Cooling Air Preheaters

During the January and February tests, the cooling air for the CAH tube bank and the LRAH panel was heated using air preheater tube bundles located downstream of the CAH. Further heating of the cooling air entering the LRAH panel was achieved electrically and by recovering heat from the CAH tube bank. Cooling air for the CAH tube bank is supplied by the first cooling air preheater tube bundle. During the January test, cooling air entering the CAH tube bank was controlled at set points ranging from 1100 to 1130 F (594 to 610 C) for nominal cooling air flow rates of 92 to 123 scfm (2.6 to 3.5 m^3/min). Cooling air temperatures at the exits of the other four preheater tube bundles were nominally 1230 to 1320 F (666 to 716 C) for flow rates totaling 100 to 150 scfm (2.8 to 4.2 m^3/min).

During the February test, cooling air entering the CAH tube bank was controlled at set points ranging from 1000 to 1025 F (538 to 552 C) for nominal cooling air flow rates of 103 to 123 scfm (2.9 to 3.5 m^3/min). Cooling air temperatures at the exits of the other four preheater tube bundles were nominally 1230 to 1320 F (666 to 716 C) for flow rates totaling 100 to 150 scfm (2.8 to 4.2 m^3/min).

Cooling air preheater temperatures are shown as a function of run time in Exhibits 2.2-15 and 2.2-16. Although the cooling air preheater heat-transfer rate degraded with time as ash deposits developed on the tube surfaces, cooling air temperature and flow rate control were adequate to support operation of the CAH tube bank and LRAH panel.

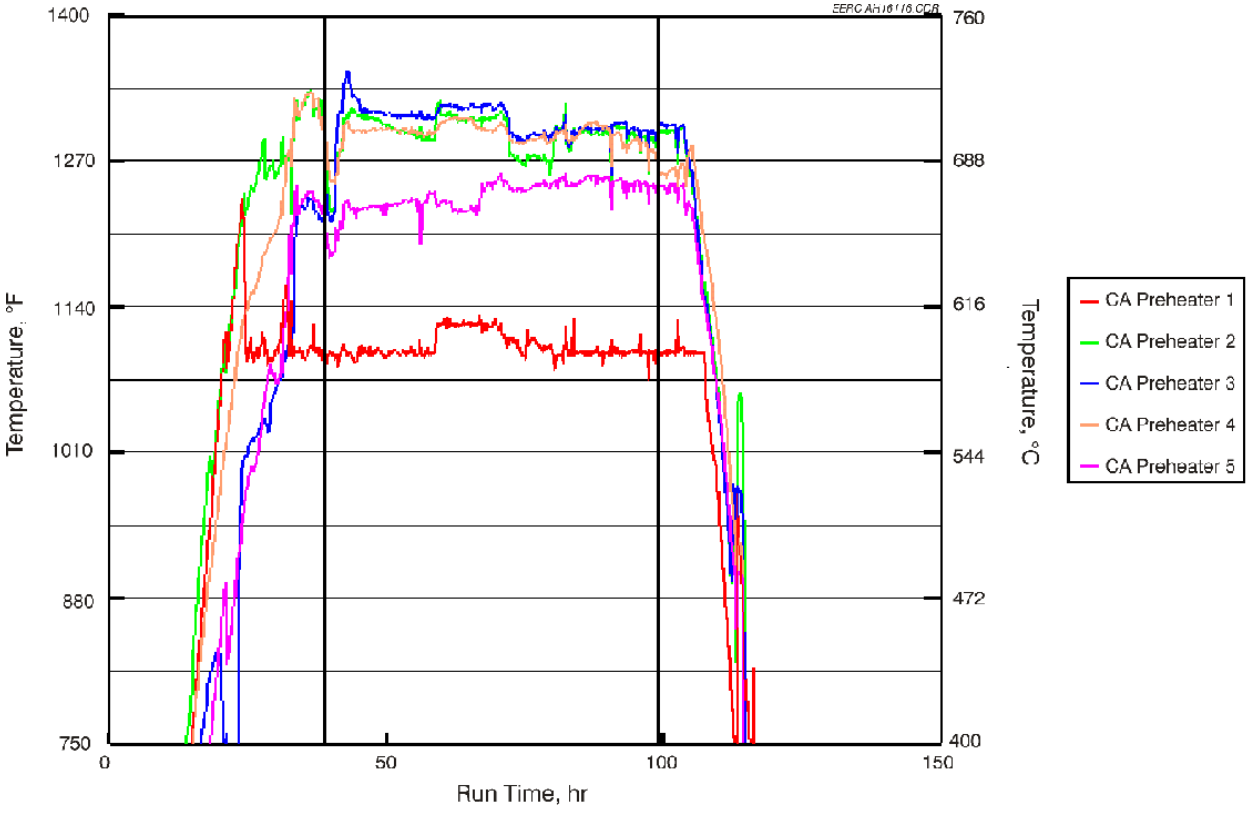

Exhibit 2.2-15
Cooling Air Preheater Temperatures Versus Run Time for the January Test

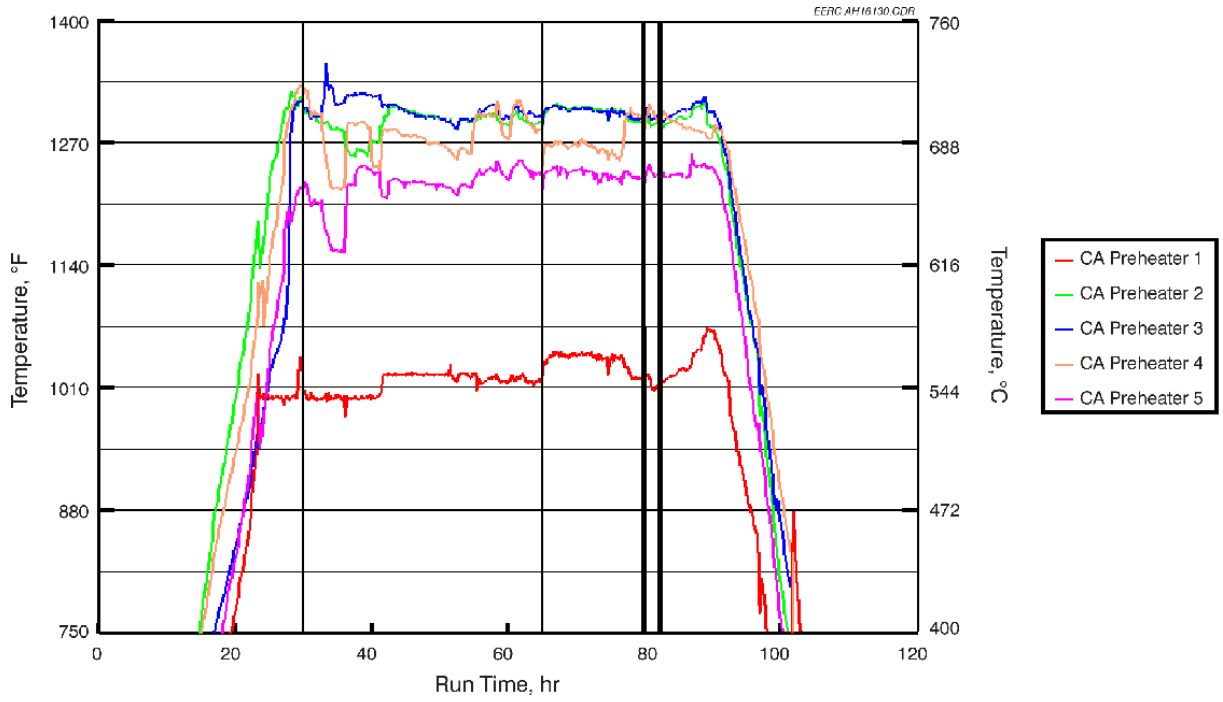

Exhibit 2.2-16
Cooling Air Preheater Temperatures Versus Run Time for the February Test

Emission Control

During gas- and coal-fired furnace operation in January and February, baghouse temperatures and temperature profiles were nominal and the electrical heaters worked well, limiting the potential for condensation on start-up and shutdown. Baghouse temperature ranged from 330 to 350 F (166 to 177 C) in January and 330 to 340 F (166 to 171 C) in February. Flue gas flow rates were 946 to 1046 scfm (26.8 to 29.6 m^3/min) and 884 to 961 scfm (2.8 to 4.2 m^3/min), respectively, in January and February. Actual flue gas flow rates through the baghouse were 1492 to 1692 acfm (42.2 to 47.9 m^3/min) and 1401 to 1535 acfm (39.7 to 43.5 m^3/min), respectively.

The 36 bags (total filtration area of 565 ft^2 [52.5 m^2]) used in the baghouse this past quarter were a 22-oz/yd^2 (747 g/m^2) woven glass with a PTFE membrane. The filter face velocities when the Illinois No. 6 and Kentucky bituminous coals were fired were 2.6 to 3.0 ft/min (0.80 to 0.91 m/min) and 2.5 to 2.7 ft/min (0.76 to 0.83 m/min), respectively. These filter face velocities are low compared to conventional pulse-jet filtration systems typically operating at or near 4 ft/min (1.2 m/min). However, a detailed evaluation of baghouse performance has not been a specific objective within the scope of work to date.

Measured inlet and outlet particulate mass loadings were nominally 0.1003 gr/scf (229.7 mg/Nm^3) and 0.0004 gr/scf (0.8015 mg/Nm^3), respectively, resulting in a particulate collection efficiency of roughly 99.6% when the Illinois No. 6 bituminous coal was fired in January. The measured inlet particulate loadings are roughly 50% lower than what was measured previously when the Illinois No. 6 bituminous coal was fired. One possible explanation for the reduced mass loading at the baghouse inlet is the change in slag screen operating conditions - higher flue gas velocity and differential pressure (the result of the slag damming observed) - which may have

increased the slag screen particulate collection efficiency. Particulate-sampling data from a future Illinois No. 6 coal-fired test should assist in determining the cause of the reduced baghouse inlet mass loading observed during the last two Illinois No. 6 coal-fired tests (August 1998 and January 1999). Calculated particulate emissions from the pulse-jet baghouse were 0.0014 lb/MMBtu. This is a lower emission rate compared to other tests with Illinois No. 6 bituminous coal (0.0024 to 0.0030 lb/MMBtu). This result is probably best explained by the performance of the new bags with respect to effective on-line cleaning and control of differential pressure.

Measured inlet and outlet particulate mass loadings were nominally 0.0428 gr/scf (98.02 mg/Nm^3) and 0.0043 gr/scf (9.8475 mg/Nm^3), respectively, resulting in a particulate collection efficiency of roughly 90% when the Kentucky bituminous coal was fired in February. These inlet particulate loadings are a factor of 2 to 5 lower than what was measured previously when the Illinois No. 6 bituminous coal was fired. One contributing factor is the smaller theoretical quantity of ash entering the SFS with the Kentucky fuel for a given firing rate, about 30% of that for the Illinois No. 6 fuel. Calculated particulate emissions from the pulse-jet baghouse were 0.0156 lb/MMBtu. This is an order-of-magnitude increase in particulate emissions compared to the January test and a significantly higher emission rate compared to tests with other coals and lignites (0.0004 to 0.0074 lb/MMBtu). Inspection of the outlet filters resulting from February sampling efforts revealed the presence of ash agglomerates in the center of both filters and no indication of a dust cake. Therefore, the EERC believes that the outlet filters in February were affected by some degree of acid condensation or ash scale/agglomerates dislodging from the surface of flue gas piping downstream from the pulse-jet baghouse.

In addition to the standard EPA Method 5 sampling completed in January and February, respirable mass emissions (defined below) were measured at the outlet of the pulse-jet baghouse using a TSI Inc. aerodynamic particle sizer (APS-33). This real-time measurement method measures particle mass in the range of 0.5 to 15 μm. The primary advantages of this system are the high spatial resolution and the short sampling time. In the APS-33, particle-laden air is passed through a thin-walled orifice, with the particles lagging behind the gas because of their higher inertia. The velocity lag is related to the aerodynamic diameter of the particles, allowing the determination of the aerodynamic dynamic diameter of a particle by measuring the velocity of a particle as it exits from the orifice. To measure the particle velocity, the APS-33 employs a laser beam split into two beams and refocused onto two rectangular planes a set distance apart in front of the orifice. The light scattered by a particle passing through these beams is collected and focused onto a photomultiplier tube, which emits two pulses separated by the time taken for the particle to cross the distance between the two planes. This time interval is measured electronically and used to calculate the particle's aerodynamic diameter.

Respirable mass is a calculated value defined by the American Council of Governmental and Industrial Hygienists for particles in the size range of 2 to <10 μm based on aerodynamic diameter. Exhibit 2.2-17 presents the respirable mass emissions data for the January (top) and February test (bottom). The data are presented on a mg/m^3 basis versus sampling time. For the Illinois No. 6 coal-fired test in January, the average respirable mass emission rate integrated over 4 hours was 0.0025 mg/m^3 versus 0.0004 mg/m^3 for a 2-hour period during the Kentucky coal-fired test in February. For the Illinois No. 6 coal-fired test, individual measurements ranged from 0.0006 to 0.004 mg/m^3. In February when the Kentucky coal was fired, individual measurements

ranged from 0.0001 to 0.0015 mg/m^3. These data support the probable contamination of the EPA Method 5 outlet filters resulting from sampling in February.

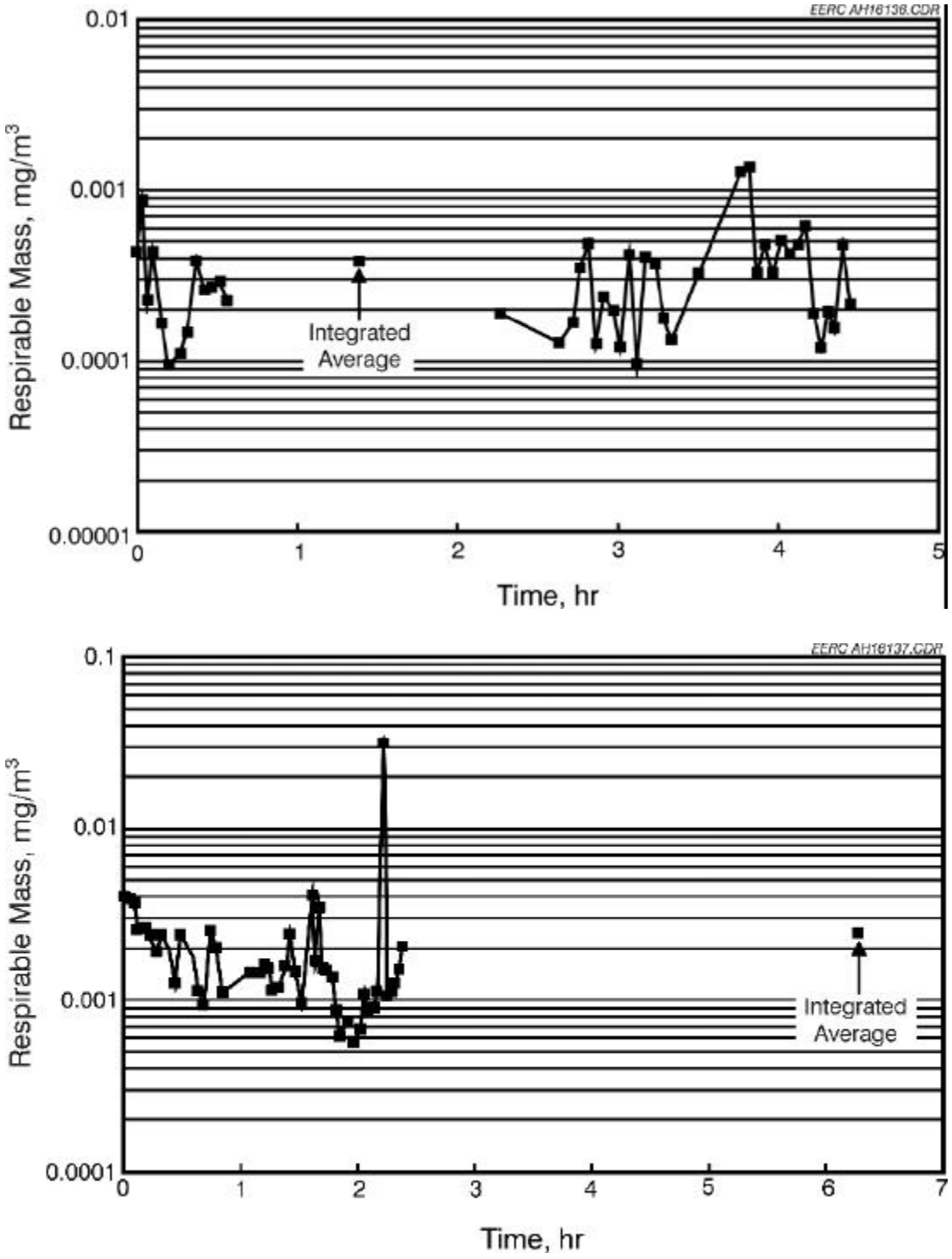

Exhibit 2.2-17
Respirable Mass Emission Data for the January (top) and February (bottom) Tests

The clean air plenum was removed from the pulse-jet baghouse following each test. One bag was pulled for inspection following the January test, with multiple bags pulled for inspection following the test in February. Inspection of multiple bags following the February test was deemed necessary because of the higher particulate emissions measured at the outlet of the baghouse as a result of EPA Method 5 sampling. In both cases, the tube sheet appeared to be very clean, consistent with the low level of particulate emissions generally measured, and the bags pulled for inspection were found to be in good condition. As a result, the bags were not pulled for cleaning after either the January or February tests.

To address the ash scale/ agglomeration question raised as a result of the February EPA Method 5 sampling at the baghouse outlet, the EERC removed, inspected, and cleaned the flue gas piping downstream of the baghouse. Some scale-type residue was found in the piping. The residue appeared to be the result of a combination of fine ash particles and acid condensation. The acid condensation most likely occurred during the January test firing the Illinois No. 6 coal, which had a substantially higher sulfur content. Sulfur trioxide measurements will be made during future tests to better document the potential for acid condensation.

Particle size analysis was completed for a composite ash sample collected from the baghouse hopper for both tests this past quarter. The data show the ash to be 100 wt% <15 μm, 80 wt% <6 μm, and 50 wt% <3 μm for the Illinois No. 6 coal. However, multicyclone sampling data indicated a larger particle size with only 30 wt% <7 μm.. For the Kentucky coal, the baghouse ash data show the ash to be 100 wt% <10 μm, 80 wt% <5 μm, and 50 wt% <3 μm. In this case, multicyclone data indicated a comparable particle size, 50 wt% <4 μm.

Analysis of the baghouse ash was also completed for carbon content as measure of combustion efficiency. The carbon content of the baghouse ash was found to be 0.50 wt% for the Illinois No. 6 coal and 0.24 wt% for the Kentucky coal, indicating a high combustion efficiency consistent with the high operating temperature of the slagging furnace.

Pulse cleaning of the bags was accomplished on-line using a reservoir pulse-air pressure of nominally 40 psig (2.8 bar) for both fuels. The baghouse differential pressure cleaning set point was 6 in. W.C. (11 mm Hg). Once the initial dust cake was formed, cleaning frequency was every 3 to 4 hours and the bags consistently cleaned down to a differential pressure of <2 in. W.C. (<4 mmHg).

Exhibit 2.2-18 shows the average gaseous emissions measured during the January and February tests. The data are based on furnace exit measurements made in the slag screen outlet. The carbon monoxide (CO) concentration of 40 ppm is a direct result of firing the main burner at a low swirl setting resulting in incomplete combustion at the sample point in the slag screen. However, no CO is observed at the baghouse outlet sampling location, indicating that the CO is oxidized in the dilution/quench zone and CAH section. Typical CO concentrations measured in the slag screen were <10 ppm in January and 0 to 40 ppm in February. These CO concentrations are consistent with previous low-swirl burner operating experience when bituminous coal was fired.

Exhibit 2.2-18
Flue Gas Emissions for Illinois No. 6 and Kentucky Coal-Fired Slagging Furnace Tests

	Concentration	lb/MMBtu
January		
O_2	3.5%–5.0%	
CO_2	12.9%–13.4%	
CO	<10 ppm	
NO_x	400–600 ppm	0.9–1.4
SO_2	1800–2800 ppm	6.0–6.5
February		
O_2	3.5%–4.7%	
CO_2	12.7%–13.9%	
CO	0–40 ppm	
NO_x	580–725 ppm	1.3–1.5
SO_2	630–850 ppm	1.0–1.4

Total NO_x emissions (reported as nitrogen dioxide) were determined to range from 0.92 to 1.34 lb/MMBtu. NO_x emissions were higher during individual test periods, represented by higher average coal feed rates. The auxiliary burner firing condition is also believed to have affected the NO_x concentrations and emissions; however, no specific tests have been conducted to document the effect of the auxiliary burner on NO_x emissions.

No attempt at controlling sulfur emissions was made. Calculated maximum theoretical sulfur dioxide emissions were 13.5 to 14.6 lb/hr or 6.5 lb/MMBtu for the Illinois No. 6 coal in January and 3.1 to 3.8 lb/hr or 1.5 lb/MMBtu for the Kentucky coal in February. These rates are based on the main burner firing rate and the sulfur content and heating value of the fuel.

Testing of the CAH Tube Bank Tests

The CAH tube bank was installed and initially evaluated during a shakedown test completed in October 1997. Cooling air flow was adequate for temperature control and to evaluate the performance of the CAH tube bank during the January and February tests. Exhibits 2.2-19 through 2.2-21 summarize CAH tube bank surface and flue gas temperatures, cooling air temperatures, and cooling air flow rate data for the January test. Exhibit 2.2-22 illustrates the location of thermocouples in the CAH tube bank, and Exhibit 2.2-23 presents a list of thermocouple descriptions.

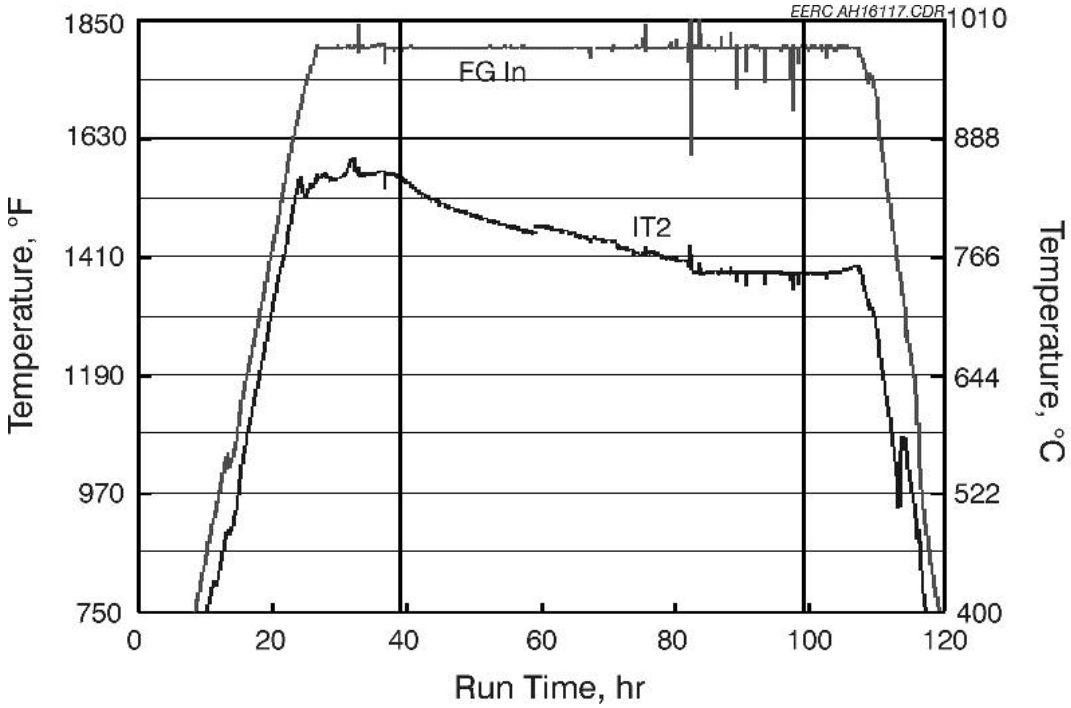

Exhibit 2.2-19
CAH Tube Surface and Flue Gas Temperatures Versus Run Time for the January Test

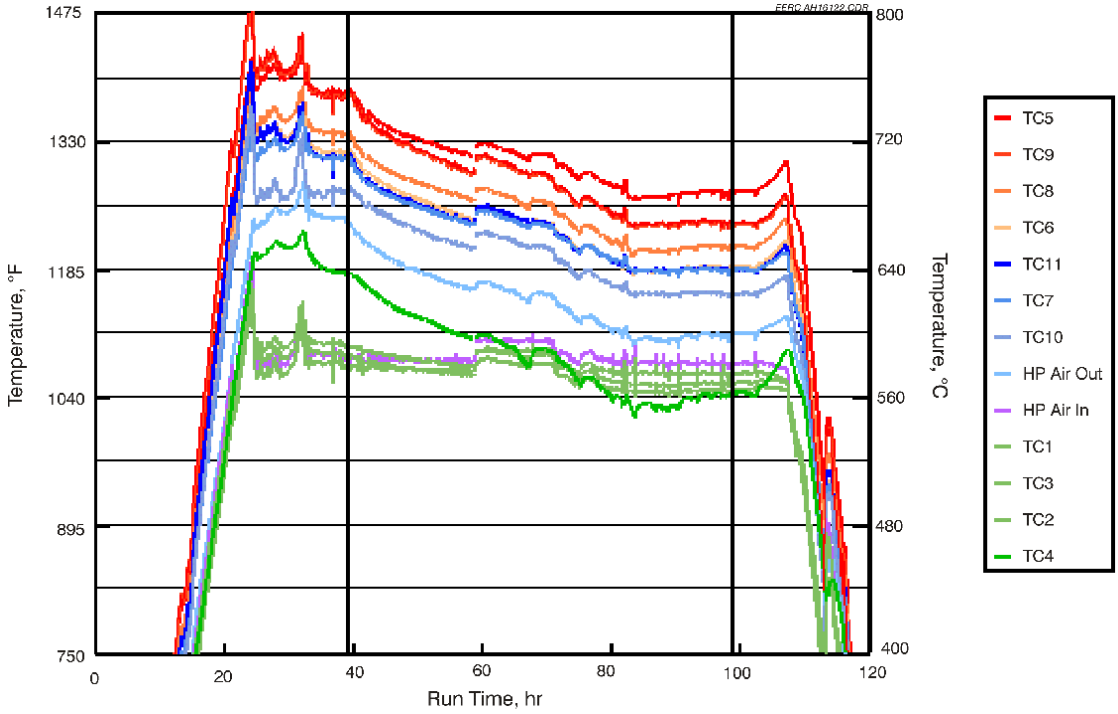

Exhibit 2.2-20
CAH Cooling Air Temperatures Versus Run Time for the January Test

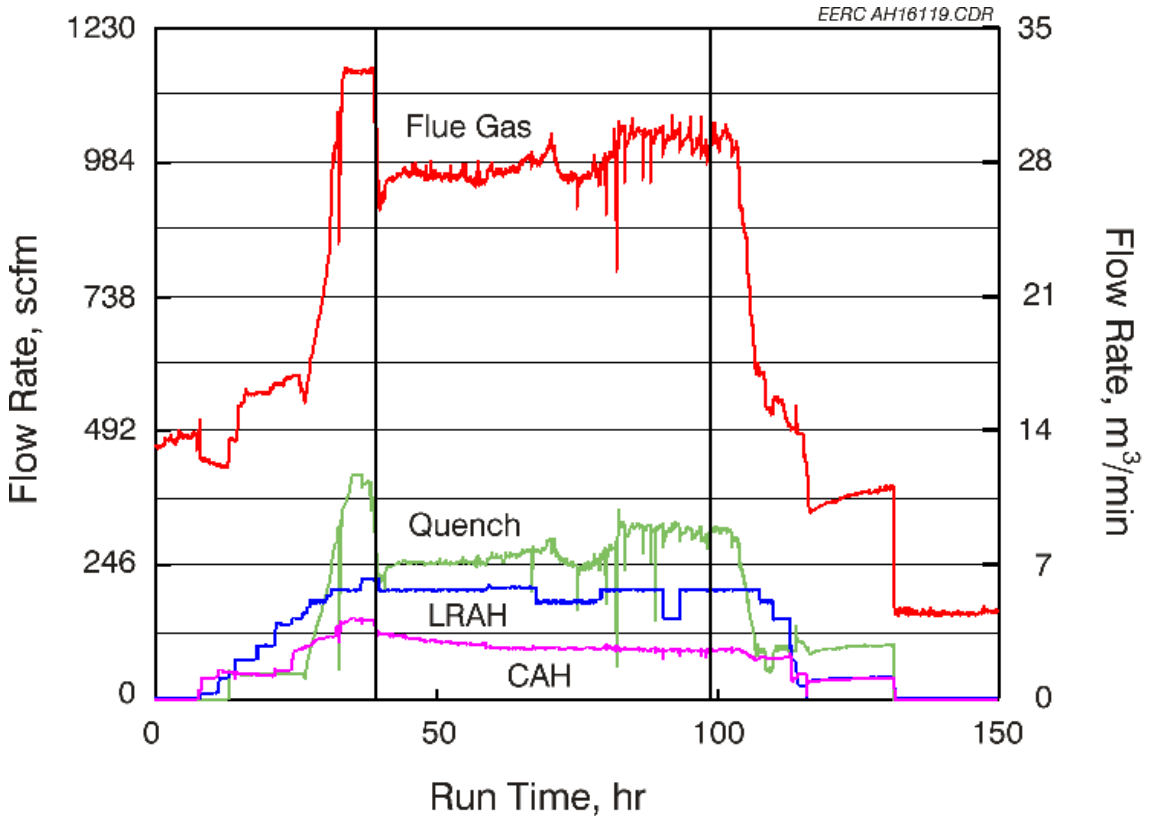

Exhibit 2.2-21
CAH Cooling, Air, LRAH Cooling Air, Quench Gas, and Flue Gas Flow Rates Versus Run Time for the January Test

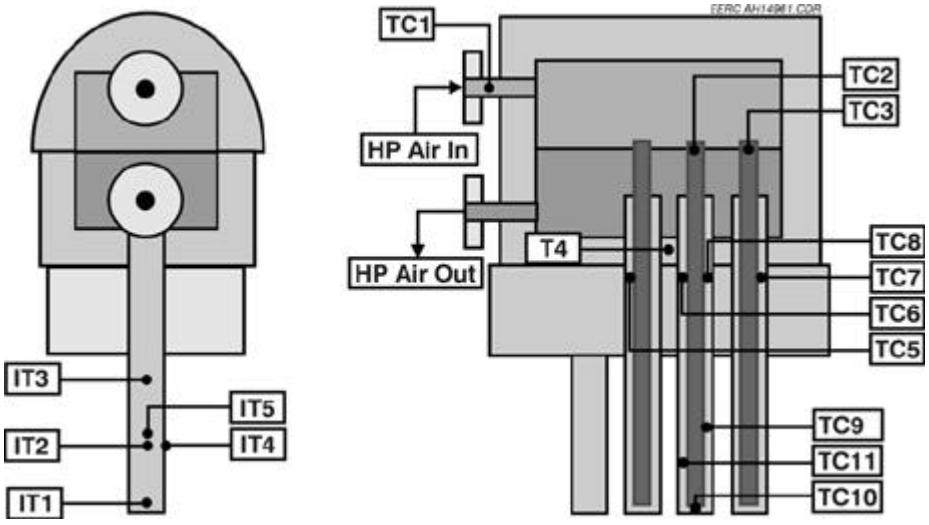

Exhibit 2.2-22
Thermocouple Locations in the CAH Tube Bank

Exhibit 2.2-23
Description of CAH Thermocouple Locations [1]

Category	No.	Label	Description
Air Inlet	1	CAHTC1	Bulk flow entering the inlet header
	2	CAHTC2	Air entering center tube
	3	CAHTC3	Air entering most downstream tube
Air Outlet	4	CAHTC6	Air leaving center tube
	5	CAHTC7	Air leaving most downstream tube
	6	CAHTC5	Air leaving most upstream tube
	7	CAHTC8	Air leaving side tube
Air in Active Region	8	CAHTC10	Bottom of center tube
	9	CAHTC11	4 in. up outside annulus, center tube
	10	CAHTC9	8 in. up outside annulus, center tube
Tube Surface	11	CAHIT1	1 in. up center tube, facing upstream (failed)
	12	CAHIT2	5 in. up center tube, facing upstream
	13	CAHIT3	8 in. up center tube, facing upstream (failed)
	14	CAHIT4	5 in. up center tube, facing to side (failed)
	15	CAHIT5	5 in. up center tube, facing downstream (failed)
Header Shell	16	CAHTC4	Next to shell on outside, between return air pipes (failed)

[1] Thermocouple locations are illustrated in Exhibit 2.2-22.

Prior to the August 1998 test, all of the CAH thermocouples were replaced or repaired in conjunction with the installation of fins on the air-cooled tubes. However, one tube surface thermocouple (CAHIT3) was damaged when the tube bank was installed in the flue gas duct. One additional CAH thermocouple failed during both the August and December 1998 tests, and a fourth thermocouple failed at the beginning of the January test. Therefore, during the January and February tests, one of the five surface thermocouples was functioning properly. There are no plans to replace these thermocouples at this time because of the time and expense that would be required.

While natural gas was fired and the tubes were clean, heat recovery from the CAH tube bank was roughly 44,000 Btu/hr (46,420 kJ/hr). The cooling air flow rate was 138 scfm (3.9 m^3/min). The inlet cooling air was 1080 F (582 C), outlet cooling air was 1240 (671), and flue gas was 1800 (982) entering the CAH tube bank. Exhibit 2.2-24 presents heat recovery in the CAH as a function of run time for the January test.

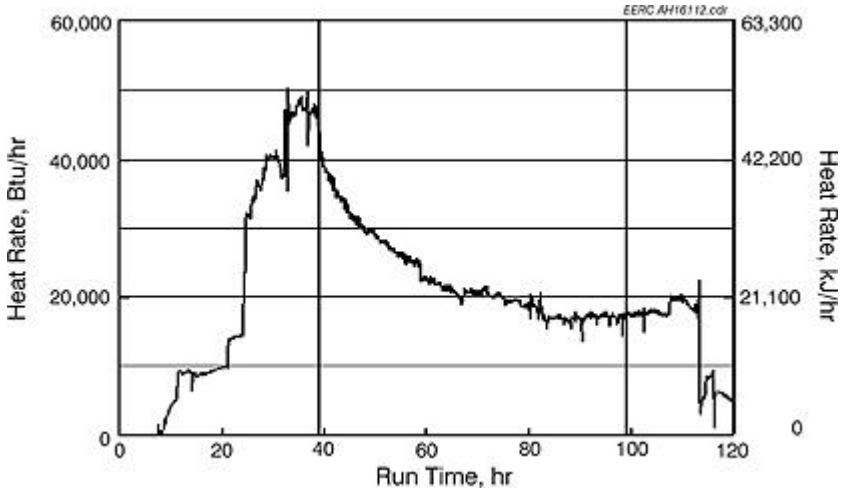

Exhibit 2.2-24
CAH Heat Recovery Versus Run Time for the January Test

When coal firing (Illinois No. 6) began, surface temperatures initially decreased at a rate of nominally 5 F/hr (3 C/hr) over nearly 20 hours as ash deposits developed on the surface of the tubes. After nearly 40 hours of coal firing, there was no further decrease in tube surface temperature. It must be noted that cooling air flow rates were also decreasing (0.01 scfm/0.0003 m^3/min) over these time frames in an attempt to maintain a relatively constant cooling air exit temperature. The minimum cooling air flow rate through the CAH tube bank was 92 scfm (2.6 m^3/min). As ash deposits developed on the tube surfaces, heat recovery from the CAH tube bank decreased from roughly 44,060 Btu/hr (46,483 kJ/hr) to 17,625 Btu/hr (18,594 kJ/hr). Heat recovery from the CAH tube bank remained at this level for nearly 17 hours of coal firing prior to the termination of the coal feed. These data are consistent with the August 1998 data observed when Illinois No. 6 coal was fired.

On the basis of these data, it appears that the addition of the fins to the air-cooled tubes improved heat recovery during the coal-fired test period. The fins appear to have reduced the rate of heat transfer degradation as ash deposits developed and helped to maintain a higher heat-transfer rate once the deposits had formed. However, no improvement in heat recovery was observed during the initial natural gas-fired period with clean tube surfaces compared to previous test periods.

EERC personnel did not clean the CAH tube bank during the January test in order to facilitate the development of ash deposits for characterization. CAH tube bank plugging was not a problem. No deposits were observed bridging the flue gas paths between the tubes. The deposits that formed were limited to the leading and trailing edges of the tubes. However, these deposits did bridge the area between the tubes in the direction of the flue gas flow.

Exhibit 2.2-25 presents a photograph of ash deposits on the surface of the tubes following the January test. The photograph shows three of the five uncooled tubes as well as two of the seven air-cooled finned tubes. The leading- and trailing-edge deposits are readily visible, with bare metal surfaces visible on the back half of the uncooled tubes. The pieces of tube deposit missing from the photograph of the air-cooled tubes fell off as the tube bank was removed from the duct.

Exhibit 2.2-25
Photograph of Ash Deposits on the CAH Tubes Following the January Test Firing Illinois No. 6 Bituminous Coal

Deposit strength is a function of ash chemistry, particle size, and temperature history. The relative strength of the deposits was indicated by the fact that the deposits generally remained intact when the CAH tube bank was removed from the duct. Also, the deposits were generally removed intact from the tube surfaces. The total weight of the deposits collected from the CAH tubes and duct was 14 lb (6.4 kg). The total weight of the deposits collected from the CAH tubes was 4 lb (1.8 kg). On a mass per unit time basis, the ash deposition rate for this Illinois No. 6 coal-fired test would be 0.07 lb/hr (30.3 g/hr) of coal firing. Incorporating the surface area of the tube bank (6.28 ft^2 or 0.58 m^2) results in a value of 0.01 lb/hr-ft^2 (52.2 g/hr-m^2). On a coal-firing-rate basis, the CAH ash deposition rate would be 0.03 lb/MMBtu (13.3 g/10^6 kJ). These calculated values are comparable to previous Illinois No. 6 tests.

Exhibits 2.2-26 through 2.2-28 summarize CAH tube bank surface and flue gas temperatures, cooling air temperatures, and cooling air flow rate data for the February test. While natural gas was fired and the tubes were clean, heat recovery from the CAH tube bank was roughly 44,474 Btu/hr (46,921 kJ/hr). The cooling air flow rate was 127 scfm (3.6 m^3/min). The inlet cooling air was 1010 F (544 C), outlet cooling air was 1195 F (646 C), and flue gas was 1800 F (982 C) entering the CAH tube bank. Exhibit 2.2-29 presents heat recovery in the CAH as a function of run time for the February test.

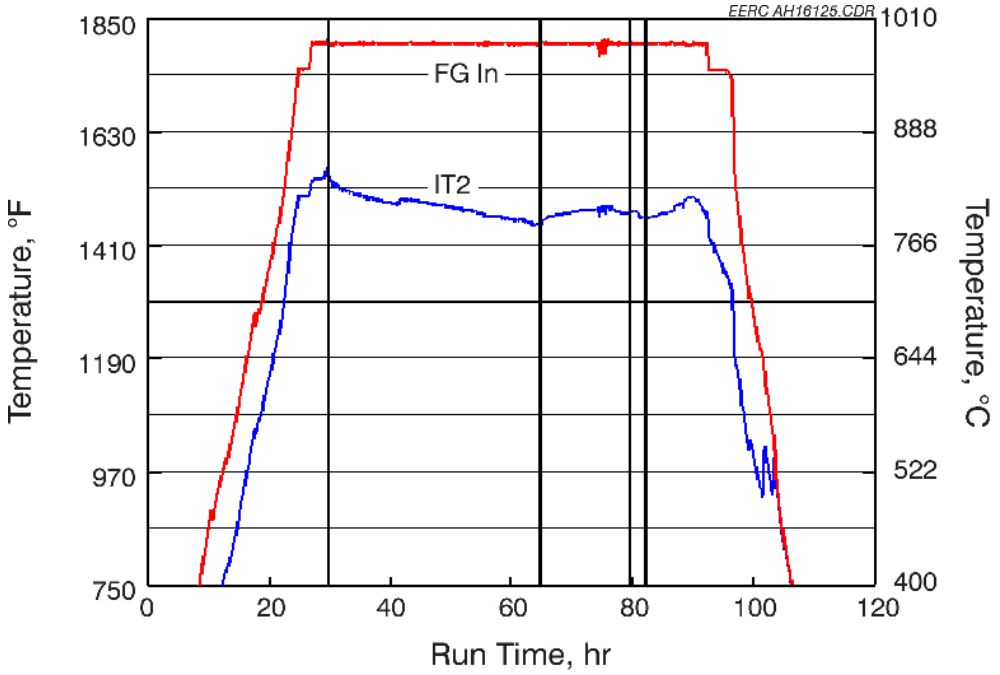

Exhibit 2.2-26
CAH Tube Surface and Flue Gas Temperatures Versus Run Time for the February Test

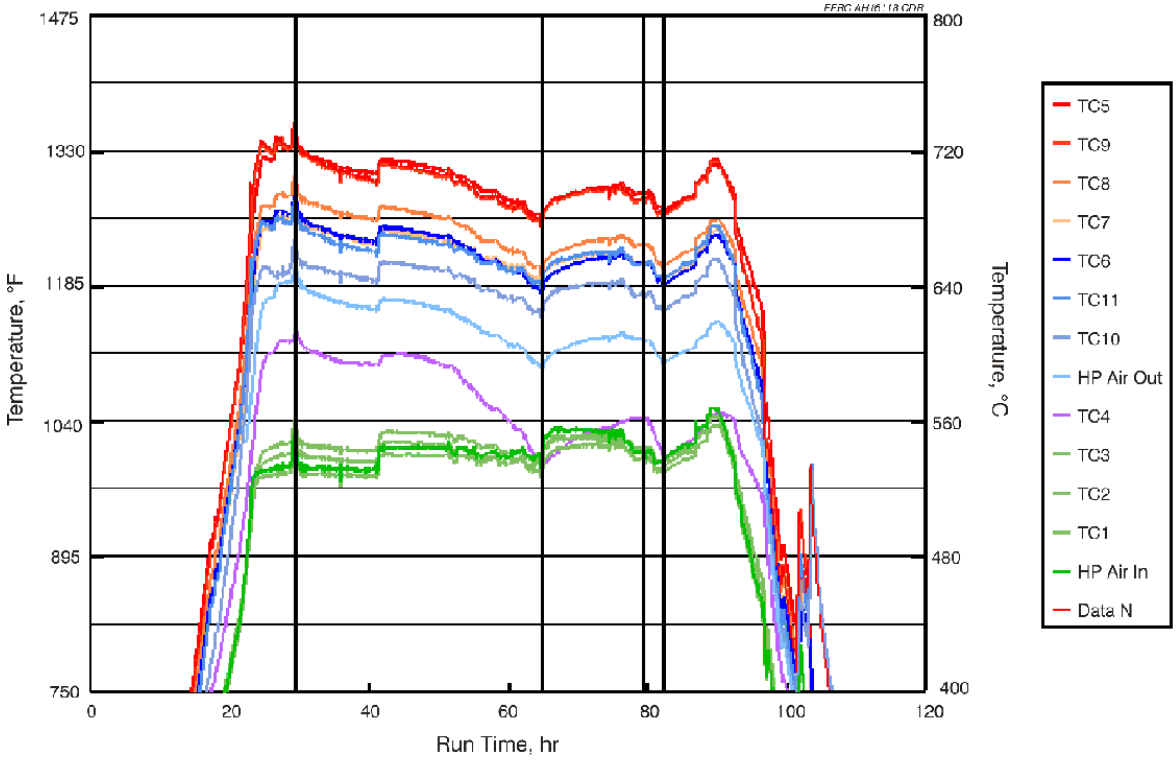

Exhibit 2.2-27
CAH Cooling Air Temperatures Versus Run Time for the February Test

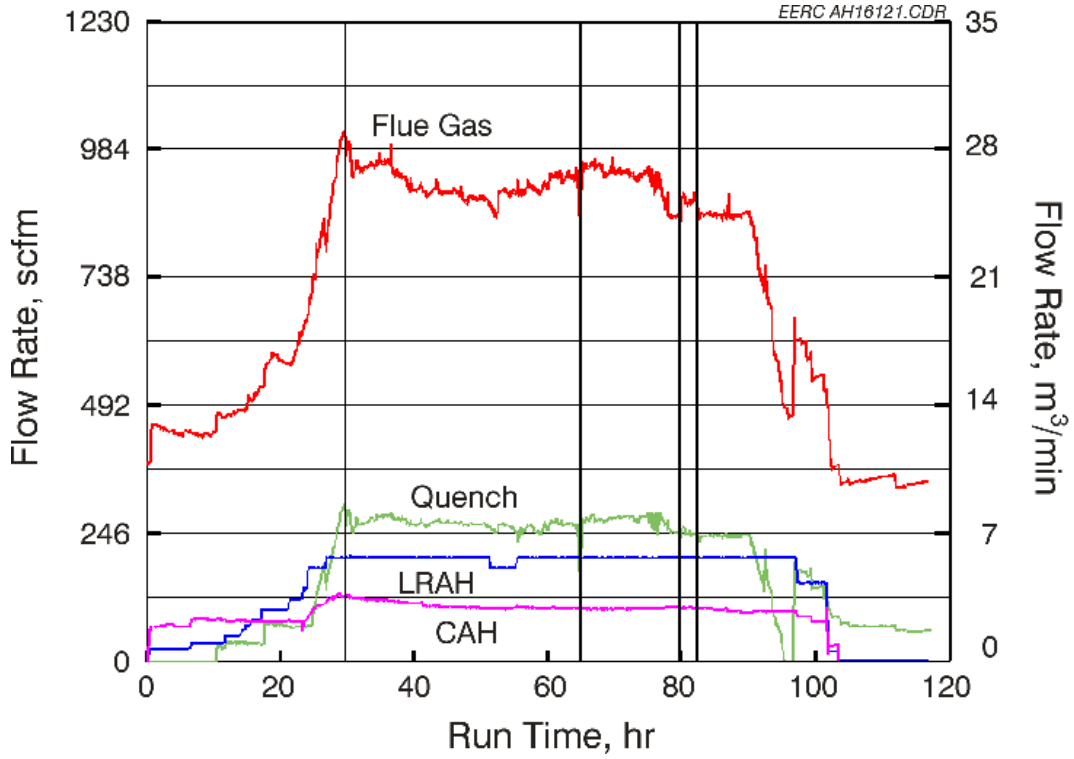

Exhibit 2.2-28
CAH Cooling Air, LRAH Cooling Air, Quench Gas, and Flue Gas Flow Rates Versus Run Time for the February Test

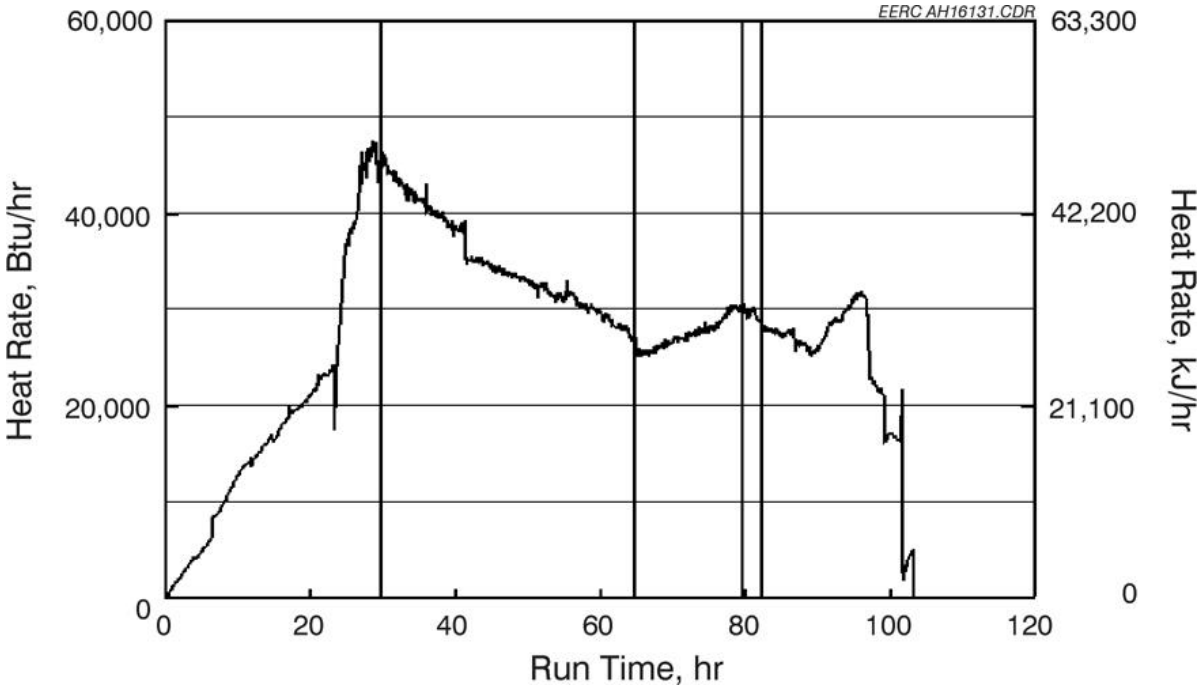

Exhibit 2.2-29
CAH Heat Recovery Versus Run Time for the February Test

When coal firing (Kentucky) began, surface temperatures initially decreased at a rate of nominally 5 F/hr (3 C/hr) over nearly 12 hours as ash deposits developed on the surface of the tubes. After nearly 40 hours of coal firing, there was no further decrease in tube surface temperature. It must be noted that cooling air flow rates were also decreasing (0.01 scfm/0.0003 m^3/min) over these time frames in an attempt to maintain a relatively constant cooling air exit temperature.

The minimum cooling air flow rate through the CAH tube bank was 104 scfm (2.9 m^3/min). As ash deposits developed on the tube surfaces, heat recovery from the CAH tube bank decreased from roughly 46,500 Btu/hr (49,058 kJ/hr) to 27,000 Btu/hr (28,485 kJ/hr). The coal feed was terminated at this time because of the plugging problems in the slag screen. When coal feed resumed, heat recovery from the CAH tube bank was nominally 30,000 Btu/hr (31,650 kJ/hr). Heat recovery decreased to nominally 29,000 Btu/hr (30,595 kJ/hr) over the final 2.5 hours of coal firing prior to the termination of the coal feed. These data indicate that heat recovery from the CAH tube bank when the Kentucky bituminous coal was fired is significantly greater as compared to the Illinois No. 6 coal data. This result is most likely due to the smaller quantity of ash in the Kentucky fuel and a difference in ash properties.

EERC personnel did not clean the CAH tube bank during the February test in order to facilitate the development of ash deposits for characterization. CAH tube bank plugging was not a problem. No deposits were observed bridging the flue gas paths between the tubes. The deposits that formed were limited to the leading and trailing edges of the tubes. In addition, these deposits did not bridge the area between the tubes in the direction of the flue gas flow.

Exhibit 2.2-30 presents a photograph of ash deposits on the surface of the tubes following the February test. The photograph shows three of the five uncooled tubes as well as two of the seven air-cooled finned tubes. The leading- and trailing-edge deposits are readily visible, with very little ash present on the side walls of either the uncooled or cooled metal surfaces. There do not appear to be any pieces of tube deposit missing in the photograph.

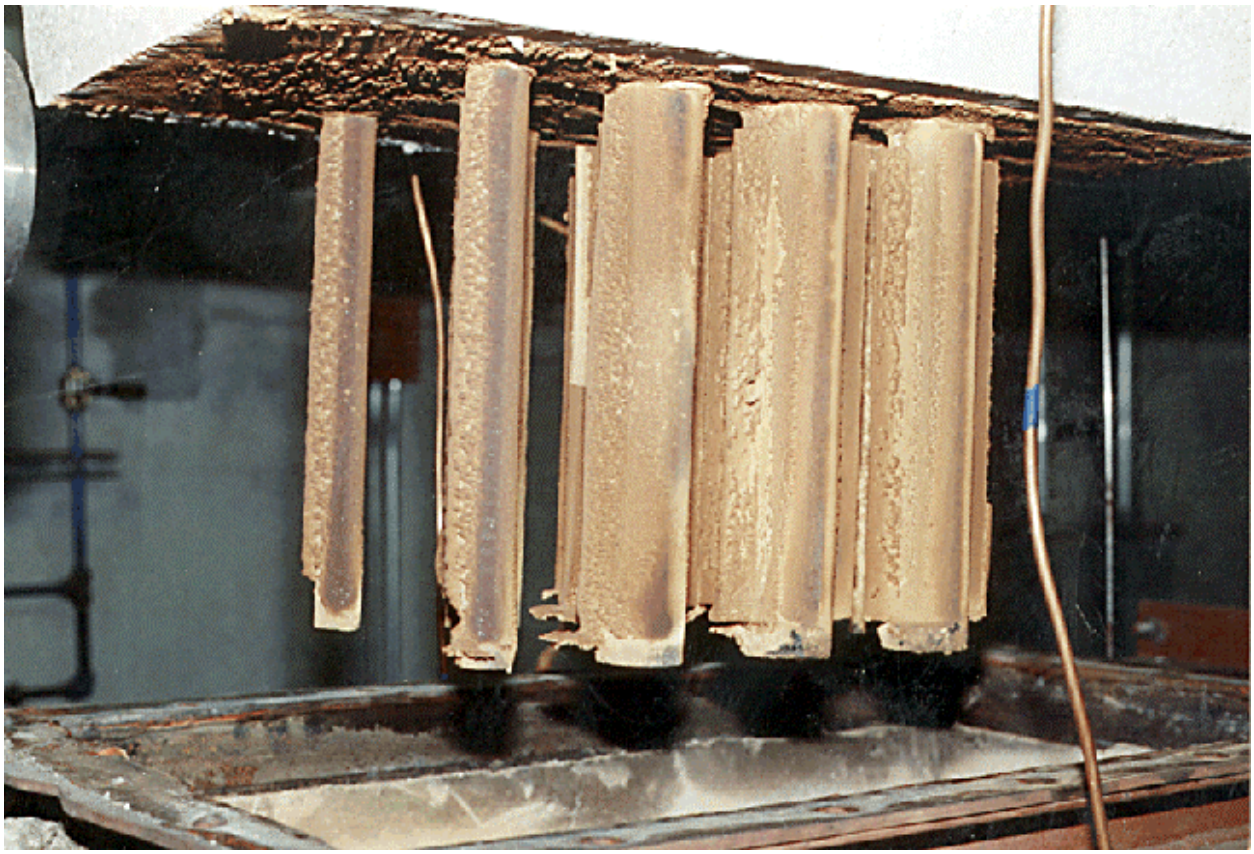

Exhibit 2.2-30
Photograph of Ash Deposits on the CAH Tubes Following the February Test Firing Kentucky Bituminous Coal

The deposits remained intact when the CAH tube bank was removed from the duct. However, the small quantity of deposit and therefore, minimal weight, may have been the primary reason the deposit remained intact when the tube bank was removed from the duct. Also, the deposits from the cooled tubes were not generally removed intact from the tube surfaces. The total weight of the deposits collected from the CAH tubes and duct was 2.2 lb (1.0 kg). The total weight of the deposits collected from the CAH tubes was 1 lb (0.5 kg). On a mass per unit time basis, the ash deposition rate for this Kentucky coal-fired test would be 0.03 lb/hr (13.6 g/hr) of coal firing. Incorporating the surface area of the tube bank (6.28 ft^2 or 0.58 m^2) results in a value of 0.005 lb/hr-ft^2 (23.4 g/hr-m^2). On a coal-firing-rate basis, the CAH ash deposition rate would be 0.01 lb/MMBtu (5.9 g/10^6 kJ). These calculated values are nominally a factor of 3 smaller than those observed for the Illinois No. 6 coal, consistent with the Kentucky coal's lower ash content and higher heating value.

Exhibit 2.2-31 shows the compositions of the deposits that formed on both the uncooled dummy tubes and the cooled tubes. The compositions show that, like the slag collected in the slag screen, the deposits are dominated by larger particles enriched in silica and iron and depleted in alumina and calcia. It is unusual that the compositions of the upstream and downstream deposits are so similar, since the upstream deposits are usually more enriched with larger particles and the downstream deposits usually more enriched with smaller particles. SEM analyses showed

that essentially all of the different deposits were composed of complex silicates, except for a thin powder layer adjacent to the tube which contained approximately 15% sulfate material.

Exhibit 2.2-31
CAH Deposit Samples

Oxides[1], wt%	Kentucky Coal	Uncooled Front	Uncooled Back	Cooled Front	Cooled Back
SiO_2	40.4	53.5	52.1	53.2	53.2
Al_2O_3	30.8	20.1	20.7	20.7	20.6
Fe_2O_3	10.6	14.1	14.2	14.5	14.1
TiO_2	1.1	1.2	1.3	1.3	1.3
P_2O_5	0.1	0.2	0.4	0.3	0.3
CaO	10.9	4.4	2.4	3.3	2.4
MgO	2.3	1.8	1.8	1.8	1.9
Na_2O	1.5	1.8	3.0	1.8	2.5
K_2O	2.3	2.8	4.2	3.1	3.8
SO_3[2]	6.7	0.3	0.2	1.0	0.4

[1] Oxide concentrations renormalized to a SO_3-free basis.

[2] SO_3 concentrations normalized with other oxides.

Testing of the LRAH Panel

Initial shakedown and testing of the LRAH panel took place in December 1997. Testing of the LRAH panel continued this past quarter following its reassembly in early January. Reassembly of the LRAH panel was necessary because of the removal of the ceramic tiles following the August 1998 test. The primary purpose of the January and February tests was to further evaluate the LRAH panel performance relative to heat transfer, tile and tube temperatures, and cooling air temperatures and flow rates. In addition, a critical aspect of LRAH panel performance is the ability of the ceramic tiles to withstand the slag attack and thermal cycling conditions in the slagging furnace. Generally, the performance of the LRAH panel this past quarter was as anticipated, with no significant process or material problems observed.

The LRAH panel ceramic tiles were thoroughly inspected upon initial installation and following each week of operation. The initial inspection revealed the presence of minor cracks in two of the five ceramic tiles. Cracks were not visible in either of the top or bottom support blocks. Exhibit 2.2-32 is a photograph of the new ceramic tiles installed on the LRAH panel inside the slagging furnace prior to the January test. The cracks visible at the time were hairline cracks in the large upper and lower tiles. The large upper tile had five visible cracks originating from the left edge and one crack originating from the top edge. Cracks originating from the left edge were about 0.75 in. (1.9 cm) in length and are not visible in the photograph. The vertical crack is visible in the photograph as a result of the application of a blue die. In addition, rough

surface pitting of the tile is evident at the end of the vertical crack in the upper center of the tile. The large lower tile had one crack originating on the left edge and a few rough surface pits along the right edge near the middle of the tile. Neither the crack nor the surface pits in the large lower tile are visible in the photograph.

Exhibit 2.2-32
Photograph of New Ceramic Tiles on the LRAH Panel Inside of the Slagging Furnace Prior to the January Test

Exhibit 2.2-33 presents photographs of the furnace interior after the January (top) and February (bottom) tests. Both photographs illustrate the excellent condition of the high-density furnace refractory as well as the darkening of the refractory with exposure to slag as a result of coal firing. Exposure of the LRAH ceramic tiles to slag during coal firing in January darkened the tiles as a result of the residual slag layer on the surface. No additional tile color change is evident following the February test. Although not obvious in the photos, the slag layer on the tiles is thin and appears to be uniform with no evidence of any extensive slag buildup. While there is some slag present in the seams between the tiles, there is no evidence of any fusion between adjacent tiles. Therefore, the 4-hour period of natural gas firing prior to SFS cooldown appears to be adequate to prevent buildup of excess slag on the surface of the tiles or in the seams between tiles for the Illinois No. 6 and Kentucky bituminous coals.

Exhibit 2.2-33
Photographs of the LRAH Panel Inside of the Slagging Furnace Following the January (top) and February (bottom) Tests

Exhibit 2.2-34 illustrates the visible cracks found in the LRAH tiles following the January (left) and February (right) tests. Overall, the tiles appear to be in good condition. Following the January test, visible cracks were only evident in two tiles, the small and large upper tiles. The small crack evident in the large lower tile prior to coal firing is covered with slag and is not evident at this time. One crack was evident in the small upper tile following the January test. The crack originates on the left edge and is <3 in. (<7.6 cm) in length. Six cracks were visible in the large upper tile following the January test, four originating from the left edge, one from the top edge, and one originating from the area of the rough surface pits and extending down toward the right edge. The four cracks originating from the left edge were visible prior to exposure of the tile to furnace conditions. However, one of the cracks has grown in length and intersects the vertical crack originating from the top edge. A fifth crack that had been observed originating from the left edge prior to tile exposure to furnace conditions is no longer evident as a result of slag covering the tile. The vertical crack in the large upper tile does not appear to have changed as a result of the January and February tests. However, the combination of the vertical crack, the crack extending from the left edge, and the new crack extending towards the right edge could be problematic with further heating and cooling cycles. The only other change in tile cracking that was observed following the February test was the appearance of a new crack originating on the lower right edge of the small upper tile.

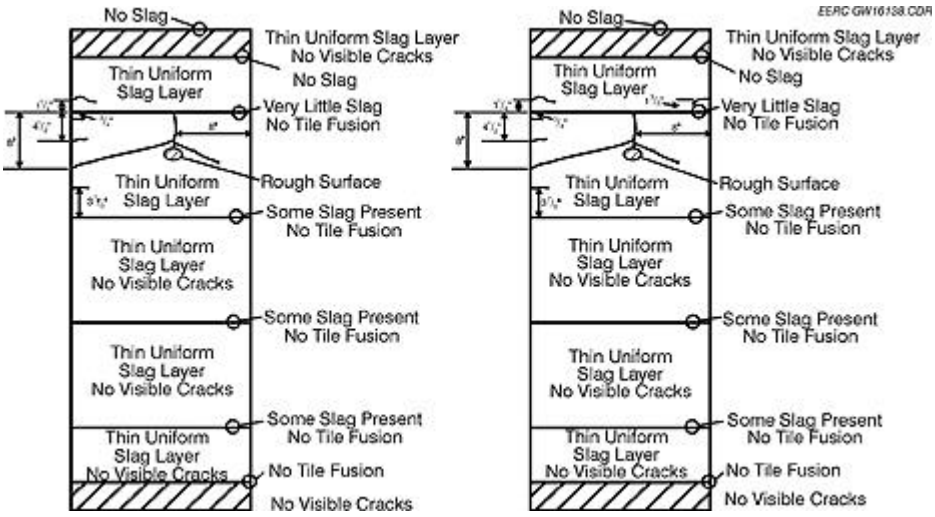

Exhibit 2.2-34
Illustrations of Cracks Found in the Ceramic Tiles/Bricks of the LRAH Panel after Testing in January (left) and February (right) 1999

Heatup/cooldown cycles are believed to be the primary cause of LRAH panel ceramic tile/brick cracking, with slag contributing to erosion/corrosion of surfaces and imparting stresses on the ceramic tile as it finds its way into seams between tiles. Exhibit 2.2-35 is a photograph of the lower support brick, small lower tile, and the lower edge of the large lower tile following the February test. The photograph shows where the flow of slag has caused erosion/corrosion of the tile surfaces. This observation is consistent with those made concerning the original LRAH tiles installed in December 1997 and removed subsequent to failure in August 1998. In addition, the photograph illustrates the small quantity of slag found in the seam between the tiles.

Exhibit 2.2-35
Photograph of the LRAH Lower Support Brick, Small Lower Tile, and the Lower Edge of the Large Lower Tile Following the February Test

Exhibits 2.2-36 through 2-38 summarize the LRAH ceramic tile temperatures, tube surface temperatures, and cooling air temperatures for the January test. The cooling air flow rate data for the LRAH panel were summarized in Exhibit 2.2-21. Exhibit 2.2-39 illustrates the location of thermocouples in the LRAH panel, and Exhibit 2.2-40 describes the LRAH thermocouples. The indicated ceramic tile surface temperatures (cavity-side) ranged from nominally 2040 to 2205 F (1116 to 1208 C), based on measurements made at the center of each of the three large tiles once the SFS had stabilized thermally (Run Hours 45 through 99). Higher tile surface temperatures (furnace-side), 2620 to 2693 F (1438 to 1479 C), were measured near the center of the large middle tile. Tile surface temperatures during the January test were somewhat higher yet comparable to the temperatures observed during the first LRAH coal-fired test completed in December 1997. However, the furnace-side tile temperature is a new thermocouple location. Therefore, a direct comparison with previous data is not appropriate.

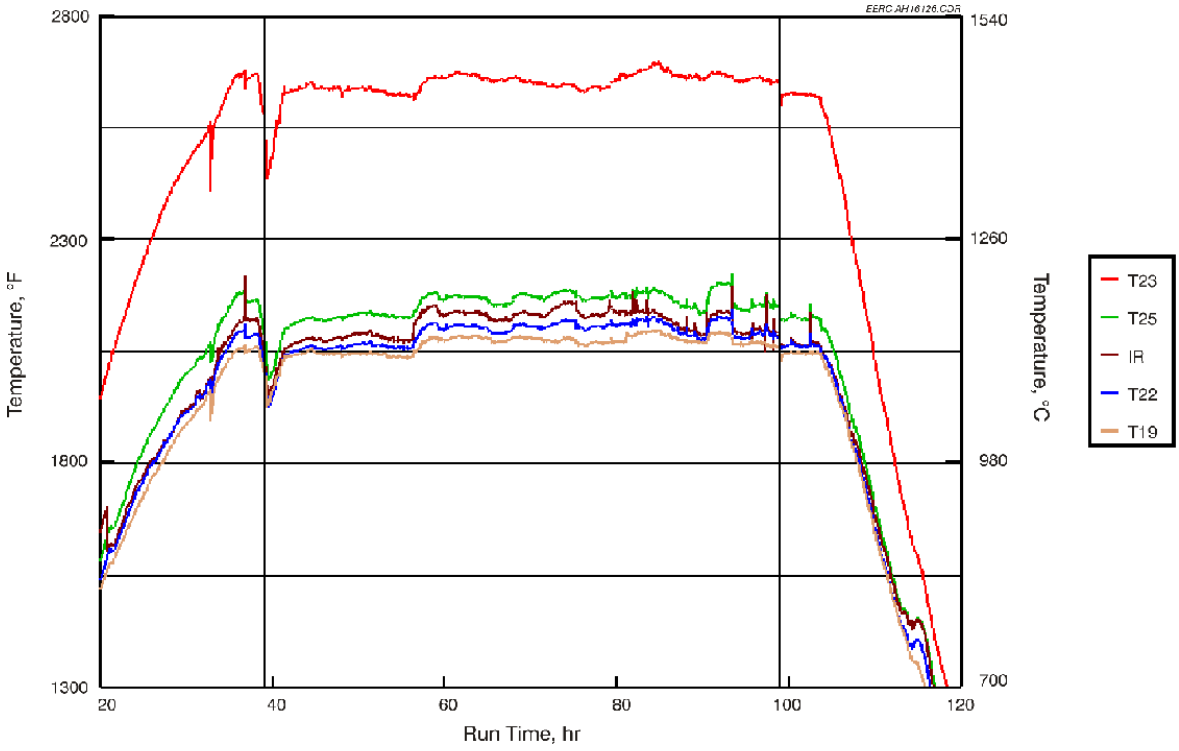

Exhibit 2.2-36
LRAH Ceramic Tile Temperatures Versus Run Time for the January Test

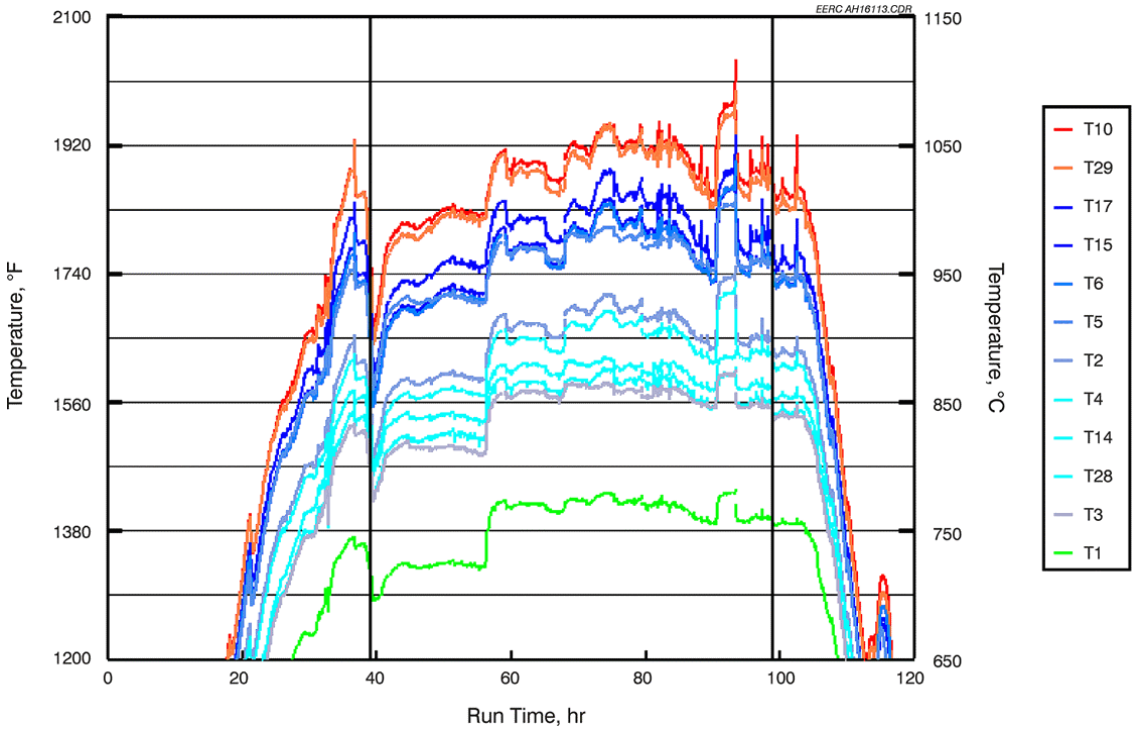

Exhibit 2.2-37
LRAH Tube Surface Temperatures Versus Run Time for the January Test

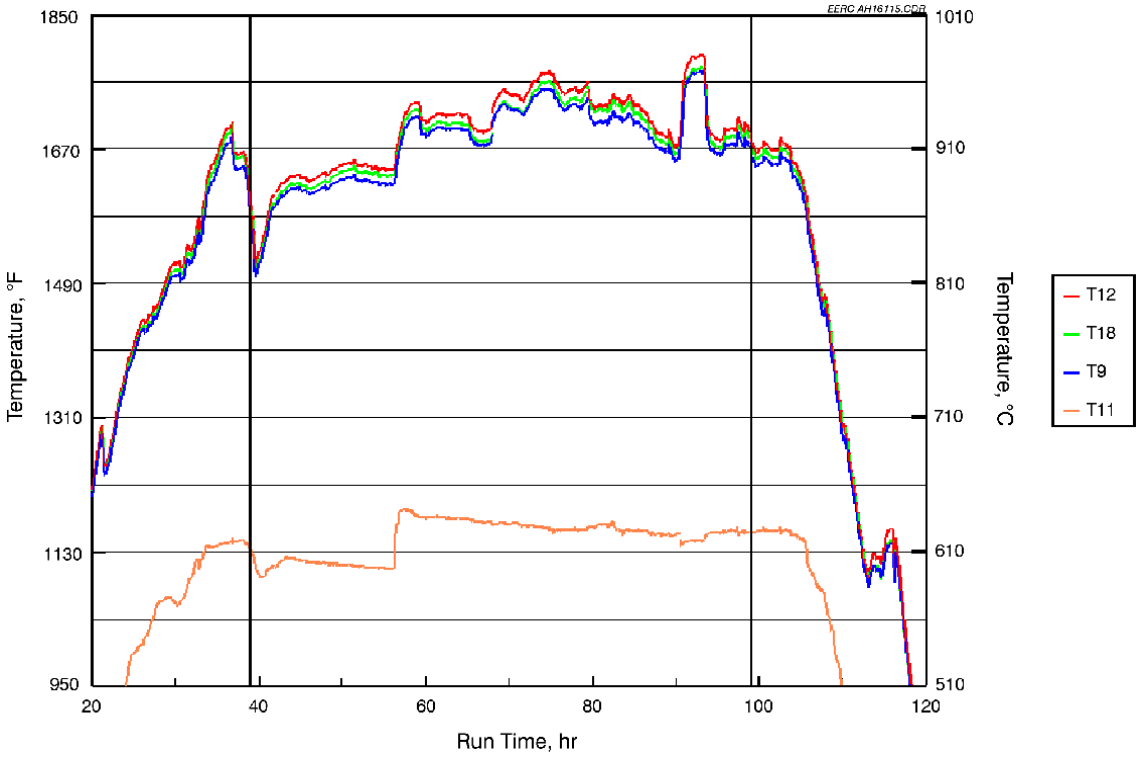

Exhibit 2.2-38
LRAH Cooling Air Temperatures Versus Run Time for the January Test

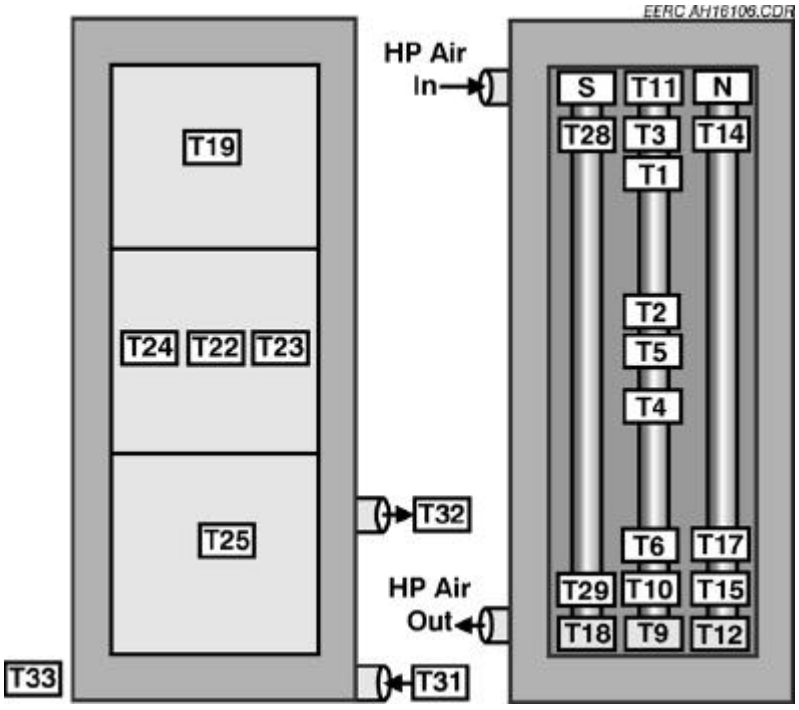

Exhibit 2.2-39
Thermocouple Locations in the LRAH Panel

Exhibit 2.2-40
Description of LRAH Panel Thermocouple Locations [1]

Category	No.	Label	Description
Air Inlet	1	HP Air In	Provided by the EERC, in pipe before inlet header
	2	RAHT11	Air entering RAH through center tube
Air Outlet	3	RAHT18	Air leaving left (south) tube
	4	RAHT9	Air leaving middle tube
	5	RAHT12	Air leaving right (north) tube
MA Tube Surface	6	RAHT1	Top of middle tube facing cold side
	7	RAHT2	Middle of middle tube facing other tube
	8	RAHT3	Top of middle tube facing toward furnace
	9	RAHT4	Middle of middle tube facing cold side
	10	RAHT5	Middle of middle tube facing toward furnace
	11	RAHT6	Bottom of middle tube facing cold side
	12	RAHT7	Removed
	13	RAHT8	Removed
	14	RAHT10	Bottom of the middle tube facing toward furnace
	15	RAHT13	Removed
	16	RAHT14	Top of north tube facing toward furnace
	17	RAHT15	Bottom of north tube facing toward furnace
	18	RAHT16	Removed
	19	RAHT17	Bottom of north tube facing toward side wall
	20	RAHT28	Top of south tube facing toward furnace
	21	RAHT29	Bottom of south tube facing toward furnace
Inner Surface of Monofrax bricks	22	RAHT19	Top tile, center
	23	RAHT20	Removed
	24	RAHT21	Removed
	25	RAHT22	Middle tile, center
	26	RAHT23	Middle tile, right center hot-side surface
	27	RAHT24	Middle tile, left side rail
	28	RAHT27	Removed
	29	RAHT25	Lower tile, center
	30	RAHT26	Removed

[1] Thermocouple locations are illustrated in Exhibit 2-39.

LRAH cooling air flow rates during the January test were controlled at 150, 180, 200, 205, and 220 scfm (4.2, 5.1, 5.7, 5.8, and 6.2 m^3/min), with most of the operational time making use of 200 scfm (5.7 m^3/min). Changes in cooling air flow rates had a definite effect on indicated tile surface temperatures. As cooling air flow rates were reduced, tile surface temperature increased. Subsequently, when cooling air flow rates were increased, tile surface temperatures decreased. This effect is most evident for cooling air flow rate changes at Run Hours 68, 79, 90, and 93.

LRAH tube surface temperatures ranged from nominally 1330 to 1970 F (721 to 1077 C). The low end of the temperature range represents the back side of the tube surfaces near the cooling air inlet, with the high end of the temperature range representing the front side of the tube

surfaces near the cooling air outlet. Changes in cooling air flow rates had noticeable effects on all tube surface temperatures. Tube surface temperature step changes were most noticeable for surface temperature measurements near the cooling air exit and on the front side of the tubes. Tube surface temperatures in January were comparable to all previous bituminous coal-fired tests.

Cooling air inlet temperature ranged from 1110 to 1190 F (599 to 644 C) but was nominally 1160 to 1190 F (644 to 666 C) for most of the coal-fired operational period. Outlet cooling air temperatures ranged from nominally 1625 to 1795 F (885 to 980 C). The effect of cooling air flow rate can be seen in the cooling air outlet temperature data. As cooling air flow rate decreases, cooling air exit temperature increases, as expected. These cooling air flow rate changes are noted at Run Hours 68, 79, 90, and 93. At Run Hour 56, a step increase in the cooling air inlet temperature results in a comparable increase in the cooling air outlet temperatures for a cooling air flow rate of 200 scfm (5.7 m^3/min).

Heat recovery data from the LRAH panel are presented in Exhibit 2.2-41 for the January test. At cooling air flow rates of 150, 180, and 200 scfm (4.2, 5.1, and 5.7 m^3/min), the heat recovered from the LRAH panel during coal firing was 120,000 Btu/hr (126,600 kJ/hr), 125,960 to 136,540 Btu/hr (132,888 to 144,050 kJ/hr), and 128,850 to 144,230 Btu/hr (135,937 to 152,163 kJ/hr), respectively. For cooling air flow rates of 180 and 200 scfm (5.1 and 5.7 m^3/min), the heat recovery ranges are a function of minor adjustments to the coal feed rate, combustion air flow rates, and main burner swirl setting. The main burner firing rate was nominally 2.1 to 2.25 MMBtu/hr (2.2 to 2.3 × 10^6 kJ/hr).

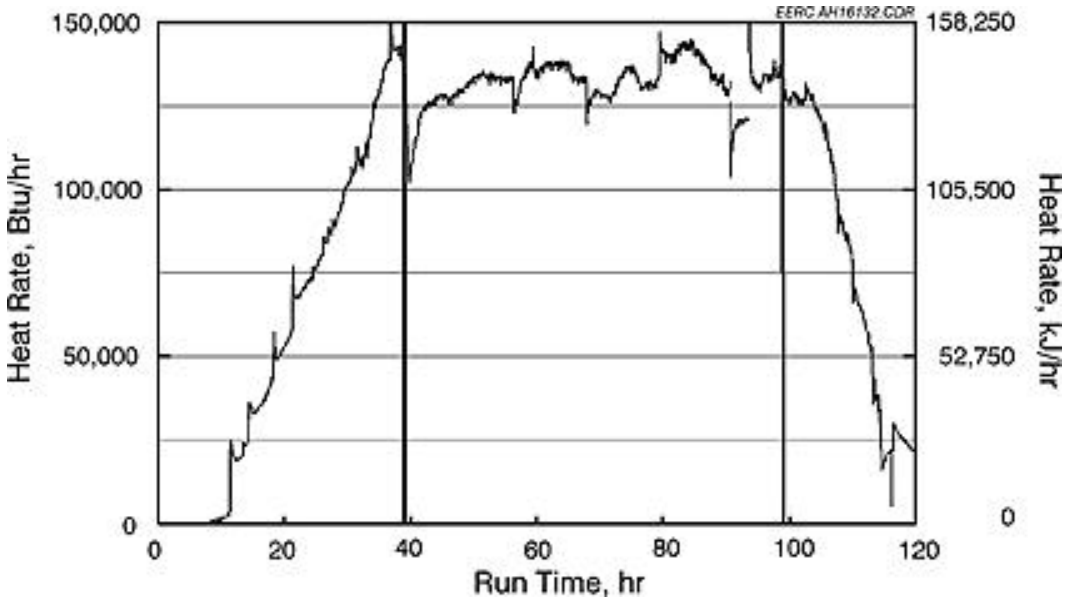

Exhibit 2.2-41
LRAH Heat Recovery Versus Run Time for the January Test

A comparison of the LRAH panel data for the January Illinois No. 6 bituminous coal-fired test and the previous tests firing the same fuel indicates that there has been a significant improvement in the heat recovery rate. During previous test periods, the heat recovery rate in the LRAH panel was <120,000 Btu/hr (<126,600 kJ/hr). However, in January the heat recovery rate was generally >120,000 Btu/hr (>126,600 kJ/hr). EERC personnel believe that the higher heat recovery rate observed in January was a function of many factors:

1) the SRAH panel was no longer in place,
2) a minimal main burner swirl setting resulted in a more uniform temperature over the length of the furnace,
3) the total furnace firing rate was somewhat higher in January than tests completed in late 1997 and early 1998, and
4) the new condition of the high-density refractory may have resulted in a slight reduction in furnace heat loss.

Another possible contributing factor may be the position of the inlet and outlet cooling air thermocouples. These thermocouples were reinstalled in January when the LRAH panel was reassembled. Although every effort was made to place the thermocouples in exactly the same position they had previously occupied, it is possible that the measurement location has been altered slightly. Further testing and data review will be necessary to develop an explanation for the higher LRAH heat recovery observed in January.

Exhibits 2.2-42 through 2.2-44 summarize the LRAH ceramic tile temperatures, tube surface temperatures, and cooling air temperatures for the February test. The cooling air flow rate data for the LRAH panel were summarized in Exhibit 2.2-28. Once the SFS had stabilized thermally (Run Hours 35 through 65 and 80 through 82), the indicated ceramic tile surface temperatures (cavity side) ranged from nominally 2070 to 2170 F (1133 to 1188 C), on the basis of measurements made at the center of each of the three large tiles. Higher tile surface temperatures (furnace-side), 2640 to 2690 F (1449 to 1477 C), were measured near the center of the large middle tile. Tile surface temperatures during the February test were comparable to those observed in January.

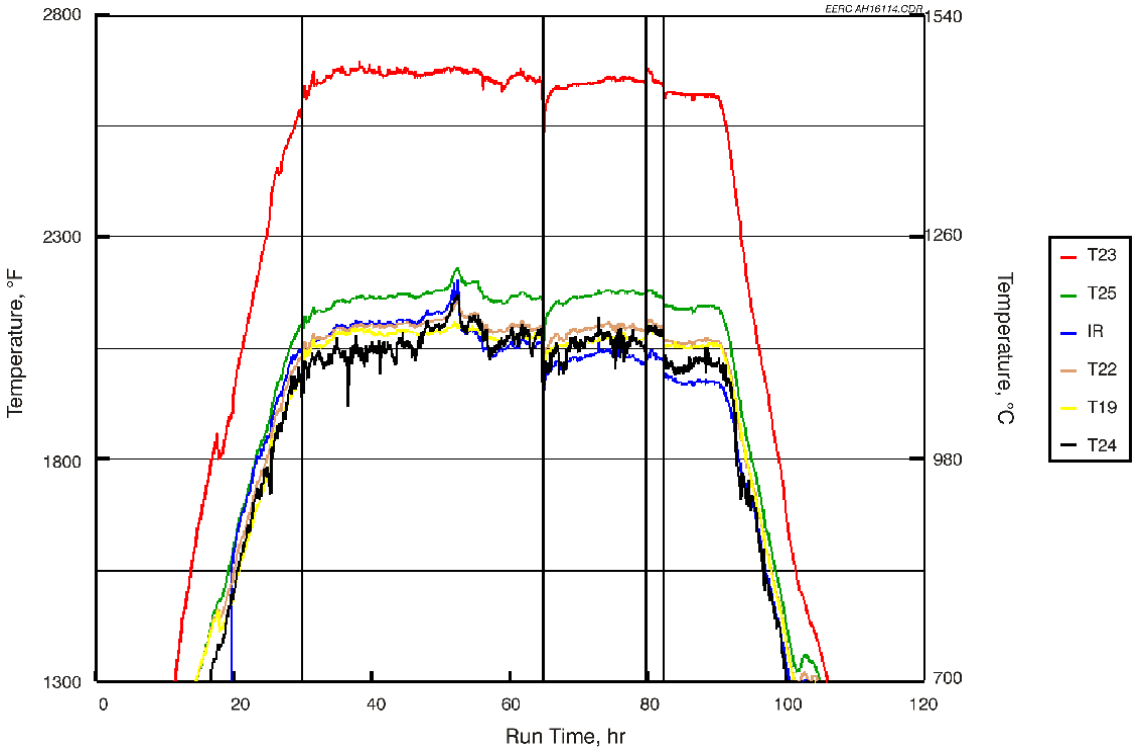

Exhibit 2.2-42
LRAH Ceramic Tile Temperatures Versus Run Time for the February Test

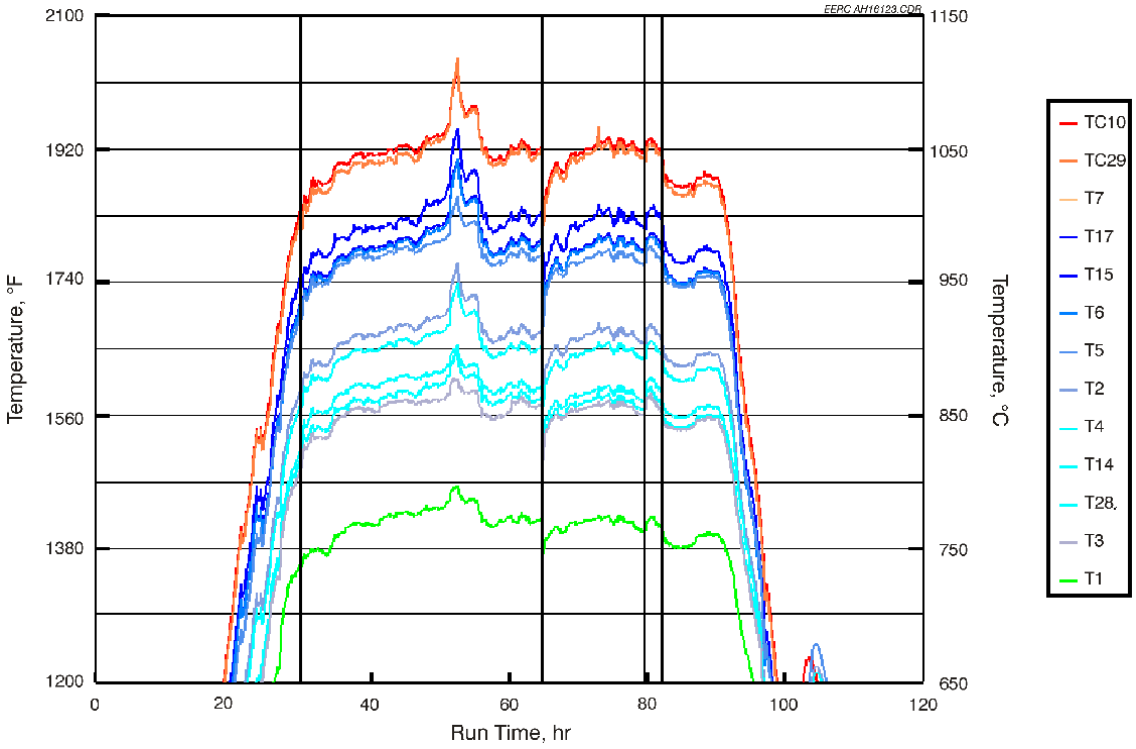

Exhibit 2.2-43
LRAH Tube Surface Temperatures Versus Run Time for the February Test

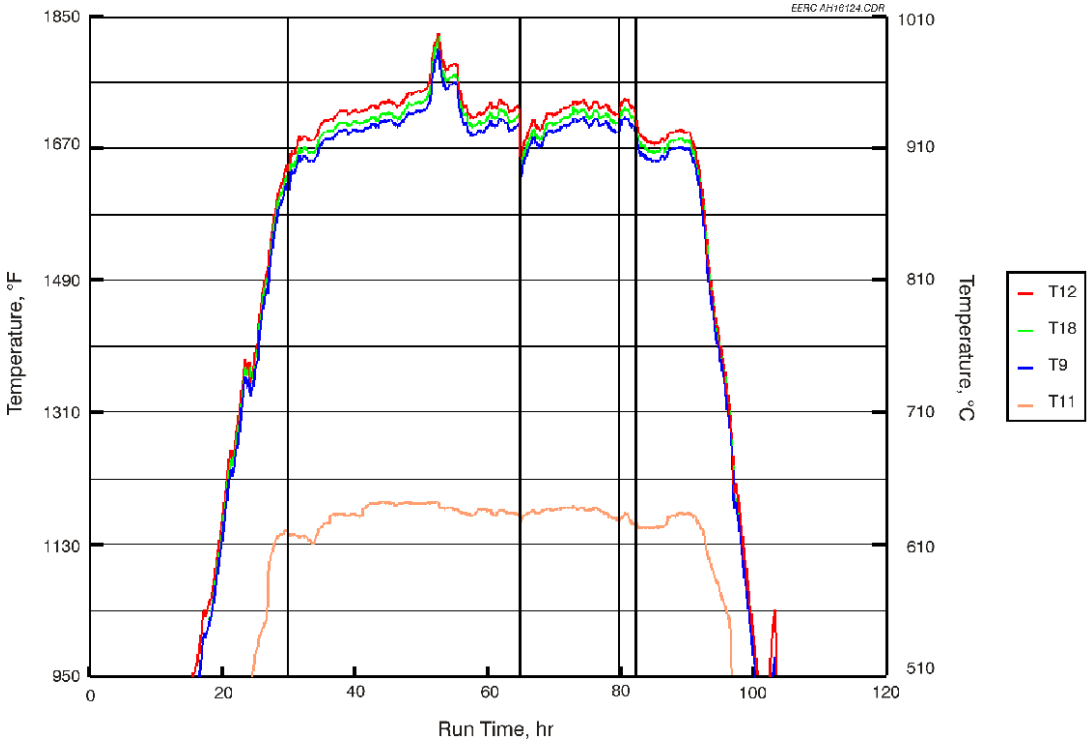

Exhibit 2.2-44
LRAH Cooling Air Temperatures Versus Run Time for the February Test

LRAH cooling air flow rates during the February test were controlled at 180 and 200 scfm (5.1 and 5.7 m^3/min), with most of the operational time making use of 200 scfm (5.7 m^3/min). Changes in cooling air flow rates had a definite effect on indicated tile surface temperatures. As cooling air flow rates were reduced, tile surface temperature increased. Subsequently, when cooling air flow rates were increased, tile surface temperatures decreased. This effect is evident for cooling air flow rate changes at Run Hours 51 and 55.

LRAH tube surface temperatures ranged from nominally 1370 to 1980 F (744 to 1083 C). The low end of the temperature range represents the back side of the tube surfaces near the cooling air inlet, with the high end of the temperature range representing the front side of the tube surfaces near the cooling air outlet. Changes in cooling air flow rates had noticeable effects on all tube surface temperatures. Tube surface temperature step changes were most noticeable for surface temperature measurements near the cooling air exit and on the front side of the tubes. Tube surface temperatures in February were comparable to all previous bituminous coal-fired tests.

Cooling air inlet temperature ranged from 1140 to 1190 F (616 to 644 C) but was nominally 1170 to 1190 F (633 to 666 C) for most of the coal-fired operational period. Outlet cooling air temperatures ranged from nominally 1650 to 1790 F (899 to 977 C). The effect of cooling air flow rate can be seen in the cooling air outlet temperature data. As cooling air flow rate decreases, cooling air exit temperature increases, as expected. These cooling air flow rate changes are noted at Run Hours 51 and 55. At Run Hours 34 and 41, a step increase in the cooling air inlet temperature results in a comparable increase in the cooling air outlet temperatures for a cooling air flow rate of 200 scfm (5.7 m^3/min).

Heat recovery data from the LRAH panel are presented in Exhibit 2.2-45 for the February test. At cooling air flow rates of 180 and 200 scfm (5.1 and 5.7 m^3/min), the heat recovered from the LRAH panel during coal firing was 131,730 to 134,615 Btu/hr (138,975 to 142,019 kJ/hr), and 132,690 to 140,385 Btu/hr (139,988 to 148,106 kJ/hr), respectively. For cooling air flow rates of 180 and 200 scfm (5.1 and 5.7 m^3/min), the heat recovery ranges are a function of minor adjustments to the coal feed rate and combustion air flow rates. The main burner firing rate was nominally 2.1 to 2.3 MMBtu/hr (2.2 to 2.3 × 10^6 kJ/hr).

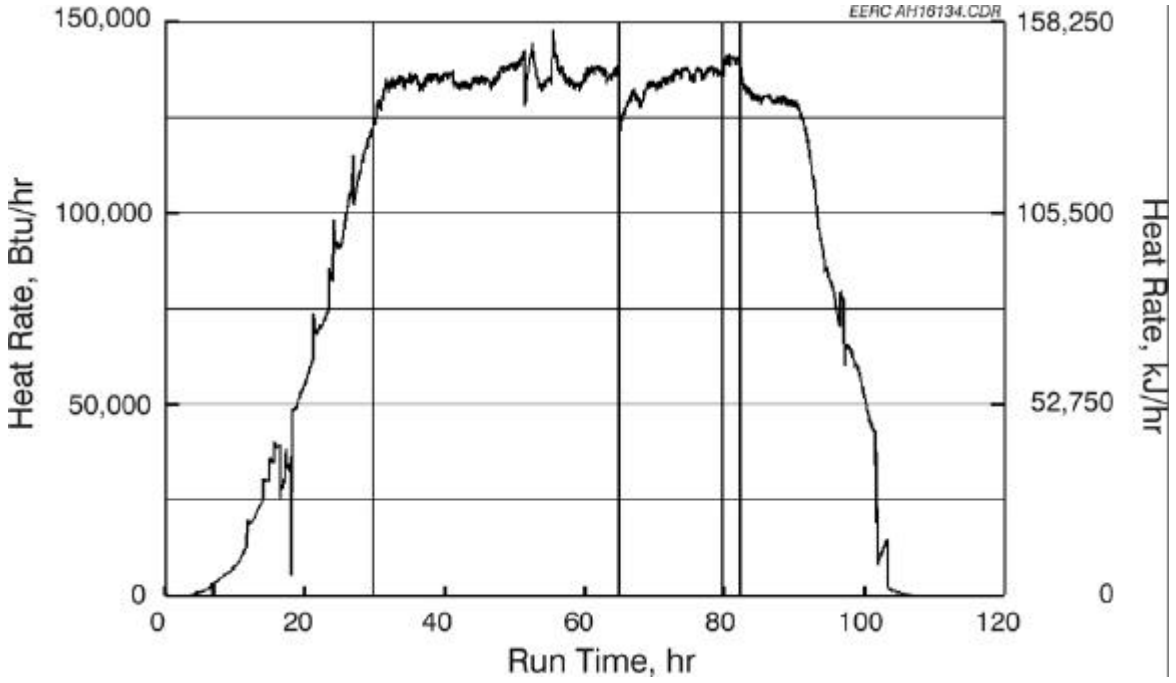

Exhibit 2.2-45
LRAH Heat Recovery Versus Run Time for the February Test

A comparison of the LRAH panel data for the February Kentucky bituminous coal-fired test and the January test firing Illinois No. 6 bituminous coal indicates a similar heat recovery rate. Again, these heat recovery rates are higher compared to bituminous coal-fired test periods in 1997 and 1998 where heat recovery rates in the LRAH panel were typically <120,000 Btu/hr (<126,600 kJ/hr). EERC personnel believe that the higher heat recovery rate observed in February was a function of the several factors that also influenced the performance in the January run.

To date, the LRAH panel has been exposed to a range of furnace-firing conditions for a total of 1221 hours. Natural gas firing represents 738 hours and coal - lignite firing represents 483 hours. In addition, the LRAH panel has been exposed to nine heating and cooling cycles. The LRAH ceramic tiles that were installed in January have been exposed to two heating and cooling cycles and 216 hours of slagging furnace operation, 118 hours of natural gas firing (including heatup and cooldown) and 98 hours of coal firing. The longest continuous coal-fired period was 80 hours, completed in March 1998. The EERC intends to fire coal for 200 hours during a test planned for April 1999.

HITAF Air Heater Materials

Refractory Materials for the Radiant Air Heater

During this quarter, an examination of the refractory panels that were tested in the small radiant air heater (SRAH) and large radiant air heater (LRAH) during 1998 was conducted. The purpose of the examination was to evaluate the panel performance and durability. Through 1998, the refractory panels in the Large RAH were exposed to fluid slags under a range of furnace firing-conditions for a total of 1005 hours (620 hr on natural gas and 385 hr on coal/lignite fuel). The Small RAH panel had been exposed similarly to a range of furnace-firing conditions for a total of 562 hours (344 hr with natural gas and 218 hr with coal and lignite).

The focus during this reporting period was on evaluating the Monofrax M radiation panels, especially those which had a chromia/alumina coating on the hot front face (slag side) and on the colder back face. The intent of the chromia coatings was to improve the resistance to slag attack, and to increase the emissivity of the base Monofrax M material. The overall performance of these refractory tiles and changes in their microstructure during the furnace runs are discussed.

Evaluation of Refractory Tiles From the RAH Furnace

Sample Location and History

Refractory tiles were removed from the LRAH and SRAH after various runs in the UNDEERC slagging furnace. Sections of these tiles were sent to URTC for examination and evaluation. The furnace run conditions are summarized in Exhibit 2.2-46. There were 7 furnace test runs for a total of 1005 hours with the fusion cast refractory tiles in the LRAH and 3 furnace test runs for a total of 562 hours in the SRAH.

Exhibit 2.2-46
Run Summary of Furnace Test Facility at UNDEERC

Date	Fuel	LRAH*			SRAH*			Comments
		Run #	Coal (hrs.)	Gas (hrs.)	Run #	Coal (hrs.)	Gas (hrs.)	
30 Nov – 4 Dec '97	Natural gas	1	- - -	104	- - -	- - -	- - -	Natural gas only
14 –19 Dec '97	Illinois #6 coal	2	35	80	- - -	- - -	- - -	Sudden temperature drop (power failure)
9 – 13 Feb '98	Illinois #6 coal	3	51	60	- - -	- - -	- - -	
16 – 20 Mar '98	Rochelle subbituminous	4	81	32	- - -	- - -	- - -	LRAH – replace top block and tile, and radiation tile
20 – 24 Apr '98	Falkirk lignite	5	50	120	1	50	120	SRAH – replace top tile and top right radiation tile
8 – 12 Jun '98	Center & Falkirk lignite	6	52	61	2	52	61	
7 – 19 Aug '98	Illinois #6 coal	7	116	163	3	116	163	LRAH-Very high temp. test. Center & bottom radiation tiles fell out
	Total		385	620		218	344	
	Total coal & gas		1005			562		

** L = Large, S = Small; RAH = Radiant Air Heater*

Exhibit 2.2-46 shows that a combination of natural gas and various types of lignite and a bituminous coal were used as the fuels. The furnace temperatures were operated above the fusion point of the coal slags, so that they would flow down over the tiles collect on a slag screen below. The composition of the slags varied widely with the type of coal used and reacted differently with the two different tile materials: Monofrax M, an α/βalumina refractory (94.5% Al_20_3 with about 4% Na_20) and Monofrax L, a magnesia/alumina spinel refractory (45% MgO, 54% Al_20_3).

The location of the tiles and support blocks in the LRAH and SRAH, and the samples returned to UTRC for evaluation are shown in Exhibit 2.2-47. Monofrax M was used exclusively in the LRAH because of its high thermal conductivity and refractoriness. The three center radiation tiles (marked B in Exhibit 2.2-47) were coated with a chromia/alumina oxide layer to increase the emissivity on the back face adjacent to the heat exchanger tubes. Sample 6, which will be discussed later in the report, was taken from the center radiation tile.

In the SRAH, Sample 2 was taken from the top left Monofrax M tile (Exhibit 2.2-47), which had been coated with a chromia/alumina oxide composition on the front (hot) face in order to enhance the resistance to slag corrosion.

The testing and evaluation of Samples 2 and 6, which are discussed in this report, are part of an ongoing evaluation of refractory performance. Exhibit 2.2-48 summarizes the status of the testing performed on the various samples that have been taken to date for characterization and evaluation. As this exhibit shows, some of the completed work has been summarized in previous quarterly reports. The results of these tests will be used to provide guidelines for improving the refractory materials and performance for future applications.

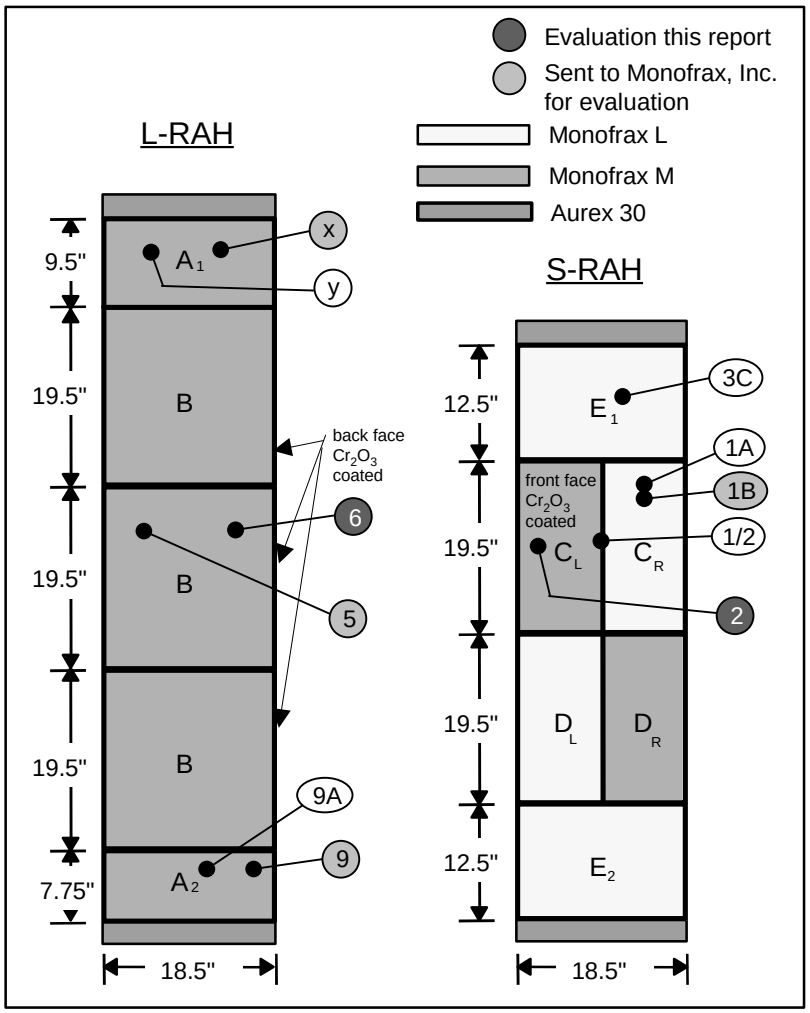

Exhibit 2.2-47
Location of samples returned to UTRC for evaluation.

Exhibit 2.2-48
Sample Description and Test Plan*

Sample	RAH	Location (Fig 1)	Material (Monofrax)	Flex. Test	Metallo-graphy	Electron Probe	Report	Source
1A	S	C_R	L	√	√	IP	4Q98	UTRC
1B	S	C_R	L	---	IP	---	---	MI
2	S	C_L	M	√	√	√	1Q99	UTRC
1/2	S	C_R / C_L	L,M	---	√	IP	4Q98	UTRC
3C	S	E_1	M	√	√	√	3+4Q98	UTRC
X	L	A_1	M	---	IP	---	---	MI
Y	L	A_1	M	---	√	√	2Q98	UTRC
5	L	B	M	---	IP	---	---	MI
6	L	B	M	√	√	√	1Q99	UTRC
9	L	A_2	M	---	IP	---	---	MI
9A	L	A_2	M	---	IP	---	---	UTRC

** Ö = completed; S = small; L = large; IP = in progress; MI = Monofrax, Inc.*

Examination and Evaluation of Selected Monofrax M Samples

In order to understand better the nature of the reactions of the slag with the Monofrax M material, the slag compositions are given in Exhibit 2.2-49. Note that all of the slags have relatively high silica, alumina, calcia, and iron oxide contents.

Exhibit 2.2-49
Typical Composition of Major Constituents in Coal Slags

Composition	Illinois #6	Rochelle Subbituminous	Falkirk Lignite
SiO_2	54	27	34
Al_2O_3	19	16	12
Fe_2O_3	16	6	7
P_2O_5	0.1	0.8	0.3
CaO	7	23	18
MgO	1	7	7
Na_2O	1	2	3
SO_3	3	16	18
Ash Fusion Temp.	(°F)	(°F)	(°F)
Initial	2340 ± 9	2250 ± 40	2180 ± 9
Fluid	2520 ± 15	2270 ± 50	2210 ± 9

Sample 2 Characterization (562 hr - SRAH)

Sample 2 was taken from the Monofrax M left top tile in the SRAH (see Exhibit 2.2-47). This tile can easily be seen in Exhibit 2.2-50A, because of its dark color that was due to a plasma sprayed chromia/alumina coating. This sample had undergone 3 furnace runs with both lignite and bituminous coal as the fuel. The slag covered tile pieces are shown in Exhibit 2.2-50B after the completion of the 3rd furnace run.

(A)

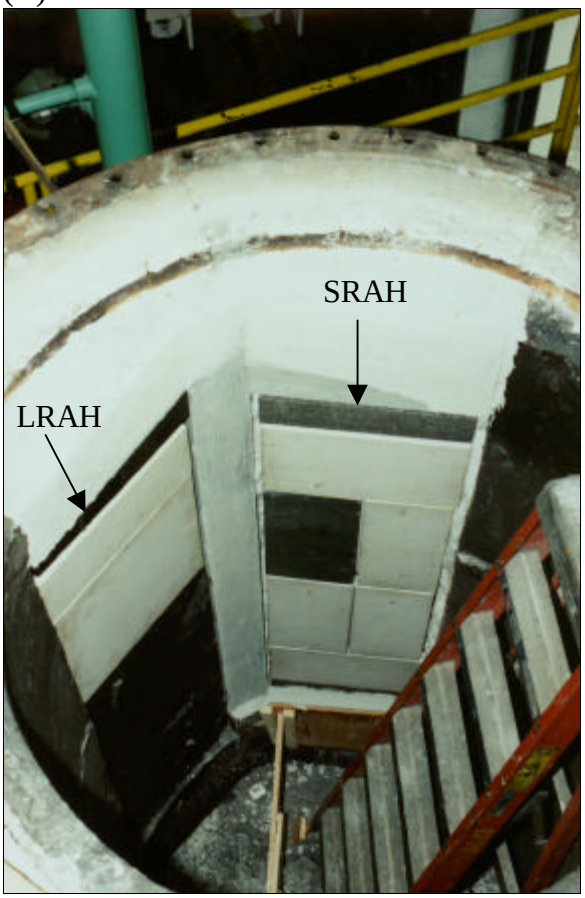

(B)

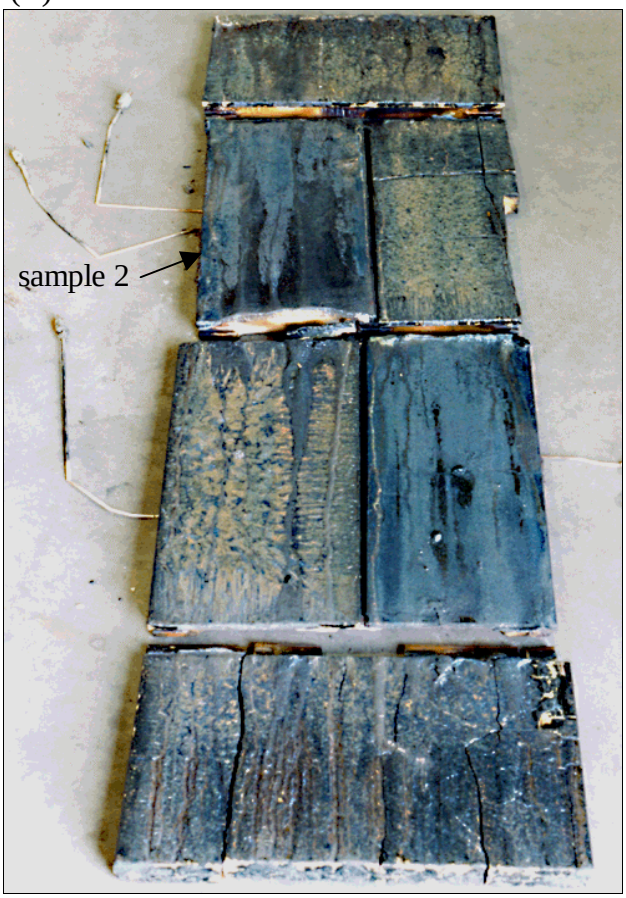

Exhibit 2.2-50
(A) Installation of SRAH panels on right side.
The dark top vertical left panel in the SRAH has been coated with Cr/Al-oxide.
(B) shows the removed slag coated panels after the 3rd SRAH furnace run.

Exhibit 2.2-51 shows the ' cold side' of the top left radiation panel and the location of sample 2, which was removed for metallographic and electron microprobe analysis. The different areas, which were scanned by the electron microprobe for composition (element) analysis, are shown also in Exhibit 2.2-51B. The slag-penetrated zone (dark coloration) was about 6mm in depth. The remaining material that was remote from the slag retained its white coloration. Flexure tests performed previously (Fourth Quarterly Report 1999), indicated that the strength of the dark region was about 1/8 that of the remaining white region after the 562 hours of furnace runs.

The compositional changes in the Monofrax M material from the slag on the surface into the dark penetrated regions and further into the white regions, as determined by electron microprobe analysis, are discussed next. Refer to Exhibit 2.2-51B for locating the different areas scanned in sample 2 by the electron microprobe. Areas 1 - 3 and 10 - 11 are discussed in this report.

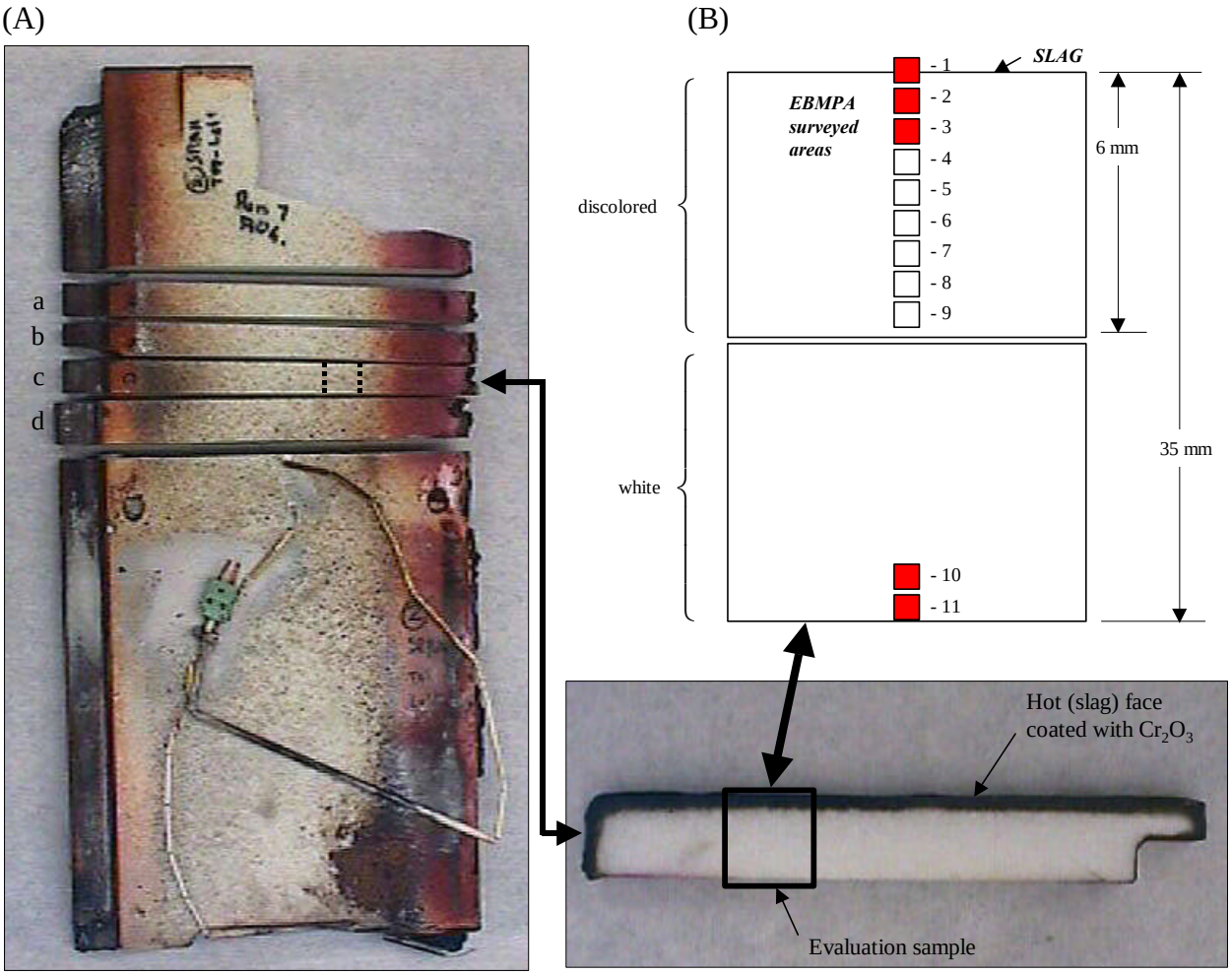

Exhibit 2.2-51
(A) Rear (cold) face of top left SRAH panel (see Exhibit 2.2-50) with sections cut for testing, and (B) location of sample cross-section for characterization and evaluation (sample 2).

Exhibit 2.2-52 shows two magnifications of the back-scattered electron image at the surface of sample 2 with the attached slag layer. The upper gray layer with the white crystals is the solidified slag. The surface had been previously exposed to different lignite and coal slags, the last run being the Illinois #6 coal (Exhibit 2.2-46).

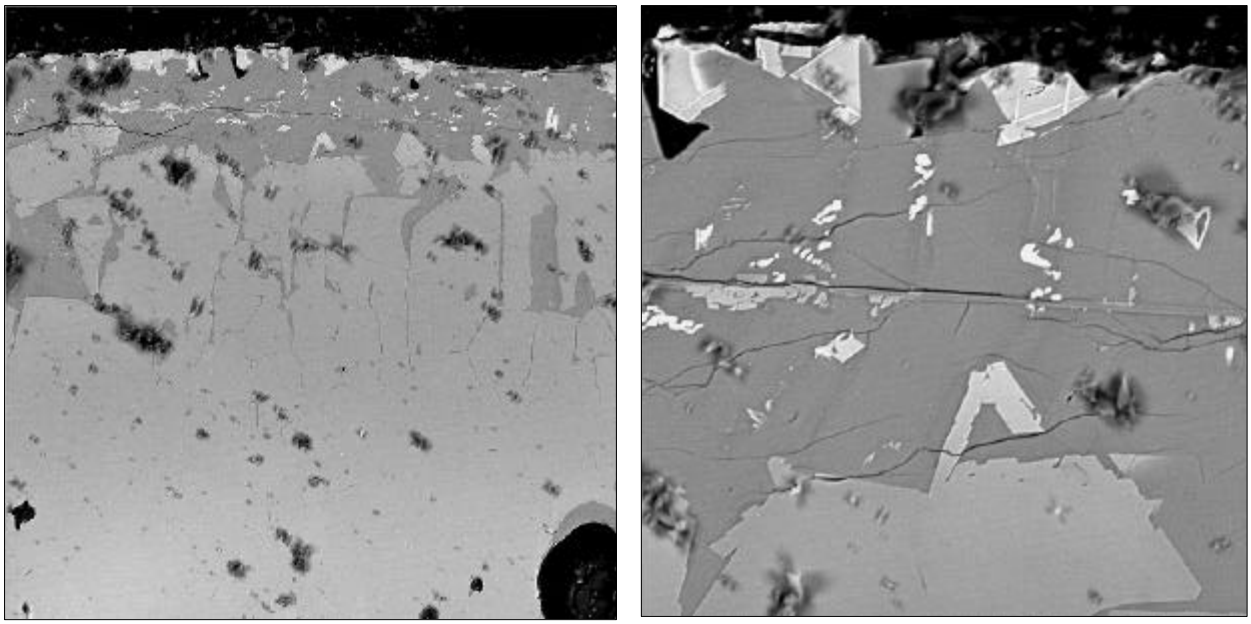

B.S.E. |-------| *125 mm* *B.S.E.* |-------| *31 mm*

Exhibit 2.2-52
Electron Probe Microanalysis of Sample 2,
Area 1 (slag surface).

The overall spectra of the elements in Area 1 is shown in Exhibit 2.2-53, where the Al peak is the strongest (from the Al_2O_3 in the Monofrax M and slag), and where there are significant, but lesser, amounts of Si, Mg, Fe from the slag (Exhibit 2.2-49). Exhibit 2.2-53 shows the element spectra of Area 1 through Area 11, which include regions of increasing depth into the Monofrax M and away from the slag surface. The changes in the relative peak heights of the different elements with increasing depth (from Area 1 to Area 2) can be seen readily in these two Exhibits. The element concentration gives a clear indication of the extent of the diffusion and reactions between the slag constituents and the α/β Al_2O_3 grains in the Monofrax M. Also, Cr (from the plasma sprayed chromia/alumina coating) can only be seen in the spectra of Area 1 and Area 2. This represents a depth of approximately 3-4 mm (0.12" - 0.16"). From Area 3 onwards to Area 11, there is no evidence of Cr. The dark regions in sample 2 contain significant amounts of slag that penetrated into the voids and cracks within the Monofrax M, and the presence of the Fe, Ca, Mg peaks confirms this. At greater depths into the interior regions (Area 10), at approximately a depth of 18mm, the Fe peak is absent and the residual Ca and Mg peaks are clearly visible, which indicates that some trace amounts of slag have penetrated deeply along some of the grain boundaries and cracks. Area 11 is a region where no slag was present; however, traces of Ca and Na that were in the original Monofrax matrix can be seen.

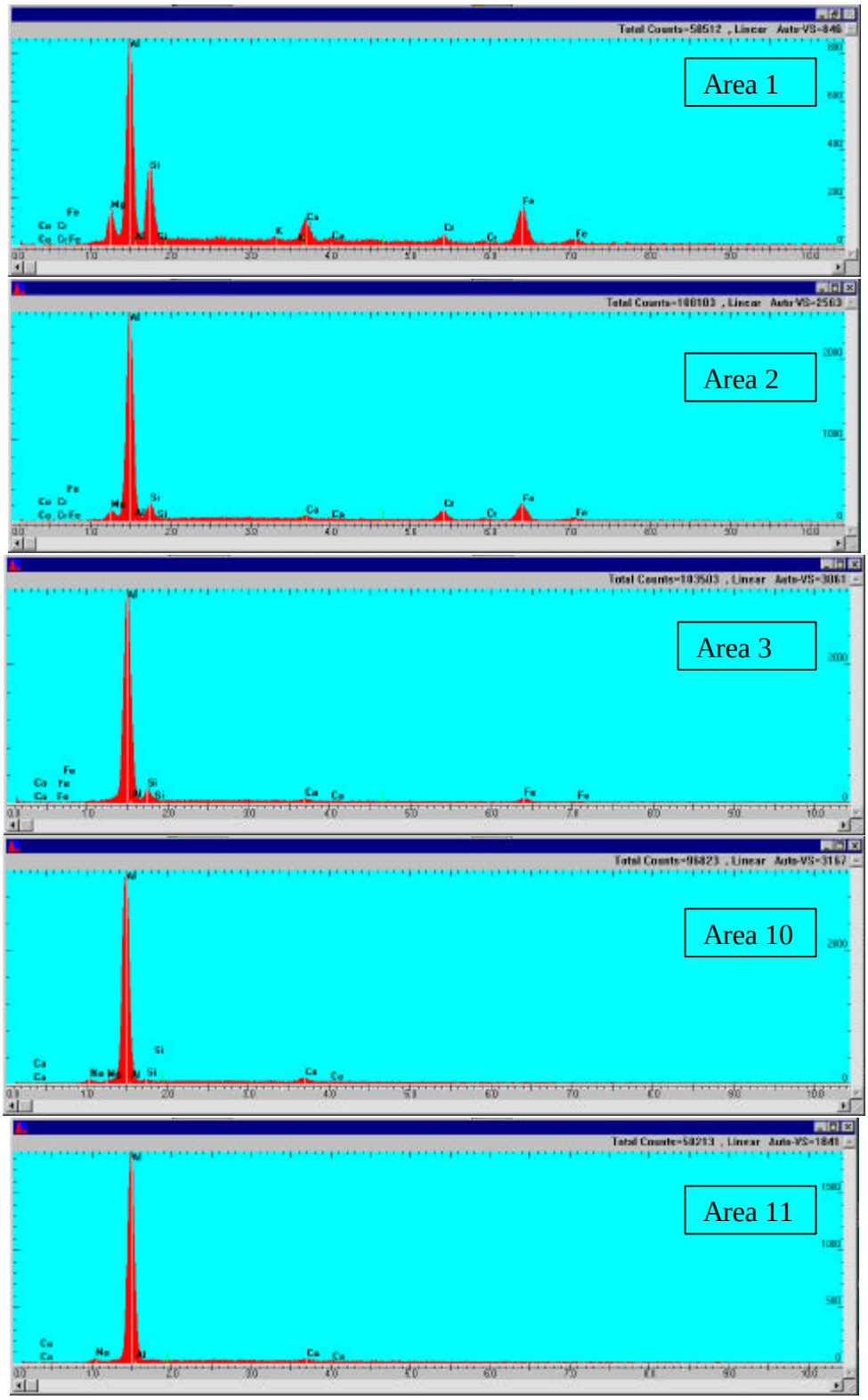

Exhibit 2.2-53
Electron Probe Spectra Showing Various Areas Of Sample 2

The electron probe element maps of Areas 1, 2, 3, 10 and 11 of sample 2 are shown in Exhibits 2.2-54 through 2.2-56, and provide a global location of the elements. The Areas 5 - 9 were also examined under the electron probe to determine the element concentrations, but no element maps were photographed, since there were little compositional differences between these areas.

An examination of the above five areas shows that there are 4 compositional zones:

1) a layer of residual slag;
2) a reacted layer of the original chromia/alumina coating;
3) a slag-penetrated region with a gradual decrease in slag constituents with increasing distance from the slag layer; and
4) the remaining original Monofrax M material.

Exhibit 2.2-54 shows the element maps of Area 1, where a distinct, 0.17 mm-thick layer of residual slag is evident from the element maps of silicon, calcium, aluminum (blue region), potassium, and spotty concentrations of magnesium and iron. All of these elements are in the slag (Exhibit 2.2-49). There is no evidence of chromium in the slag.

The next adjacent layer or region contains the chromia/alumina coating and resides within Area 1 and Area 2 (Exhibits 2.2-54 & 2.2-55). The microprobe element maps show that iron and magnesium have diffused into this region from the slag layer along with silicon and calcium. At the lower boundary of this chromia (30% Cr_2O_3-70% Al_2O_3) coated region is a distinct interface, as shown by the termination of the chromium, magnesium, and iron element maps. Note that the chromia/alumina coating composition has been modified by the reactions of the iron and magnesium from the slag. Both of these elements appear to be uniformly dispersed, while the silicon, calcium, and potassium are concentrated as thin layers in voids between the grain boundaries. The original chromia/alumina coating was 15.6 mils (0.4 mm) thick, while this chromia containing layer is about 40 mils (1 mm) thick. This indicates that a considerable amount of the slag penetrated into the chromia/alumina coating and reacted with it.

Exhibit 2.2-54 is a region (Area 3) showing a high concentration of aluminum (yellow green color), and is a continuation of the region below the chromia boundary shown in Exhibit 2.2-55. This region has been well penetrated by the slag elements Si, Ca, Mg, K, Fe and Na. Both the Fe and Mg have diffused into the alumina, where as the Si, Ca, K were concentrated in the voids and at the grain boundaries of the alumina grains. The three regions just discussed appear as the dark colored zone in Exhibit 2.2-51B, which is 6 mm (0.24") thick.

The fourth compositional zone described above is the white region shown in Exhibit 2.2-51B, and is located 33 – 35 mm (1.3" - 1.4") away from the slag layer. Exhibits 2.2-57 (Area 10) & 2.2-58 (Area 11) show that the microstructure contains primarily large grains of α–alumina (light yellow green) and β-alumina (yellow green), and also contains sodium. There is some silicon and calcium that surround the grains, and these are minor elements in the Monofrax M. By comparing the maps in Exhibits 2.2-57 and 2.2-58 of the unreacted Monofrax M, the differences in microstructure and composition due to the reaction and penetration of the slag are readily evident when comparing these element maps with those of Exhibits 2.2-54 through 2.2-56.

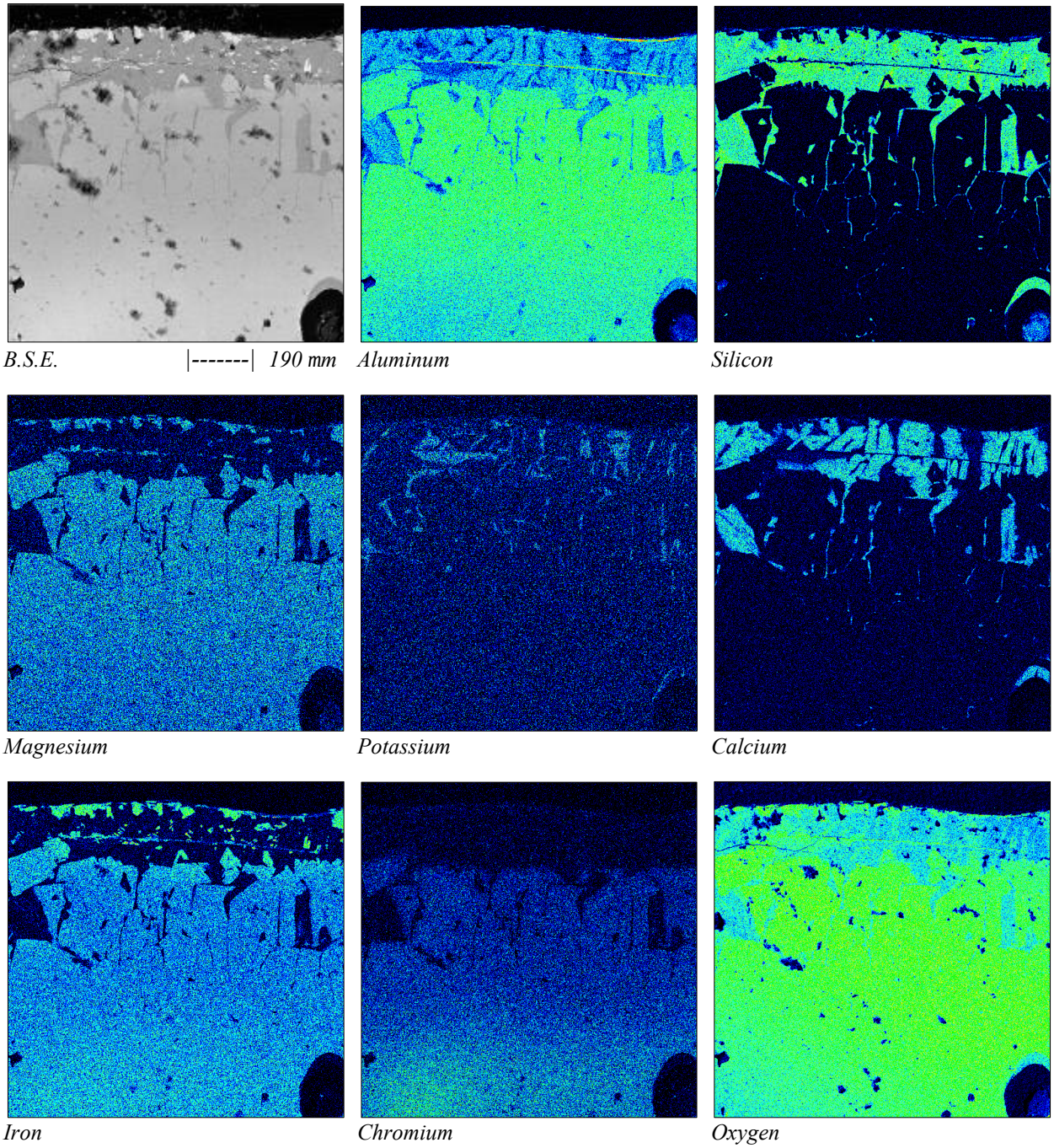

Exhibit 2.2-54
Electron Probe Microanalysis Showing Element Maps in Sample 2, Area 1 (slag surface)

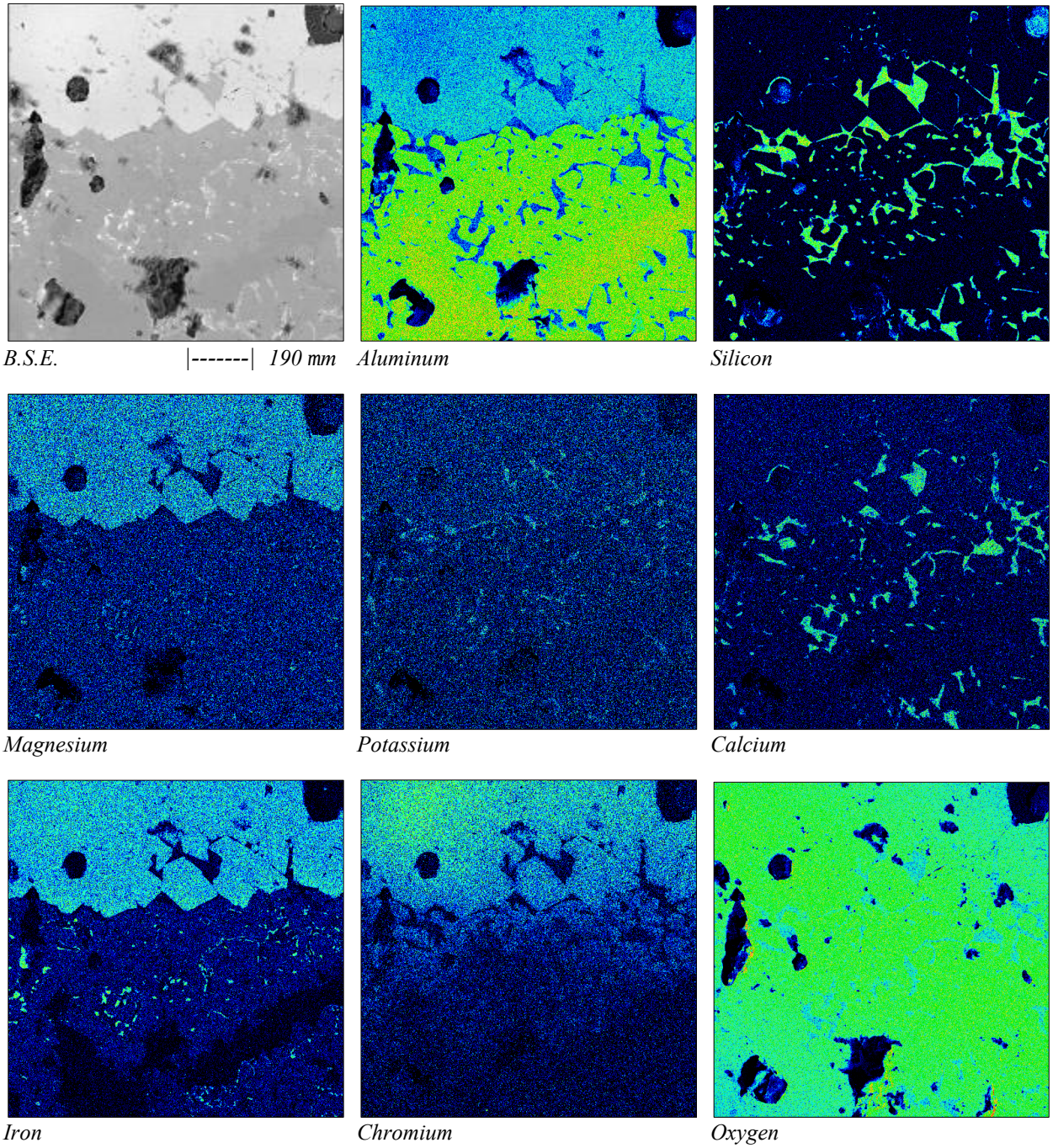

Exhibit 2.2-55
Electron Probe Microanalysis Showing Element Maps in Sample 2, Area 2

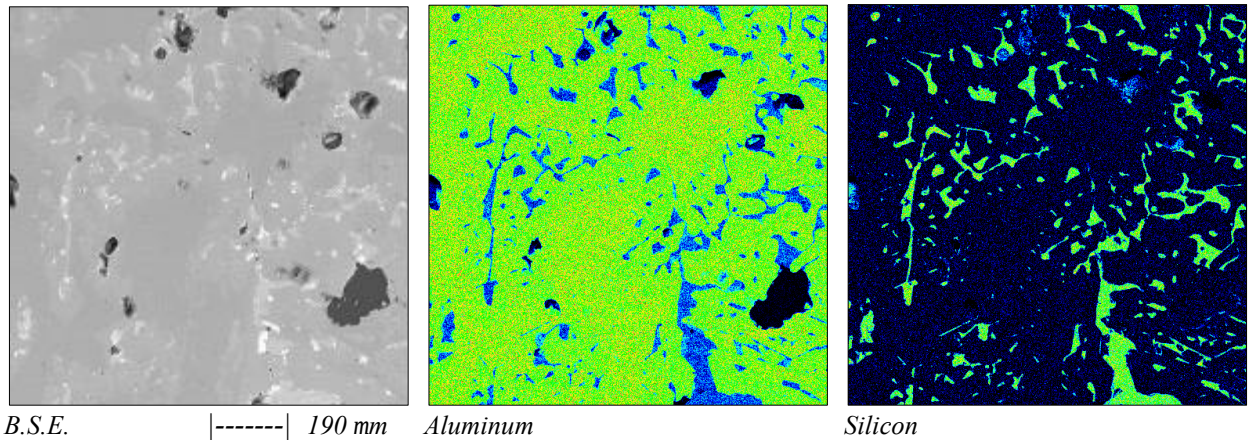

Exhibit 2.2-56
Electron Probe Microanalysis Showing Element Maps In Sample 2, Area 3

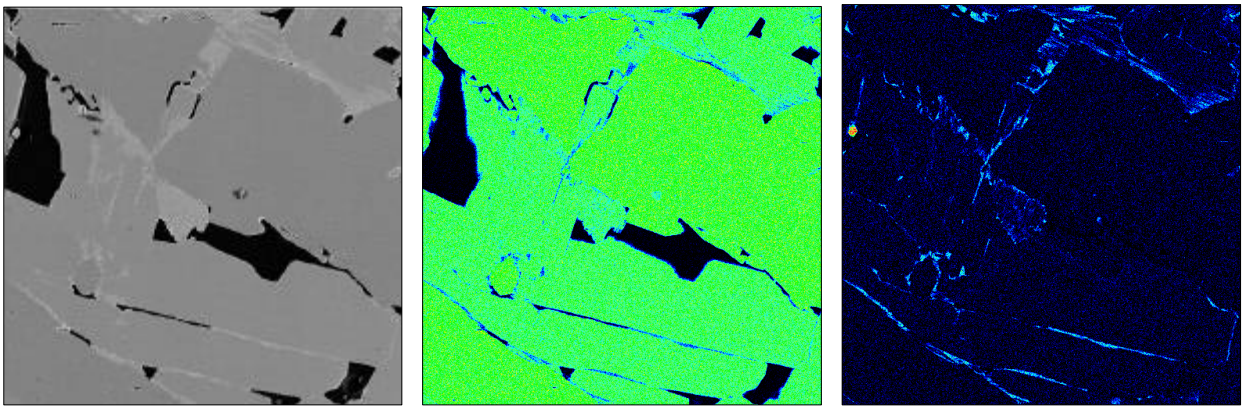

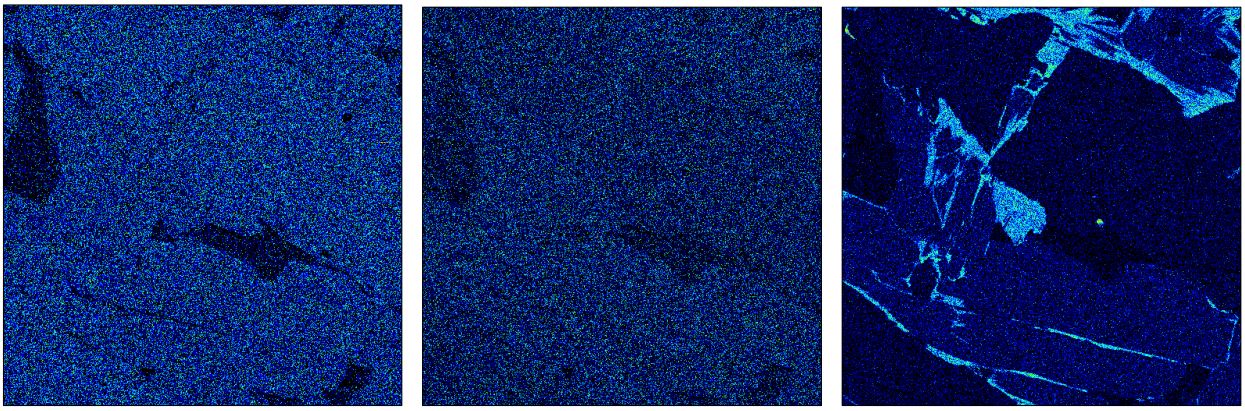

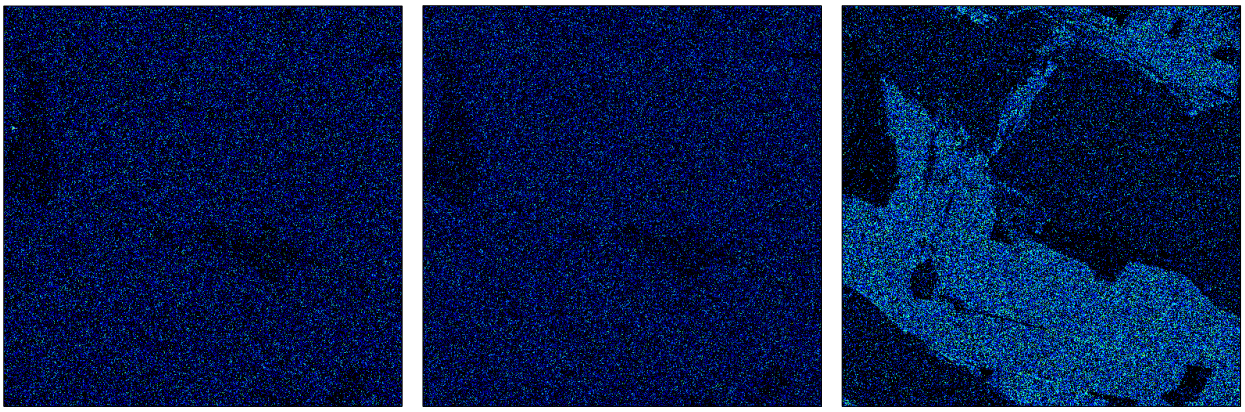

Exhibit 2.2-57
Electron Probe Microanalysis Showing Element Maps In Sample 2, Area 10

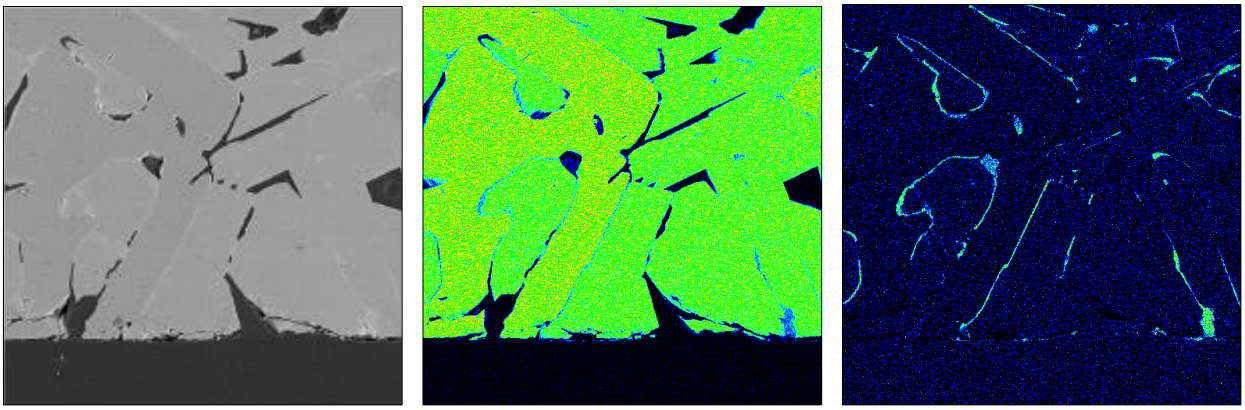

B.S.E. |-------| *190 mm* *Aluminum* *Silicon*

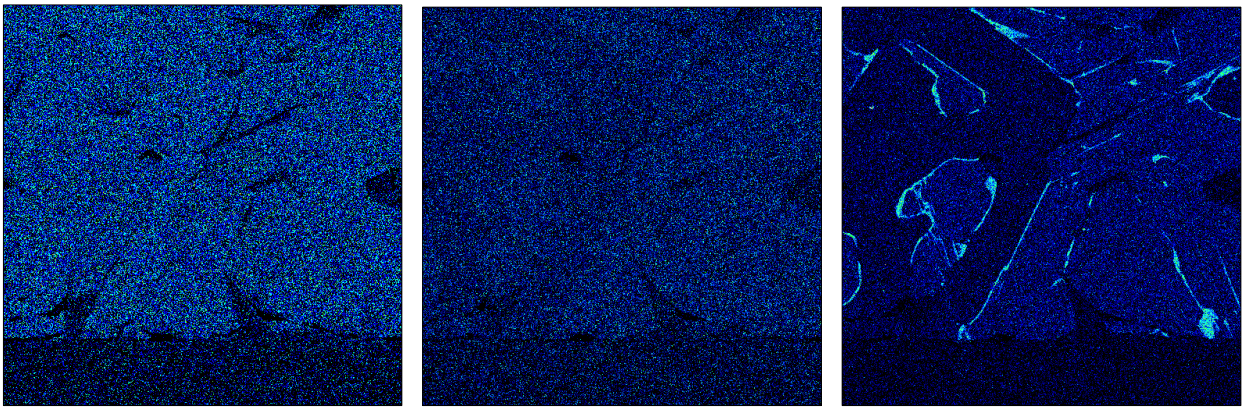

Magnesium *Potassium* *Calcium*

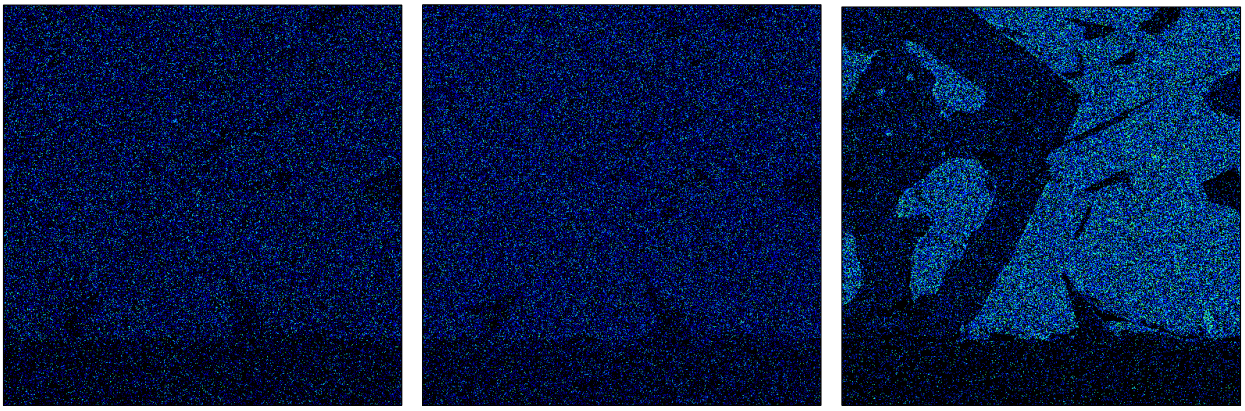

Iron *Chromium* *Sodium*

Exhibit 2.2-58
Electron Probe Microanalysis Showing Element Maps In Sample 2, Area 11

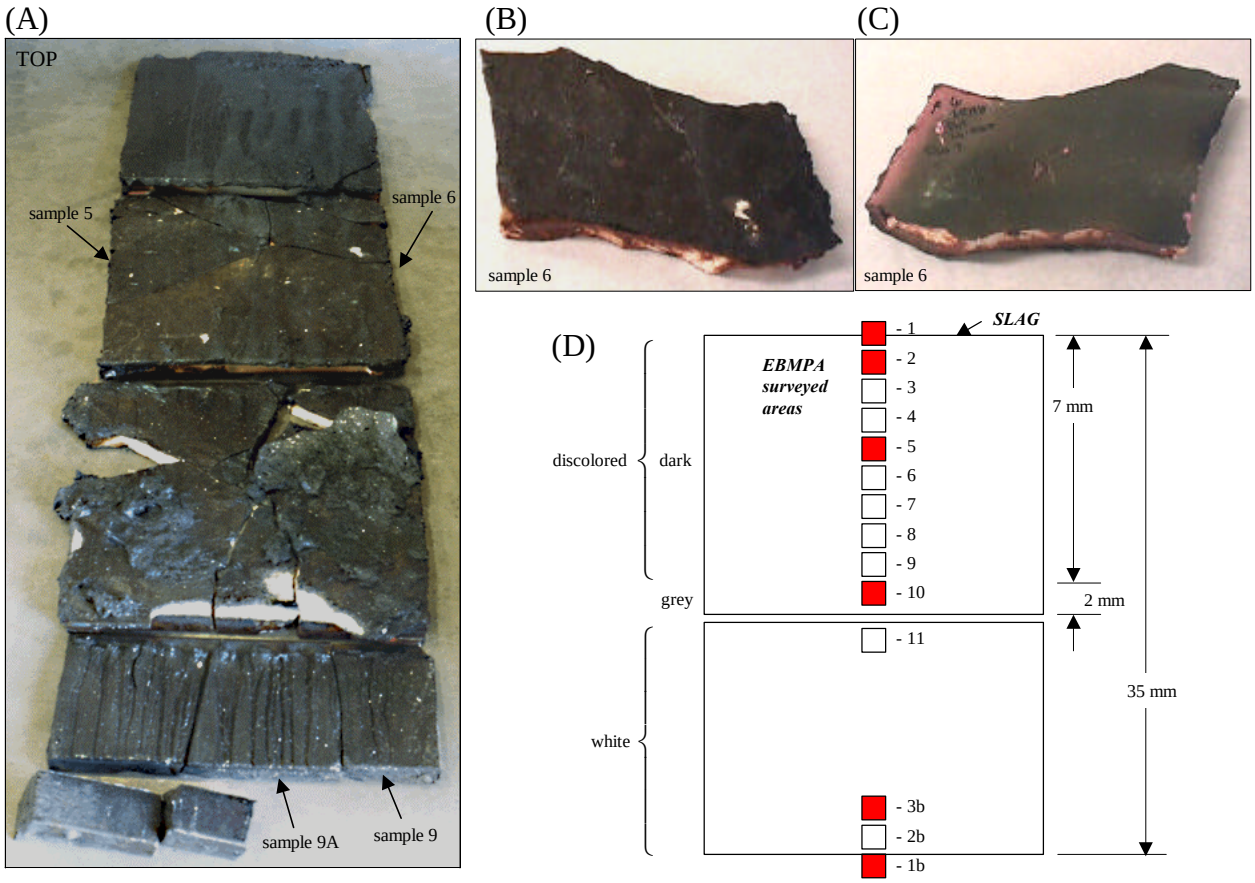

Exhibit 2.2-59
(A) Slag Covered Tiles Removed from the LRAH after 7 Furnace Runs.
(B) hot face (slag covered) side of sample 6,
(C) cold face with Cr_2O_3/Al_2O_3 coating, and
(D) location of electron microprobe survey areas.

Sample 6 Characterization [1005 hr – LRAH]

Sample 6, which was taken from the center radiation tile in the Large Radiant Air Heater panel, is shown Exhibit 2.2-59. Exhibit 2.2-59A & 2.2-59B shows the residual slag on the hot face of the tile. This tile was previously coated with chromia/alumina on the back (cool) face, and the coating can be seen in Exhibit 2.2-59C. Electron microprobe analysis was also performed on various areas of the sample, which is shown in Exhibit 2.2-59D. This sample had twice the number of hours of furnace runs as sample 2 and had some notable differences. The dark, discolored zone was slightly larger (7mm thick). In addition, there was an intermediate 2mm-thick grey transition zone between the discolored and white regions. Both samples 2 and 6 were from tiles that went through the last three runs in the furnace (Exhibit 2.2-46) before being removed for characterization and evaluation. Their exposure to the last three lignite and coal slags was similar.

Exhibit 2.2-60 shows the microstructure of sample 6, and Exhibit 2.2-61 shows the element spectra of the area adjacent to the slag (Area 1). Unlike sample 2, there was no discrete slag layer. The back scattered electron (B.S.E.) image shows that the slag is an integral part of the

surface of the Monofrax M, and that the original surface alumina grains partly dissolved. This is better seen in the element maps, which are discussed on page 2.2-70.

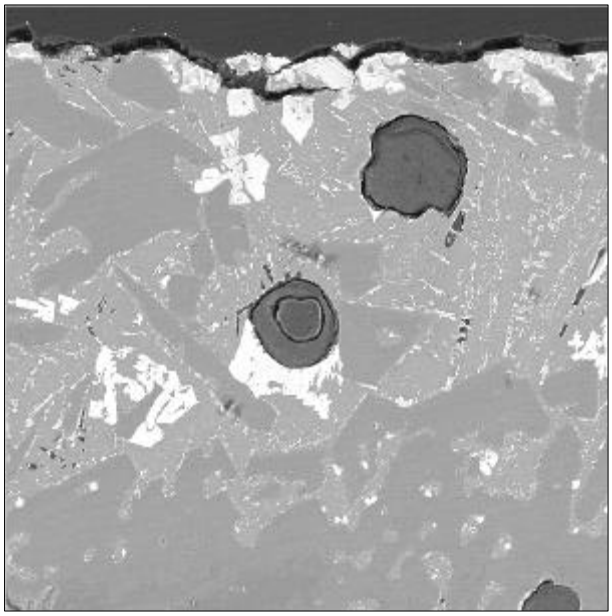

B.S.E. |-------| *125 mm*

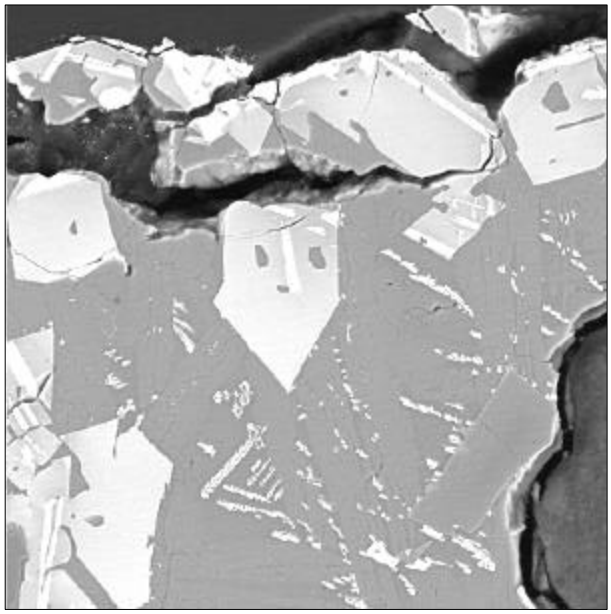

B.S.E. |-------| *31 mm*

Exhibit 2.2-60
Electron Probe Microanalysis of Sample 6, Area 1 (slag surface)

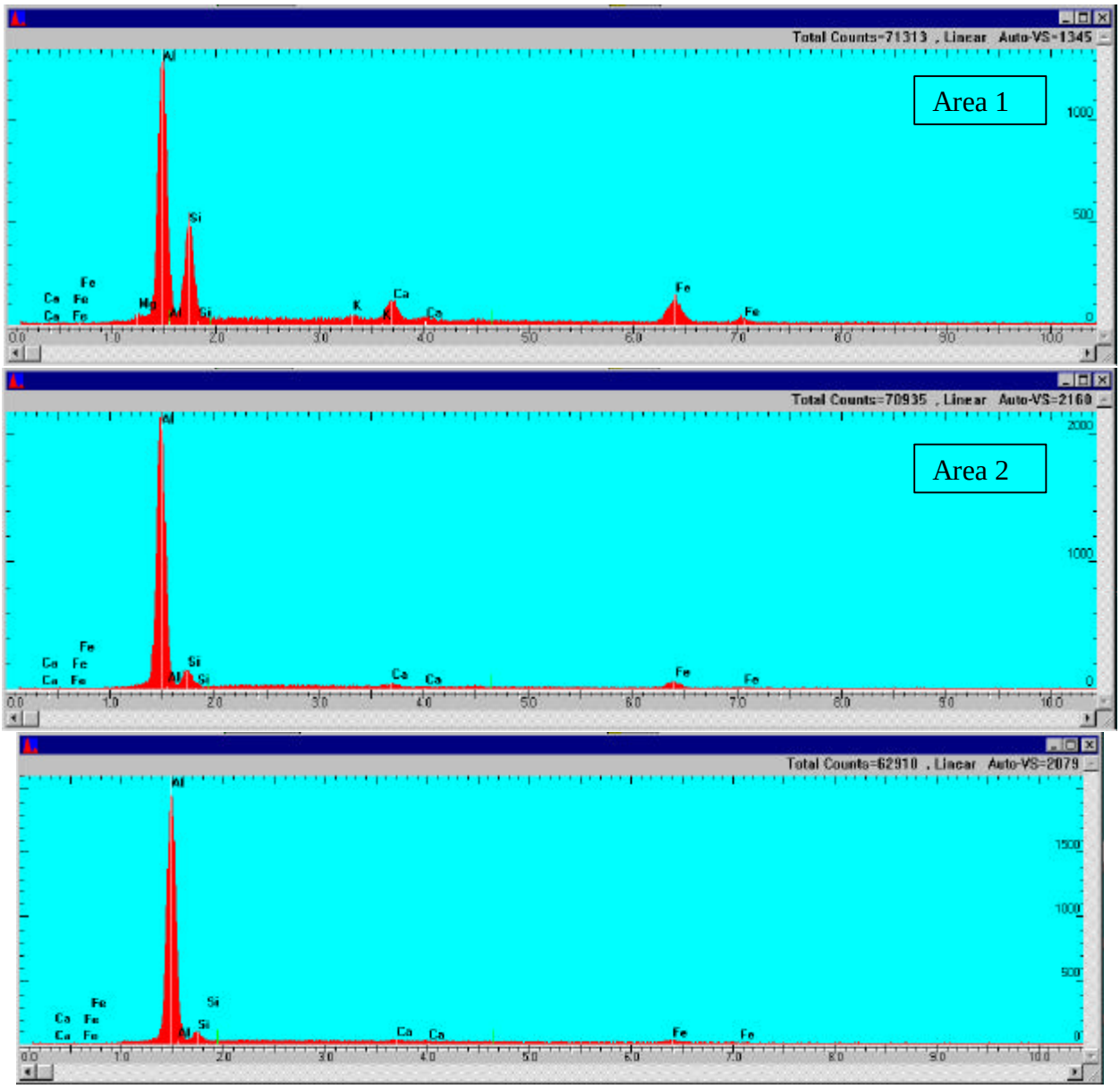

Exhibit 2.2-61
Electron Probe Spectra showing Various Areas of Sample 6

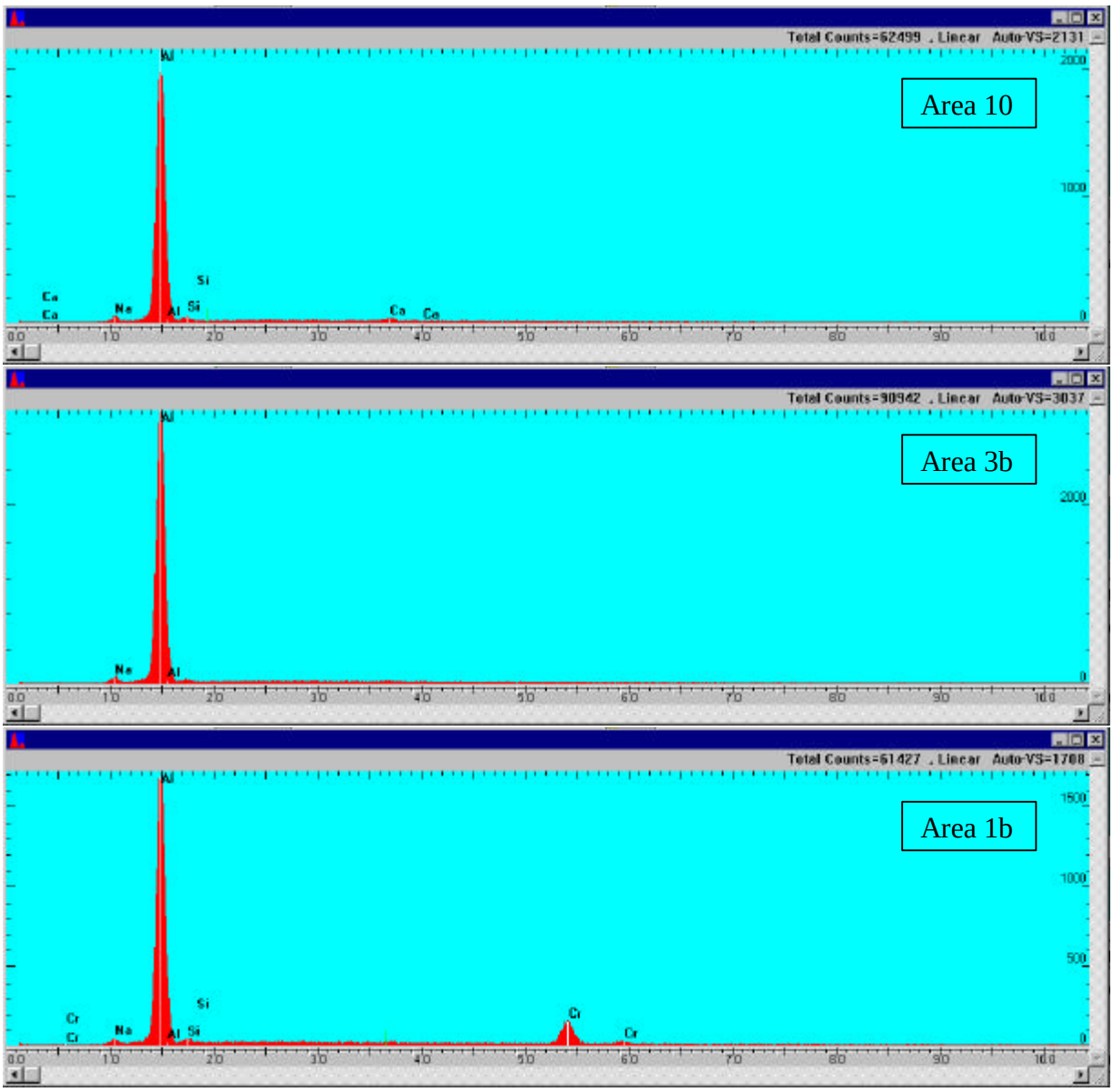

Exhibit 2.2-61 (cont.)
Electron Probe Spectra showing Various Areas of Sample 6

The element spectra of Area 1 in Sample 2 (Exhibit 2.2-53) and Sample 6 (Exhibit 2.2-61) are similar, with a very strong aluminum peak, followed by moderate silicon, iron and magnesium peaks. The chromium peak in Exhibit 2.2-53 is missing in Exhibit 2.2-61, as would be expected. Again the Area 2 element peaks are similar between the two samples, except that the iron peak is much weaker in Sample 6. The element spectra 2mm to 5mm from the slag surface into the dark region are very similar in the two samples (Area 3 in sample 2 and Area 5 in sample 6). One of the main differences between Area 1 and Area 3 & 5 is that the iron and silicon peaks are greatly diminished. In Area 10 of Exhibit 2.2-61, the iron peak is missing, and there are some very weak peaks of silicon, sodium, and calcium. In Area 3b, which is in the unaltered (white) Monofrax M region, only a very weak peak of sodium and the very strong aluminum peak are visible. The chromium peak is visible in Area 1b (Exhibit 2.2-61).

Exhibit 2.2-62 shows the element maps of Area 1 in Sample 6. The penetration of the slag is deeper than in Area 1 of Sample 2 (Exhibit 2.2-54), and is not limited to a discrete layer. The aluminum (blue dolor), silicon, calcium, iron, magnesium and potassium are all present in the slag. The unreacted alumina grains (yellow green) in Exhibit 2.2-62 can be seen to be dissolving (getting smaller) and are separating from the Monofrax M matrix and are moving into the slag. With increasing distance from the slag surface, viz., going to the element maps of Areas 2 and 5, the amount of silicon, calcium, and iron diminish significantly (Exhibit 2.2-63 & Exhibit 2.2-64). In contrast, the amount of aluminum increases along with the sodium, which indicate that not all of the β-alumina has lost its sodium and converted to the α-phase. In regions remote from the slag (Area 10 or 3b, Exhibits. 2.2-65 and 2.2-66, respectively) only aluminum and sodium elements can be seen, which are from the α- and β- alumina grains. Thin layers of silicon and calcium, which concentrate at the alumina grain boundaries and in the voids between the grains are also visible in these Exhibits. The chromia/alumina coating on the back surface of the tile can be seen as the chromium and aluminum (blue color) element map in Exhibit 2.2-67.

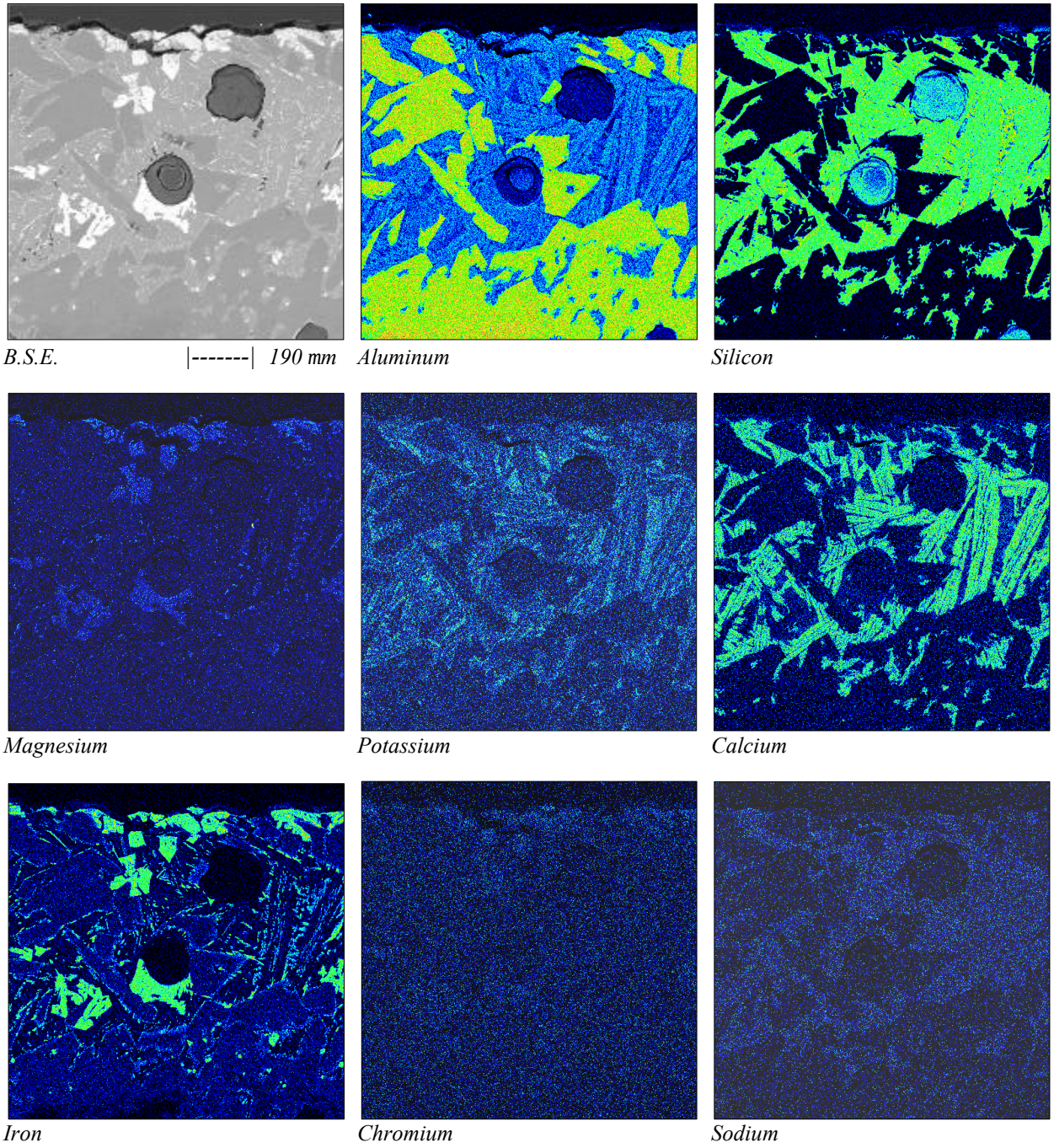

Exhibit 2.2-62
Electron Probe Microanalysis showing Element Maps in Sample 6, Area 1 (slag surface)

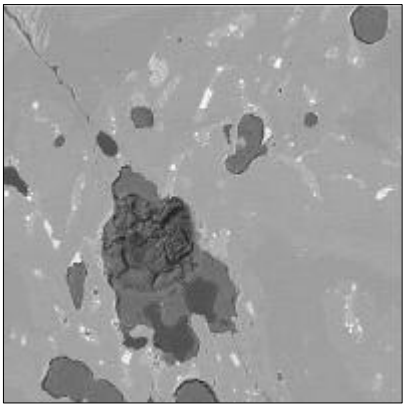

B.S.E. |-------| *190 mm*

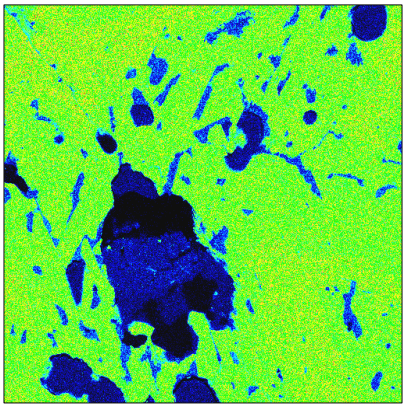

Aluminum

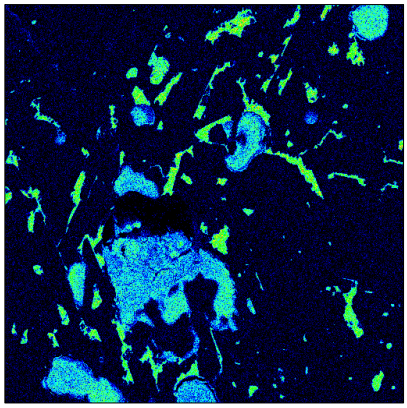

Silicon

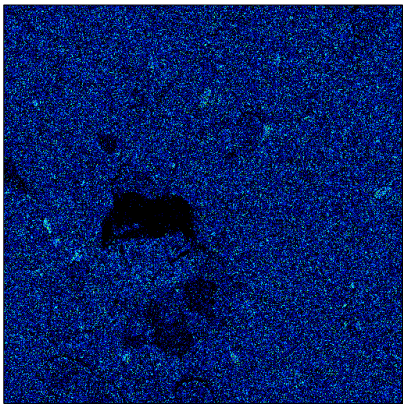

Magnesium

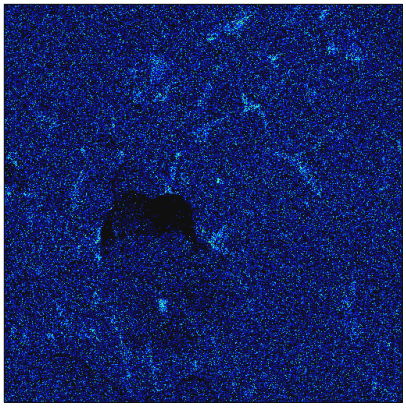

Potassium

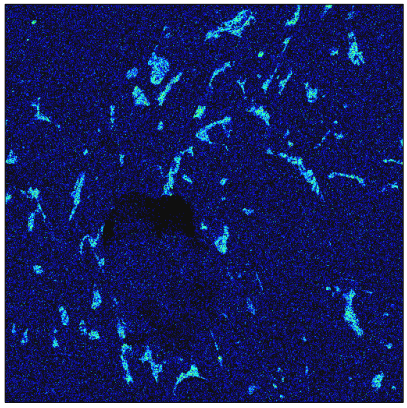

Calcium

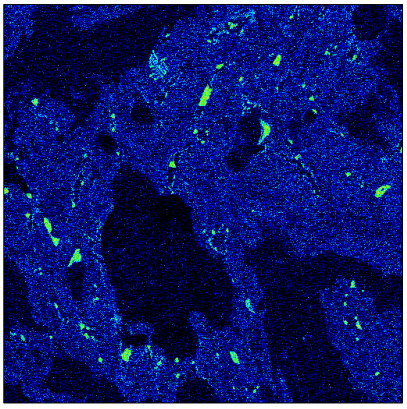

Iron

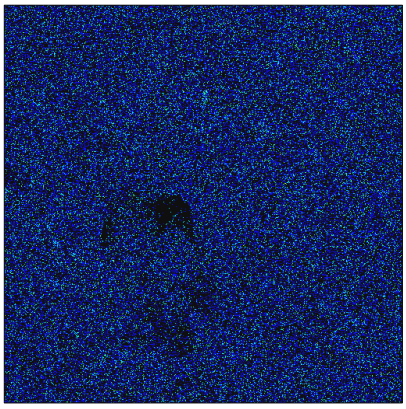

Chromium

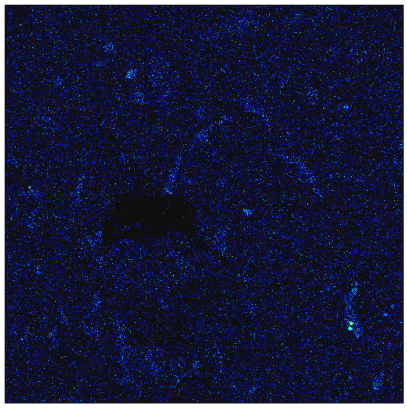

Sodium

Exhibit 2.2-63
Electron Probe Microanalysis showing Element Maps in Sample 6, Area 2

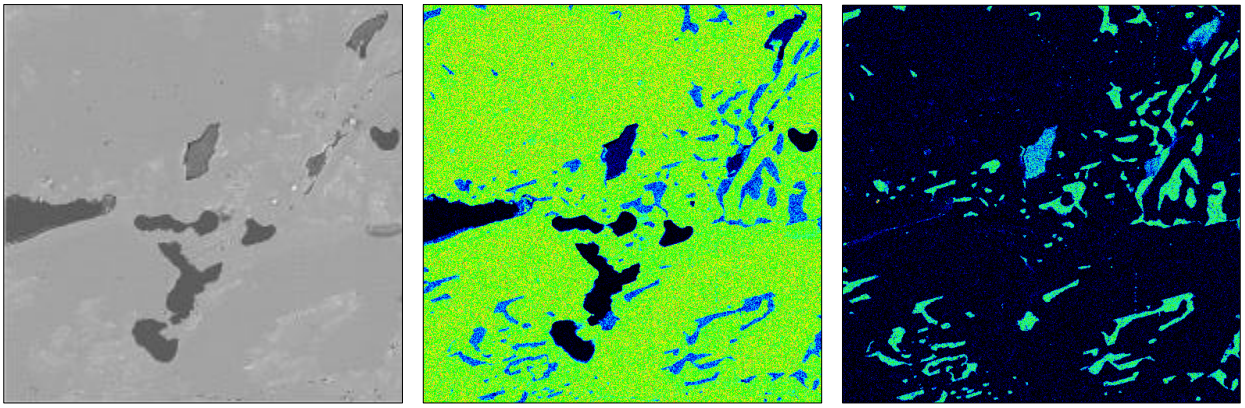

B.S.E. |-------| *190 mm* *Aluminum* *Silicon*

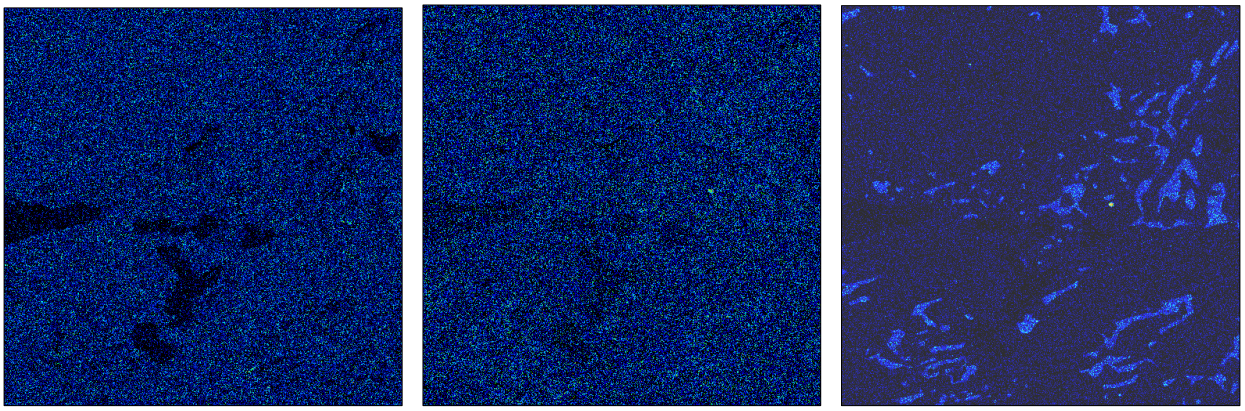

Magnesium *Potassium* *Calcium*

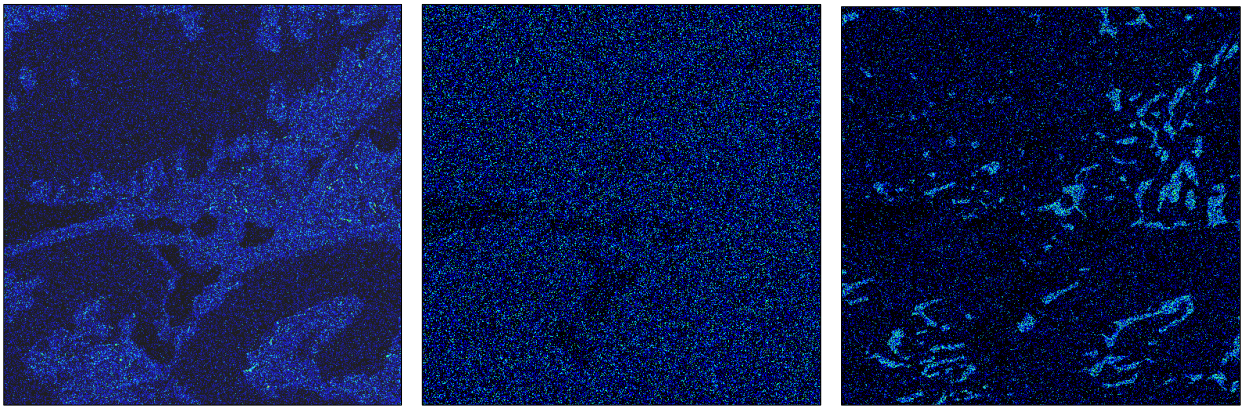

Iron *Chromium* *Sodium*

Exhibit 2.2-64
Electron Probe Microanalysis showing Element Maps in Sample 6, Area 5

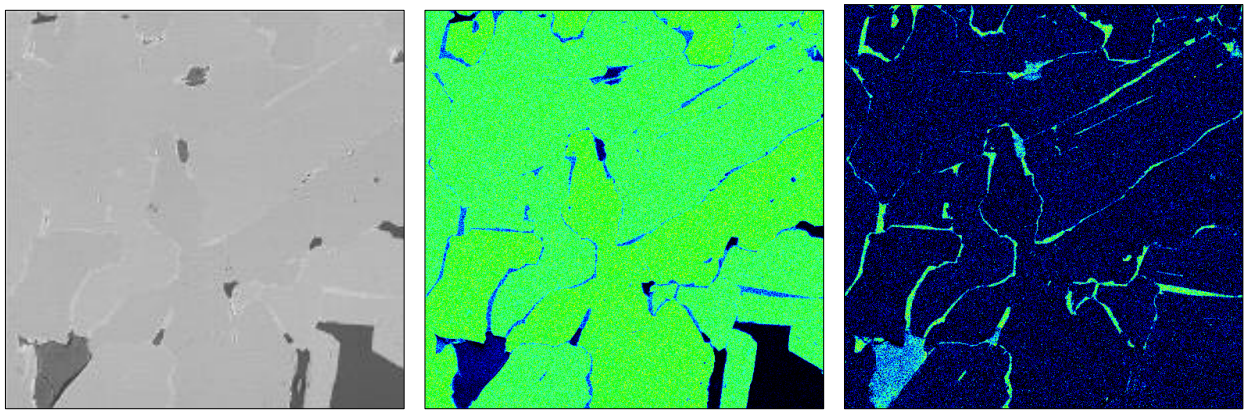

B.S.E. |-------| *190 mm* *Aluminum* *Silicon*

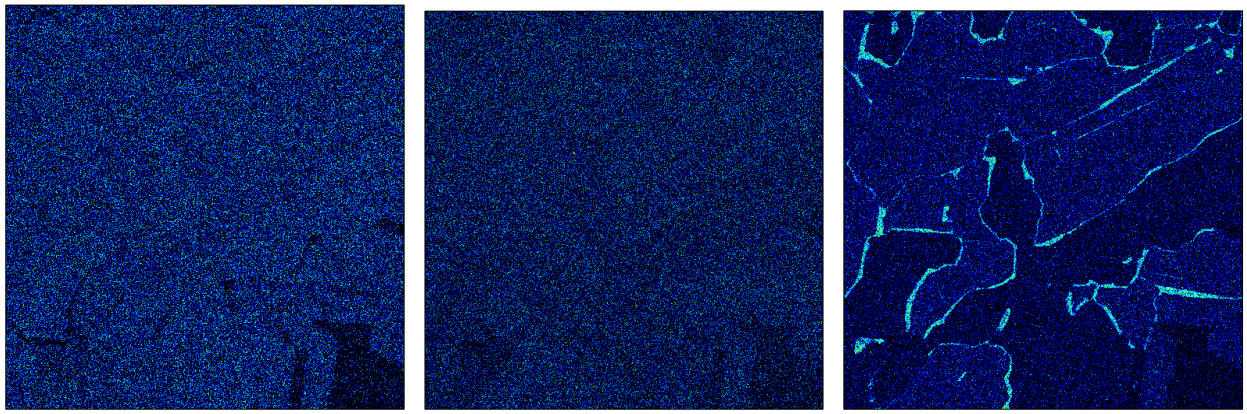

Magnesium *Potassium* *Calcium*

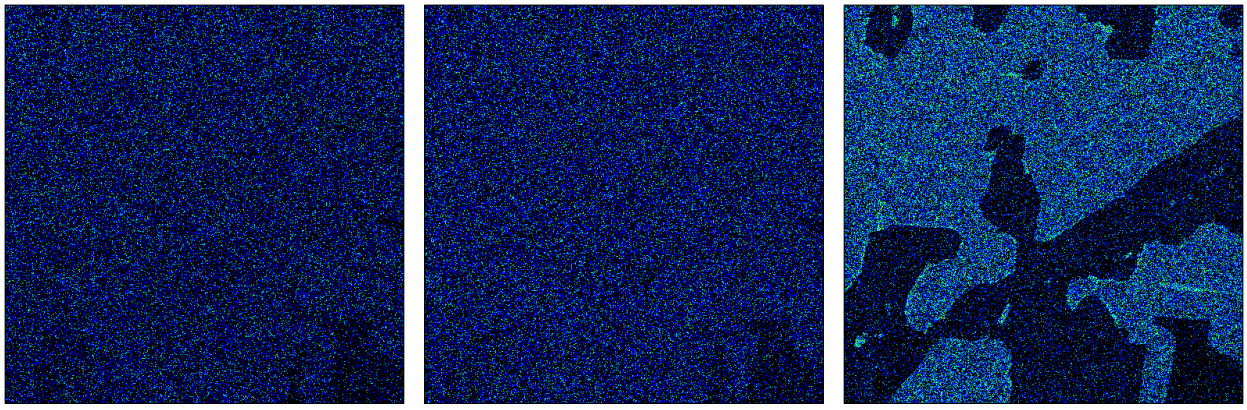

Iron *Chromium* *Sodium*

Exhibit 2.2-65
Electron Probe Microanalysis showing Element Maps in Sample 6, Area 10

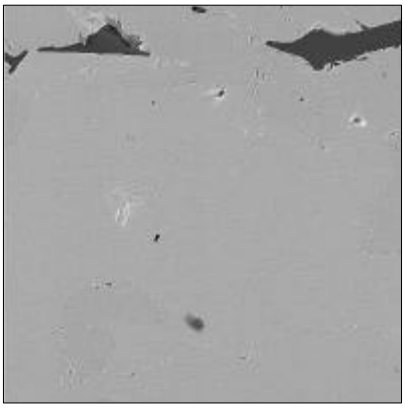

B.S.E. |-------| *190 mm*

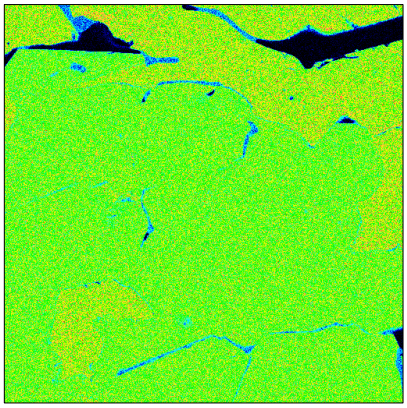

Aluminum

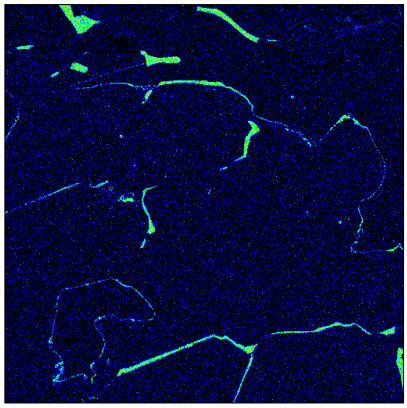

Silicon

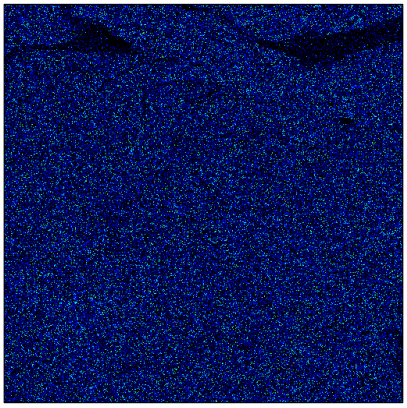

Magnesium

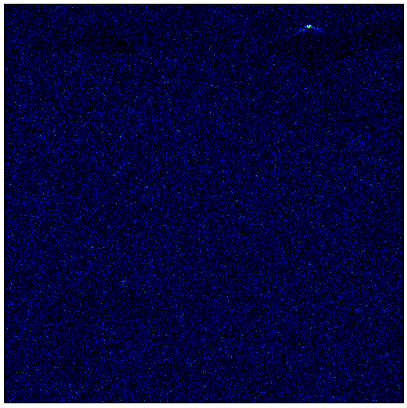

Potassium

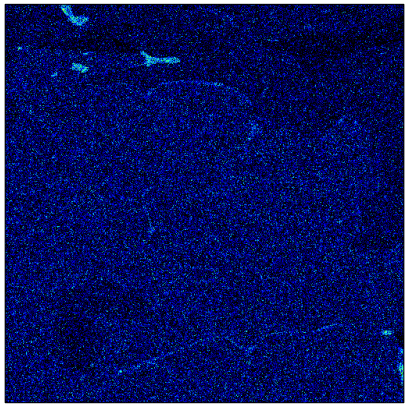

Calcium

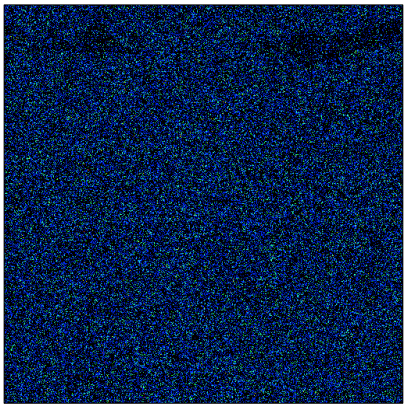

Iron

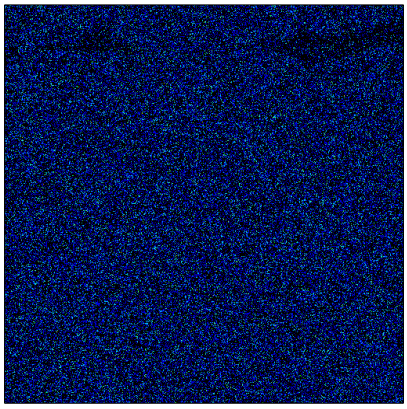

Chromium

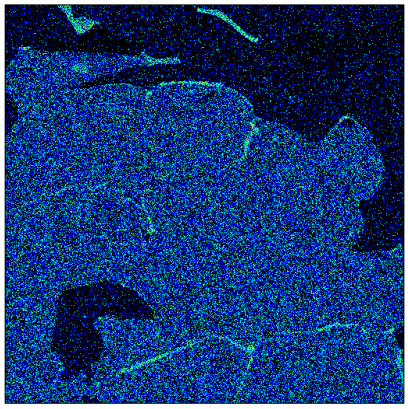

Sodium

Exhibit 2.2-66
Electron Probe Microanalysis showing Element Maps in Sample 6, Area 3b

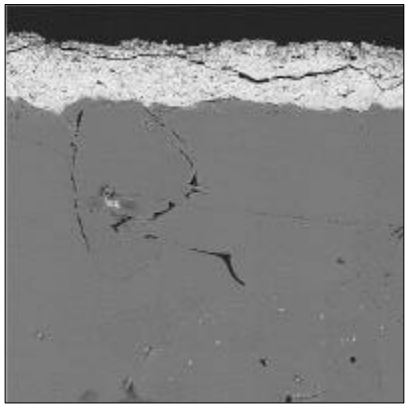

B.S.E. |-------| *190 mm*

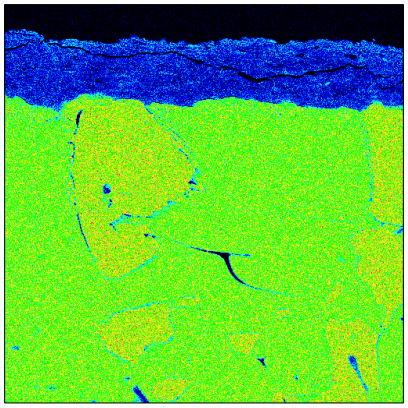

Aluminum

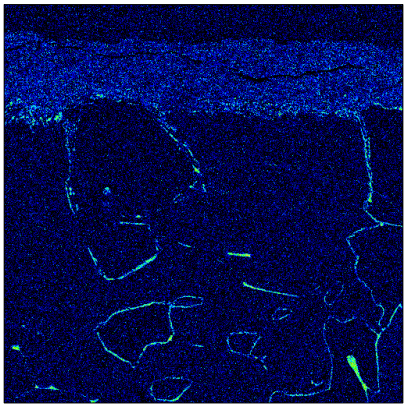

Silicon

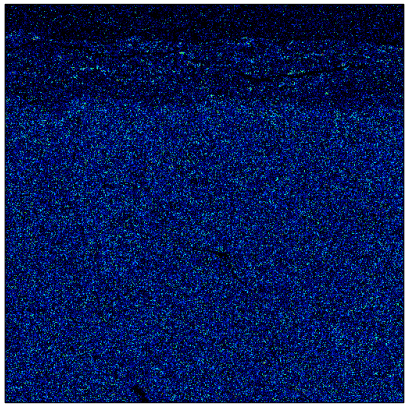

Magnesium

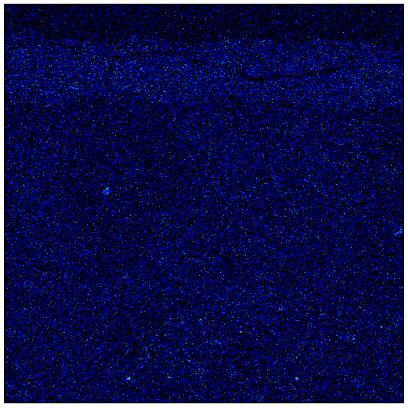

Potassium

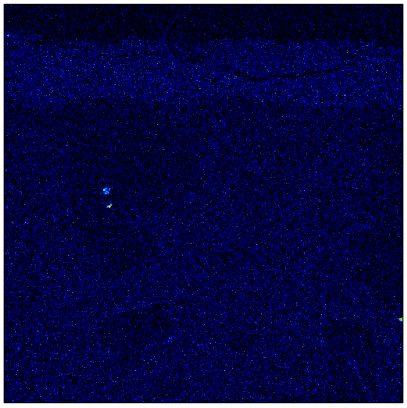

Calcium

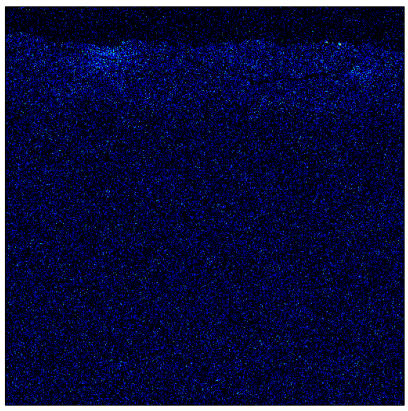

Iron

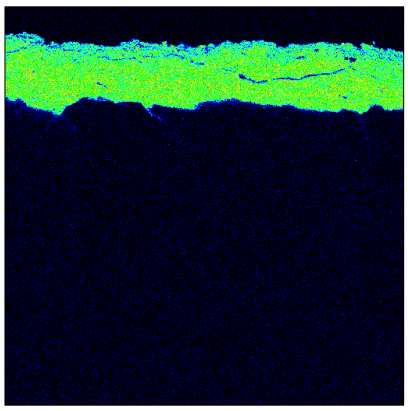

Chromium

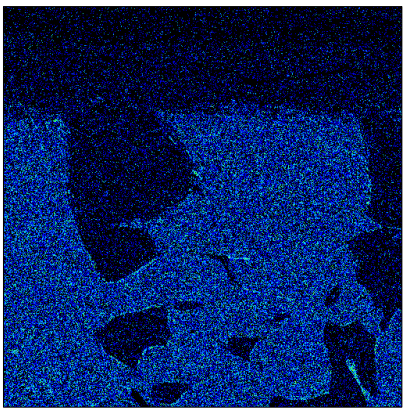

Sodium

Exhibit 2.2-67
Electron Probe Microanalysis showing Element Maps in Sample 6, Area 1b

Discussion

The fusion-cast Monofrax M material was selected for the heat exchanger tiles primarily because of its high thermal conductivity and refractoriness. It was not the best choice for resistance to slag attack, but overall it had the best combination of properties for the RAH.

The accelerated (high temperature) laboratory slag tests indicated that the life of the Monofrax M material was susceptible to significant corrosion and erosion in 100-hour exposures. However, the Monofrax M tiles proved to be durable and reliable in the RAH under the heating conditions and exposure to various slags during the 1005 hours of furnace time. Examination of the removed tiles indicated that little or minimal changes occurred in the tile dimensions (especially in the thickness). There was reaction and dissolution of the alumina surface grains with the different slags, but this was generally limited to the outer 1 - 3 mm. The discoloration due to the penetration of slag constituents down grain boundaries and into crack and voids was limited to 6 - 7mm, but in this region the β-alumina grains converted to α-alumina, and the main changes in composition occurred in the regions between grains. The shape and size of the original grains were changed only slightly. The discoloration of the white Monofrax M was noticeable in the early runs, but apparently the continued rate of discoloration into the material decreased with increasing exposure time. Samples with 562 hours of furnace time had a discoloration depth averaging about 5 - 6mm, while those with 1006 hours had an average depth of 7 - 8mm.

The application of a plasma sprayed chromia/alumina layer on the face of a tile did not seem to reduce the thickness of the discolored zone. However, it did have a significant effect on limiting the extent of the major corrosive action of the slag to the outer 1mm from the surface. The as- sprayed coating was porous so that the slag was able to penetrate it, but the extent of the reactions of the slag with the alumina grains below the coating was lessened.

Overall, the discolored zone (away from the surface) contained minor amounts of slag constituents and did not seem to adversely affect the structural performance of the Monofrax M. The penetration of slag into thin cracks appeared to have a beneficial effect, since it filled the cracks and bonded the alumina grains together.

Task 6 Commercial Plant Update

HIPPS Repowering.

Cycle Analysis

The emphasis on repowering this quarter continues to be the identification of HIPPS using coal as the majority fuel which would demonstrate efficiencies comparable to those realized by the Advanced Turbine System (ATS) Program (~60% LHV). Two approaches have been taken: the first is the "conventional" repowering where a gas turbine(s) is used to supply additional power as well as heated air for use in the steam bottoming cycle; and the second uses a high temperature fuel cell in addition to the gas turbine.

While any type gas turbine can be used for repowering, the use of aeroderivative gas turbines for repowering has several advantages over the heavy frame machine: quick start up and high availability being two of the major advantages. To establish the range of performance obtainable with aeroderivative gas turbine, a series of analyses of repowering a nominal 125 MW steam plant were made using the Pratt & Whitney FT8 as the base gas turbine. A typical configuration for repowering is shown in Exhibit 6-1. The results of these analyses are shown in Exhibit 6-2.

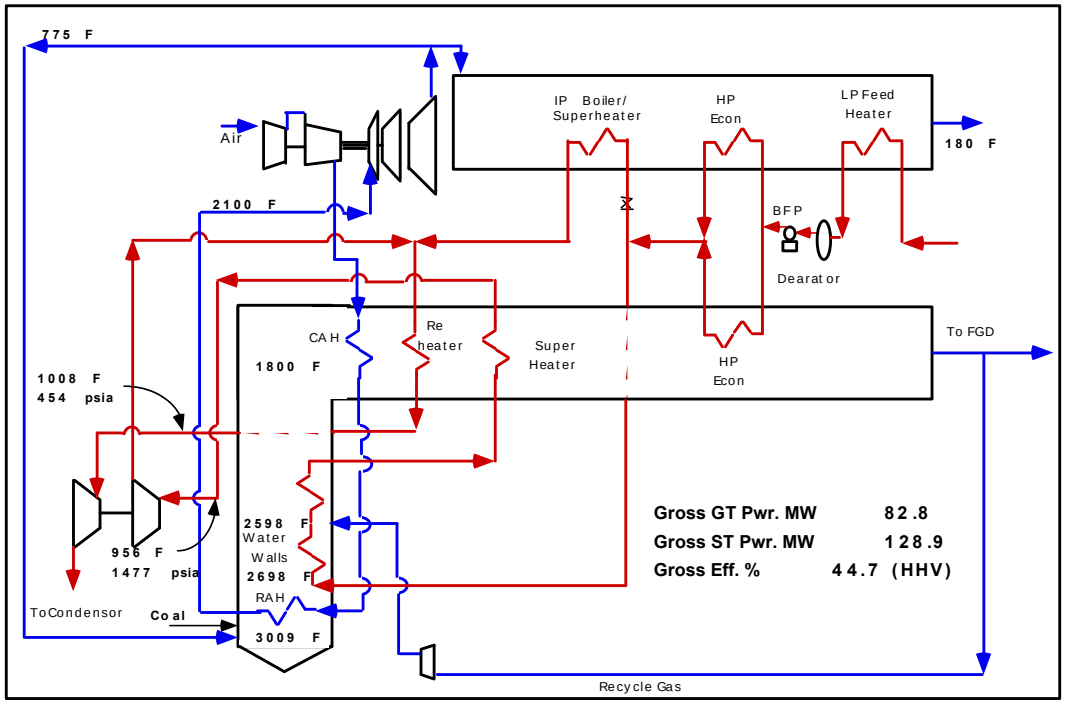

Exhibit 6-1
HIPPS Repowering with Aeroderivative Gas Turbine

Exhibit 6-2
FT8 Gas & Coal (HITAF) Performance

Case	1	2	3	4	5	6	7
	UTRC FT8	HITAF 1800F	HITAF 2100F	HITAF 2208F	HITAF 2300F	HITAF 2400F	HITAF 2500F
Number of GT engines	1	4	4	4	4	4	4
Type of fuel	Nat Gas	Coal	Coal	Coal & Gas	Coal & Gas	Coal & Gas	Coal & Gas
System Performance							
Total net power, MW	25.5	191.2	202.8	212.1	219.3	225.6	233.6
Gross Gas Turbine power, M	26.0	64.3	82.8	92.0	99.2	105.5	113.6
Gross Steam Turbine power, MW	0	136.0	128.9	129.1	129.1	129.1	129.1
Cycle Efficiency, %, net (LHV gas)	38.7						
Cycle Efficiency, %, gross (HHV c&g)	NA	42.3	44.7	45.4	45.9	46.1	46.6
Gas Turbine Performance							
GT HPT temp, F	2208	1800	2100	2208	2300	2400	2500
GT LPT temp, F	1642	1308	1515	1608	1676	1735	1810
GT power turbine temp, F	1337	995	1195	1285	1355	1415	1490
GT exhaust temp, F	857	667	775	825	862	896	937
GT stack temp, F	857	180	180	180	180	180	180
Turbine Cooling (% Inlet)	18.4	10.5	17.7	18.5	19.6	21.6	22.4
Fuel flow rate, lbs/sec	3.024	NA	NA	1.0	1.8	2.7	3.6
Gas /Coal Ratio, %	1.0	0.	0.	4.9	8.8	12.7	16.4
HITAFF Combustor							
Coal flow rate, lbs/sec	NA	35.52	35.52	34.7	34.1	33.4	32.7
Radiant sect., GT Outlet temp, F	NA	1800	2100	2100	2100	2100	2100
Convective HX outlet temp, F	NA	1300	1300	1300	1300	1300	1300
HITAF HRSG stack temp, F	NA	300	300	315	335	367	386

Repowered Steam System							
Throttle flow, lbs/sec	NA	209.9	199.1	199.4	199.4	199.4	199.4
Pressure, psia	NA	1477	1477	1477	1477	1477	1477
Temperature, F	NA	956	956	956	956	956	956
Steam Turbine flow parameter (*)							
W T /P	NA	5.35	5.07	5.07	5.07	5.07	5.07
Reheat turbine flow, lbs/sec	NA	209.9	199.1	199.1	199.1	199.1	199.1
Pressure, psia	NA	454	454	454	454	454	454
Temperature, F	NA	1008	1008	1008	1008	1008	1008

(*) Base, DOE steam station, FP=5.48

The baseline engine information is given in column 1; the engine has an output of 25.5 MW and an efficiency of 38.8% (LHV) using natural gas as a fuel. In column 2, an all coal HIPPS version is given. Here, the HITAF radiator outlet temperature is limited to 1800 F and, with no gas used to boost the temperature, the gas turbine output is reduced to approximately 18 MW. To raise enough steam for the nominal 125 MW steam system, four FT8 turbines are required. Because the steam raised in the HRSG displaced most of the extraction steam, the steam turbine output is raised to 136 MW. The overall output is increased to over 190 MW and the efficiency is 42.3 % (HHV) compared to the original steam station output of 122 MW with an efficiency of 35.5%.

When advanced materials are used in the HITAF radiator, the outlet temperature can be performance increases to 203 MW at 44.7%. The use of natural gas to boost the gas turbine inlet temperature to its design point (column 4) results in further increase in power (212 MW) and efficiency (45.4%). This system is approximately 95% coal fired. The remaining columns show the effect of increasing the turbine inlet temperature by using increasing amounts of natural gas in the boost combustors. As would be expected, both power and efficiency increase. The impact on overall system economic is, however, a function of the ratio of cost of coal to cost of gas.

The second approach being considered for repowering uses a high temperature fuel cell, either a molten carbonate (MCFC) type (operating temperature around 600 F) or a solid oxide (SOFC) type (operating temperature around 1800 F). A preliminary configuration for a SOFC system is shown in Exhibit 6-3.

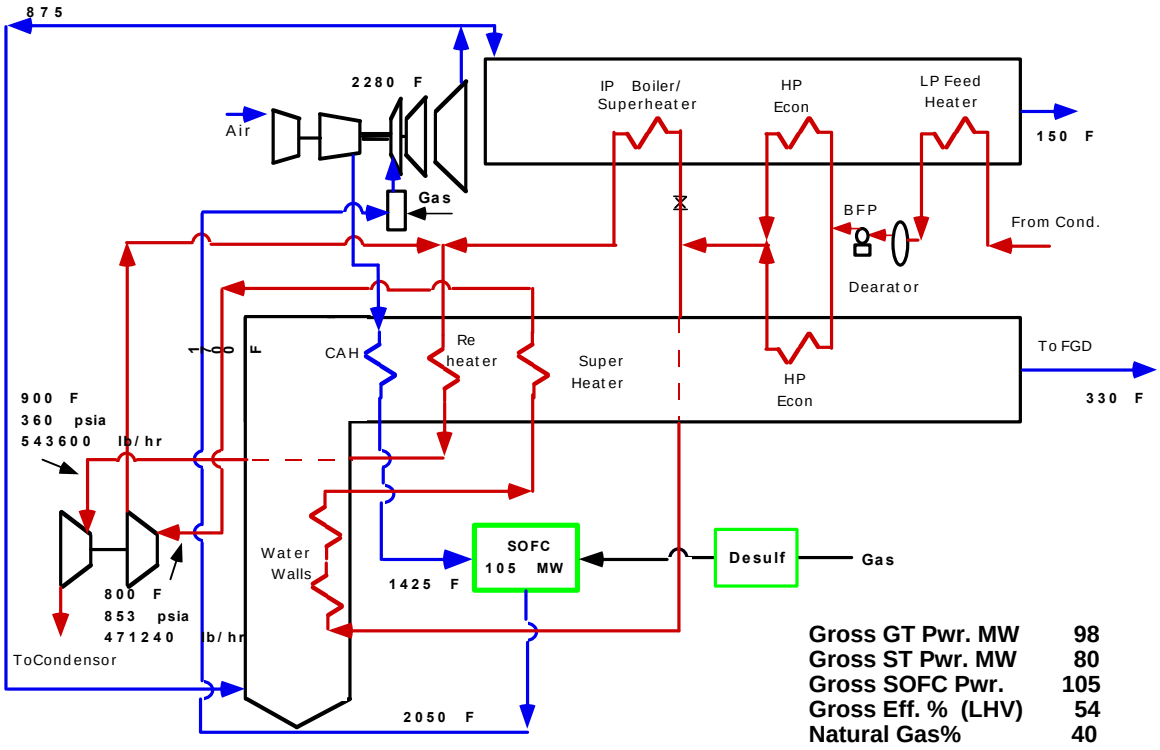

Exhibit 6-3
HIPPS Repowering with a SOFC and GT

The values shown in Exhibit 6-3 are based on very preliminary estimates. A computer simulation model of a SOFC is being constructed for use in the overall HIPPS power system model. When that model is completed and validated, a more thorough analysis will be performed.